An analysis of the requirement for septate junction proteins in essential morphogenetic events

BY

Sonia Marie Hall

Submitted to the graduate degree program in Molecular Biosciences and the Graduate Faculty of the University of Kansas in partial fulfillment of the requirements for the degree of Doctor of Philosophy.

_____
Chairperson – Dr. Robert Ward

_____
Dr. Stuart MacDonald

_____
Dr. Matthew Buechner

_____
Dr. Erik Lundquist

_____
Dr. Justin Blumenstiel

Date defended: June 15, 2015

The dissertation committee for Sonia Marie Hall
certifies that this is the approved version of the following dissertation:

An analysis of the requirement for septate junction proteins in essential morphogenetic events

_____
Chairperson – Dr. Robert Ward

Date approved: June 15, 2015

Abstract

Proper organismal development depends upon highly regulated cellular rearrangements and cell shape changes that are driven by intrinsic stabilizing and dynamic forces within an epithelium. These morphological processes require coordination of signaling pathways, cytoskeletal changes, and cell adhesion. To identify essential regulators of morphogenesis, our lab conducted three screens to identify genes involved in regulating morphogenesis. From this screen, we identified a novel component of the septate junction (SJ), *Macroglobulin complement related (Mcr)*. The SJ provides a barrier between epithelial cells to regulate paracellular flow, allowing for organ compartmentalization. The SJ requires over twenty proteins for its organization and function. While the function of the SJ is of critical importance to development and homeostasis, its role in morphogenesis was unclear. We examined whether the identification of *Mcr* in a screen for morphogenesis was an isolated role of *Mcr* or a concerted requirement for the entire SJ complex. To explore this question, we conducted an analysis of nine SJ genes and examined the penetrance of defects in head involution, dorsal closure, and salivary gland organogenesis. From this analysis, we determined that each SJ component examined has an essential role in regulating morphogenesis by contributing to cell shape changes and rearrangements.

Acknowledgements

The opportunity to attend and complete graduate school would not have been possible without the support of my family. My husband, Derek, has been a constant source of love and encouragement. I have navigated many challenging obstacles along this journey that would not have been manageable without his friendship, love, and compassion. For his support, I am eternally grateful. My daughter Hanna, who learned to read by assisting me in studying for my exams, made it possible for me to balance my academic endeavors with my family life. I acknowledge the sacrifices that she has made that have contributed to making this work possible. To my curious son Kristian, I thank you for constantly questioning why things are they way they are and teaching me to think more broadly about how interrelated things are in the natural world. Each of you has made me a more complete person, mother, wife, and scientist.

To my mentor, Dr. Robert Ward, I thank you for allowing me the opportunity to train under your guidance. I appreciate your patience and confidence in my ability to develop and explore our project. Your support of my professional endeavors that extended beyond the door of the lab and far from the reach of the bench has been instrumental in shaping the direction of my career. I appreciate your faith in me to be able to manage these commitments in addition to my project.

Dr. Brian Ackley and the members of the Ackley lab, I would like to extend my appreciation to you for your generosity in the use of your confocal microscope. I appreciate the time that each you took away from your own work training me to use the equipment, troubleshooting, as well as insightful conversations about science

and life. Dana and Samantha, I greatly value the advice and guidance you provided me during the completion of my degree and postdoctoral job search.

John Connolly and Linda Wiley, thank you for your tireless support of not only me but also all students and faculty within our department. I would also like to thank members of the Ward lab for their support, assistance, and friendship during my graduate training. Finally, Lynn Villafuerte, you have become a dear friend and trusted mentor during my time here at KU. I appreciate you providing opportunities for me to further my mentoring skills, encouraging my passion for education and outreach, and empowering me to trust in my abilities. I will carry the strength I have gained from your guidance and friendship throughout my life.

Table of Contents

Page number

List of Figures

Figure **Page number**

List of Tables

Table **Page number**

Chapter I
Introduction

The formation and maintenance of an epithelium is a fundamental requirement in multicellular organisms, allowing for the formation of distinct three-dimensional organ compartments that can carry out essential functions such as directed secretion, nutrient absorption, and protection from the invasion of pathogens. An intact mature epithelium requires three major features: 1. defined apical and basal domains that polarize the epithelium for directed vesicle secretion; 2. membrane scaffolds that allow for cell-cell adhesion and anchoring of cytoskeletal components; 3. establishment and maintenance of a paracellular barrier. Vertebrates and invertebrates have slightly different mechanisms for establishing and maintaining the essential architecture of an epithelium, yet many of the components are conserved across species, notably the claudin and cadherin protein families. *Drosophila melanogaster* has served as a key model in understanding the cellular mechanisms that drive the formation of specialized membrane domains during development and homeostasis.

Epithelial cell membranes are subdivided into three primary domains: apical, lateral, and basal. In an organ, the apical surface is in contact with the chemically distinct luminal environment. The basal side is anchored to extracellular matrix proteins of the basal lamina. Spanning the region between the apical and basal domains is the lateral membrane domain. This membrane can be further divided into the apical-lateral and basolateral regions. It is within the apical-lateral region that specialized protein complexes, called junctions, form to provide cell-cell adhesion and paracellular barrier function. (Fig. 1.1)

Cells organized into a complex tissue require cell-cell adhesion, stabilization, and the ability to communicate with their neighbors to coordinate cellular and tissue level events during morphogenesis. Much of our understanding of the role of these mechanisms has been revealed through extensive study of the apical-lateral membrane complex referred to as the adherens junction (AJ). The AJ is a large protein complex that interacts at the cytoplasmic side of the membrane with the actin cytoskeleton to drive contractility that leads to changes in cell shape. The transmembrane proteins of the AJ, including cadherins, function to mechanically and chemically link neighboring cells within a tissue, maintaining and propagating tissue-wide communication and the distribution of force.

The junction responsible for the occluding function of the epithelium is adjacent to the AJ. In vertebrates, this junction is called the tight junction (TJ) and is located apical to the AJ. The TJ is composed of over forty proteins (Schneeberger and Lynch 2004; Yamazaki et al. 2011) including cytoplasmic proteins that interact with actin and transmembrane proteins to bring adjacent membranes into close apposition. It is believed that claudins are responsible for the regulation of the permeability of the tight junction.

The occluding function in *Drosophila* and other invertebrates is provided by the septate junction (SJ), which is located basal to the AJ. It is a large protein complex that forms an electron-dense ladder-like array that spans the intermembrane space between adjacent lateral membranes. Over the last twenty years, the use of *Drosophila* as a model has provided us the ability to study the establishment and maintenance of the barrier using genetics and cell biology. Over

20 proteins have been identified as playing a role in the SJ, the majority of which are transmembrane proteins. Many of these proteins have been shown to localize to or transiently associate with the SJ. Here I review the known functions and interactions of these SJ proteins, our current understanding of the maturation of the junction, and the contribution of this work to our greater understanding of the biology of the lateral membrane.

Septate Junction Biogenesis

Pivotal observational studies have provided the field with considerable insight into the mechanistic regulation that facilitates the redistribution of SJ proteins from the basolateral membrane to the apical-lateral region of the SJ. Specifically, SJ proteins that are initially broadly distributed along the lateral membrane at stage are retargeted to the SJ between stages 13 and 14 via the endocytic and recycling pathways as small subcomplexes that require Ly6 proteins. By stage 15, SJ proteins are refined at the region of the SJ where they form a core complex where the loss of a single core component results in the mislocalization and increased mobility along the lateral membrane. For the complexes to become fixed within the plane of the membrane and form a tight barrier by stage 16, intercellular communication between core complexes of adjacent lateral membranes is required (Genova and Fehon 2003; Oshima and Fehon 2011) (Fig. 1.2).

Our understanding of the regulatory mechanisms required for biogenesis of the SJ were extended with the discovery of *Melanotransferrin* (*Mtf*) ((Tiklová et al. 2010). *Mtf* was identified as encoding a GPI-linked iron binding protein that undergoes cleavage of the GPI anchor, allowing it to function tissue non-

autonomously for SJ organization and function. In addition, structure function analysis indicates that the iron binding sites are essential for stabilization of core SJ components. At stage 13, Mtf was found to locolize and co-immunoprecipitate with Rab5 and Rab11, which that suggests endocytosis and recycling are required for the internalization and redistribution of Mtf for SJ localization. This finding raised an interesting possibility that the redistribution of core SJ proteins from the basolateral membrane to the refinement at the SJ by stage 16 was facilitated through the endocytic and recycling pathways. They extended their analysis and identified that Cor, Gli, and Sinu also co-localize with Rab5 and Rab11 at stage 13. However, at stage 16, when there is very little turnover of core SJ components, this co-localization is no longer observed.

The discovery of four Ly6 genes, *Boudin* (*Bou*), *crooked* (*crok*), *coiled* (*coil*), and *cold* (*cold*) extended our understanding of the subcellular trafficking of SJ components when they were identified as being required for the assembly of core SJ components (Hijazi et al. 2009; Nilton et al. 2010). This family of proteins is related to the vertebrate urokinase/plasminogen activator receptor (uPAR) and Ly6 protein family. In vertebrates, Ly6 proteins appear to be involved in cell adhesion, cell signaling, and have also been identified to modulate allosteric interactions, indicating that this protein family plays a fundamental role in cell biology (Nilton et al. 2010; Hijazi et al. 2009).

The role of Bou, Crok, Cold, and Coil in the SJ is unique when compared to other SJ proteins. Until the discovery of these Ly6 proteins, proteins involved in SJ organization and function had been identified to localize to the SJ where they form a

highly interdependent structure. The *Drosophila* Ly6 proteins, only transiently associate with core SJ components while they are being trafficked within the cell. It was identified by Nilton et al. (2010) that Crok and Cold are responsible for the trafficking of Nrx-IV and Cor where they co-localize with early, recycling, and late endosomes, as well as with lysosomes. Interestingly, Crok and Cold were not found to be required for the trafficking of Atpα or Nrg. These findings further our understanding of the differential trafficking of core SJ components. In addition, it raises the possibility that small subcomplexes of SJ proteins begin to assemble prior to their incorporation into a large junctional complex. This idea of subcomplex formation taken together with the known cellular function of vertebrate Ly6 proteins led Nilton et al. (2010) to hypothesize that the role of Ly6 in the biogenesis of the SJ could be due to their ability to regulate specific interactions, facilitating modifications that are required for the final maturation of the SJ.

Another unique component involved in organizing the SJ are the lipid phosphate phosphatase (LPP) encoding genes, *wunen (wun)* and *wunen2 (wun2)* (Ile et al. 2012). Lpps function as transmembrane enzymes that regulate the phosphorylation of sphingolipids and glycerolipids that facilitate cell signaling. Wun localizes at the apical surface of tracheal cells and also co-localizes with markers of the AJ and SJ. In comparison, Wun2 localizes to the apical surface and along the length of the lateral membrane. Maternal and zygotic loss of *wun* and *wun2* leads to a decrease in the AJ protein DE-cadherin and disrupted SJ organization in the embryonic trachea. Surprisingly, this interaction is not observed in any other ectodermally derived epithelial tissues. While Wunens seem dispensable in several

tissues, the observation that modifications of the lipid bilayer can regulate SJ organization and function raises interesting questions regading the role of lipid modifications in regulating the membrane dynamics of the SJ.

Currently, the field lacks a comprehensive understanding of how individual SJ proteins become incorporated into the SJ complex. Studies conducted by Oshima and Fehon (2011) explored the dynamics of proteins that localize to the SJ using fluorescence recovery after photobleaching (FRAP). At stages 11 and 12, they showed that SJ proteins are very mobile within the lateral membrane. This suggests that during this developmental time period, SJ core components do not form a stable complex. In comparison, at mid-to late-stage 13 SJ core components become immobile. This was contrasted by that of the SJ associated protein Dlg, that continues to exhibit greater mobility after the SJ has begun to assemble, demonstrating that core components of the SJ are stabilized and localized to the SJ by a mechanism independent of other lateral membrane proteins. This analysis allowed for the identification of similar membrane kinetics for the core SJ proteins Cor, NrxIV, Nrv2, Nrg, Atpα and Mcr (Oshima and Fehon 2011; S. Hall et al. 2014). The application of FRAP has provided a mechanism to distinguish between core SJ components and SJ-associated proteins.

Core components of the *Drosophila* SJ

Claudins

Claudin-family proteins have been identified as key regulators of vertebrate and invertebrate epithelial permeability (Furuse 2010; Behr, Riedel, and Schuh 2003; Wu et al. 2004; Nelson, Furuse, and Beitel 2010). Their basic structure

consists of four transmembrane domains connected by two large extracellular loops, one intracellular loop and N and C terminal cytoplasmic tails. Twenty-four claudin proteins have been identified in mammals and seven are predicted to be encoded in the *Drosophila* genome. A sequence alignment and analysis by Wu et al. (2004) showed that *Drosophila* and human claudins do not cluster together and have extensive sequence divergence both within and between species.

Of the seven *Drosophila* claudins, Kune, Sinu, and Mega function to regulate the organization and function of the SJ (Behr, Riedel, and Schuh 2003; Wu et al. 2004; Nelson, Furuse, and Beitel 2010). These findings reveal conserved molecular and functional components between vertebrate and invertebrate occluding junctions. In vertebrates, claudins have been found to form homo- and heterophilic interactions within the same cell (Furuse, Sasaki, and Tsukita 1999; Blasig et al. 2006)and between adjacent cells. These interactions have been shown to regulate essential biological functions, including the migration of germ cells between the TJs of Sertoli cells (Smith and Braun 2012). This process requires the transient incorporation of CLDN3 into new forming TJs during germ cell passage, which is then later replaced by CLDN11. Interestingly, the regular spacing of neighboring cells in the SJ preclude claudins from being the intercellular adhesion molecule in the SJ. This information positions the field to explore if claudin proteins in the mature epithelia of *Drosophila* display a differential localization that could facilitate remodeling of the SJ during complex morphogenetic events when cells are required to divide or rearrange while also maintaining tissue integrity.

Na+/K+ Atpase

The Na^+/K^+ Atpase is an essential component of the plasma membrane that creates an electrochemical gradient through the exchange of three Na^+ into and two K^+ out of the cell for every molecule of ATP hydrolyzed. The heterodimer consists of an α-subunit with ten transmembrane domains that create the Na^+ and K^+ channels (Chow and Forte 1995), as well as, the β-subunit with a single transmembrane domain. The vertebrate Na^+/K^+ Atpase primarily localizes basal to the AJ, similar to the *Drosophila* homologues, and also demonstrates cell-type specific localization patterns that includes a close association with the TJ in retinal cells. The *Drosophila* genome encodes one α-subunit, *Atpα,* and three β-subunits, *nervana1* (*Nrv1), nervana2 (Nrv2)* and *nervana3 (Nrv3)*.

Experiments altering the concentration of Na^+ and K^+ and chemically blocking pump function demonstrated that Na^+/K^+ Atpase pump activity is required for TJ assembly and maintenance (Rajasekaran et al. 2001; Madan, Rose, and Watson 2007; Cibrián-Uhalte et al. 2007; Violette, Madan, and Watson 2006; Krupinski and Beitel 2009). Surprisingly, work conducted by Paul et al. (2007) revealed, using a catalytically inactive *Atpα* isoform, that the pump function of the Na^+/K^+ Atpase is not required in *Drosophila* for the assembly of the SJ. Additionally, they identified that only the extracellular domain of Nrv2 is required for SJ organization, further indicating that the Na^+/K^+ Atpase functions as a transmembrane component of the lateral membrane scaffolding and not an ion pump. These findings raise interesting questions about the evolution of the occluding junction and its connection to the larger cell biology of the lateral membrane.

Ig superfamily proteins

Immunoglobulin (Ig)-containing proteins are often involved in protein-protein interactions that contribute to cell adhesion. The SJ contains two members of the Ig superfamily, *Neuroglian (Nrg)* and *Lachesin (Lac)* (Genova and Fehon 2003; Llimargas et al. 2004). *Nrg* encodes a transmembrane adhesion molecule that contains six Ig domains, five fibronectin type III domains, and an ankyrin-binding motif. *Nrg* is homologous to the vertebrate neurofascin-155 that is involved in barrier function in the paranodal loops (Bieber et al. 1989; Charles et al. 2002). Nrg is a transmembrane component of the SJ that was identified to physically interact with Cor and Nrx-IV(Genova and Fehon 2003). Lac is a GPI-linked protein that contains three Ig domains, homologous to the vertebrate IgLONs. *Lac* mutant animals display an enlarged tracheal phenotype that contains breaks. Llimargas et al., (2004) concluded that this change in size is not due to an increase in cell number but speculate that this is due to abnormal cell size. In addition, they suggest that abnormal cell shape contributes to abnormal force distribution that leads to loss of cell adhesion. Force distribution and cell adhesion are essential for correct cell shape changes and cell rearrangements that are required for the final form and function of tissues. A closer examination of how these lateral membrane proteins regulate fundamental cell processes will provide important insight into our understanding of development.

Coracle, Neurexin, Contactin, varicose

SJ complex proteins demonstrate a strong interdependence for SJ organization due to extensive protein-protein interactions that exist between a network of cytoplasmic, transmembrane, and GPI-linked proteins. Seminal work conducted in the laboratory of Rick Fehon provided the beginning of our understanding of the interactions of the subcellular components of the SJ. *coracle* (*cor*), which encodes a cytoplasmic organizing protein from the protein 4.1 family, was identified in a screen as a dominant modifier that suppresses the rough eye phenotypes of mutations in the *EGF-receptor homologue* (*Egfr*). While mutations in *Egfr* result in tissue overgrowth and abnormal cell differention, histological analysis showed that mutations in *coracle* mutant eyes resulted in cells that were abnormally shaped and positioned rather than abnormal growth or differentiation (Lamb et al. 1998). Cor was found to be associated with the plasma membrane at the region of the SJ (Fehon, Dawson, and Artavanis-Tsakonas 1994). Using phenotypic analysis, it was shown by Ward et al (1998) that the membrane localization of Cor was due to an interaction with the transmembrane SJ protein Neurexin-IV (NrxIV). This interaction is due to physical interactions between the CNTR of Cor and the cytoplasmic tail of Nrx. This co-dependence has become a defining characteristic of all core components of the SJ.

Later work directed at the identification of mutations that contribute to defects in tracheal development identified two additional core components of the SJ, *contactin* and *varicose. varicose* (*vari*), encodes a membrane-associated guanylate kinase (MAGUK) (Wu et al. 2007) that is homologus to the vertebrate PALS2, which localizes basolaterally in epithelial cells and is not involved in cell polarity or

paracellular barrier function (Wu et al. 2007). Using co-immunoprecipitation, Wu et al. (2007) identified a strong binding affinity between the PDZ-domain of Vari and the C-terminus of Nrx-IV, which suggests that Vari is part of the membrane scaffolding of the SJ. *contactin (cont)* which encodes a GPI-linked protein homologous to the vertebrate contactin subfamily, is required in the glial cells of the peripheral nervous system (Faivre-Sarrailh et al. 2004). Contactin was also identified to require Nrx-IV for plasma membrane localization.

This data suggests a model where Cont is localized to the extracellular surface where it is able to interact with the extracellular environment and additional transmembrane and GPI-linked SJ proteins, such as Nrx-IV, Kune, and Atpα. In addition, Cor and Vari stabilize Nrx-IVand function to organize the cytoplasmic region of the SJ, leading to the interdependence that defines core components of the SJ.

Septae Formation and Ultrastructure

Analysis using electron microscopy (EM) revealed that septae begin to form at stage 14, where they are broadly spaced or aggregate in small numbers (Tepass and Hartenstein 1994). Septa increase in density until they form a continuous band, covering up to two-thirds of the lateral membrane surface (Tepass and Hartenstein 1994). To better understand SJ biogenesis and the role of individual SJ proteins, EM analysis has been used in combination with genetic approaches. These studies indicate a two-step process for building the SJ, formation and organization. In the absence of Cont, Nrg, Lac, Sinu, or Mega, septa form but appear discontinuous and fail to cluster at the region of the SJ. In the absence of Nrx-IV, septa fail to form,

which indicates that Nrx-IVis required for septa formation. The functional integrity of the SJ can be tested by injecting a 10kD Rhodamine-labeled dextran dye into the hemocoel of stage 17 embryos. A physiologically tight SJ will prevent the passage of the dye into the lumen of tissues like the salivary gland and trachea. In SJ mutant animals, disrupted occluding function is observed when the dextran freely passes between cells, filling the lumen with dye. While many SJ genes have been characterized, there is limited information regarding changes in ultrastructure. A comprehensive analysis of tissue-specific changes to the formation and organization of septae will allow for increased understanding of how these proteins work together for the final maturation of the SJ.

Discussion

Our understanding of the function of SJ proteins has focused on their role in the organization, structure, and function of the occluding junction. While we have identified a variety of core and associated SJ components, it is likely that there are many more genes involved in the SJ that have not yet been identified. A systematic screen to identify new regulators of SJ biogenesis and maintenance could provide further understanding of the regulation of SJ biogenesis within the larger context of development. Here, I present our identification of a novel core component of the SJ called *Macroglobulin complement related* (*Mcr*) in a screen for imaginal disc morphogenesis (S. Hall et al. 2014). This gene was originally identified as playing a role in innate immunity (Stroschein-Stevenson et al. 2006), which suggests a potential connection between the SJ and immunity that has not been explored.

This large collection of cell adhesion molecules is known to localize along the lateral membrane in the middle of embryogenesis where they demonstrate mobility. It has also been identified, that SJ components are involved in vesicle trafficking that alters the mobility of core components. This regulated trafficking may be required to facilitate interactions that are specific to the occluding function or to redeploy SJ proteins within the cell when dynamic cellular and tissue-level events must take place during development or tissue repair. A subset of SJ components was shown to regulate apical-basal polarity, raising an interesting possibility that SJ proteins may function as subcomplexes prior to their incorporation in the occluding junction. Further exploration is needed to understand how these proteins interact before they assemble into highly interdependent SJ complex.

The idea of dual roles for SJ components is not isolated to Mcr. Laprise et al., (2009) showed that a collection of core SJ proteins, Cor, Nrx-IV, Nrv2, and Atpα, function redundantly with the basolateral protein Yurt to regulate the maintenance of apical-basal polarity during organogenesis before SJs have formed. In addition, mutations in *cor* and *Nrx-IV* result in defective dorsal closure (Ward et al. 1998; Baumgartner et al. 1996). These findings support the idea that SJ proteins participate in processes outside of the paracellular barrier to regulate cellular mechanisms that contribute to morphogenesis. Here I present our exploration of this idea, using a collection of well-characterized SJ mutant lines. I discuss our examination of these mutations for defects in head involution and dorsal closure. Our analysis identified a clear requirement for each of these proteins in regulating early morphogenetic events before a SJ has formed suggesting this is not simply a

pleiotropic effect of a few SJ genes. These findings open the field to a new area of exploration to understand the larger role of the lateral membrane during morphogenesis.

Section 1.1 Figures

Figure 1.1

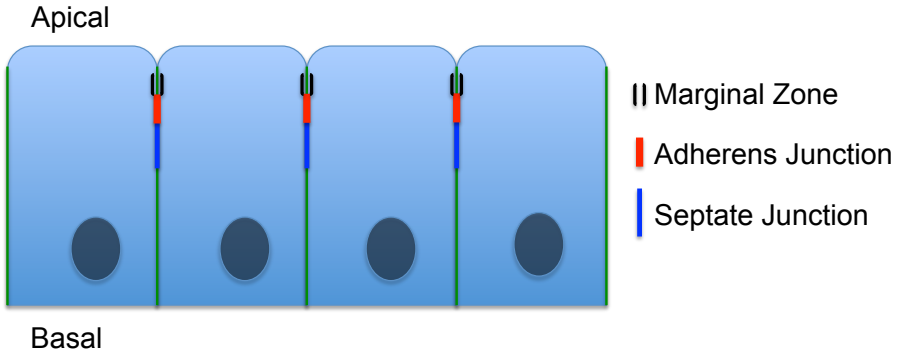

Figure 1.1 Schematic diagram of a mature epithelim A mature intact epithelium has distinct membrane regions including: apical, in contact with a unique environment; basal, maintains contact with the interior of the organism; and lateral (solid green lines). The lateral membrane contains specific regions that allow for specific functions, the marginal zone (Double black bars), adherens junction (red bars), and the SJ (blue bars).

Figure 1.2

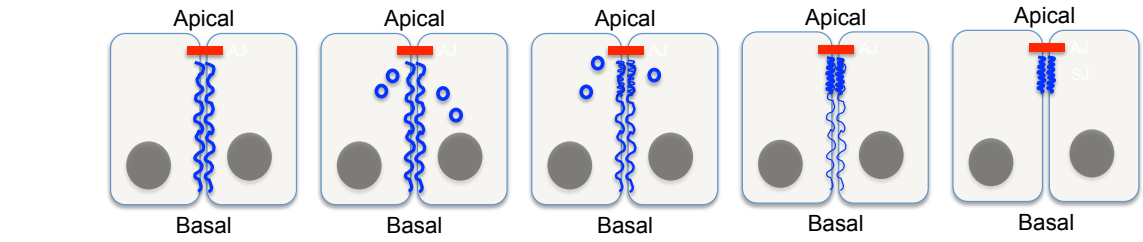

	12	13	14	15	16
SJ protein localization:	basolateral	basolateral/ endosomes	basolateral/ apical enriched	mostly apical	fully apical
Mobility in membrane:	fully mobile	becoming fixed	fixed	fixed	fixed
Barrier function:	leaky	leaky	leaky	tight	tight

Figure 1.2 SJ biogenesis requires endocytosis and recycling for maturation SJ proteins are broadly localized along the lateral membrane at stage 12. These proteins are then endocytosed and recycled at stages 13 and 14. The SJ complex becomes fixed within the plane of the membrane at stage 15 allowing for occluding function. Stage 16 marks the final maturation of the junction where mobility along the lateral membrane has decreased and the SJ is tight and functional.

Chapter II

Macroglobulin complement related (*Mcr*) encodes a protein required for septate junction organization and paracellular barrier function in *Drosophila*

The material in this Chapter has been published as "Hall, Sonia, Courtney Bone, Kenzi Oshima, Liang Zhang, Molly McGraw, Bethany Lucas, Richard G Fehon, and Robert E Ward. 2014. "Macroglobulin Complement-Related Encodes a Protein Required for Septate Junction Organization and Paracellular Barrier Function in Drosophila." *Development (Cambridge, England)* 141 (4) (February): 889–98. doi:10.1242/dev.102152. http://www.ncbi.nlm.nih.gov/pubmed/24496625."

Section 2.1 Abstract

Polarized epithelia play critical roles as barriers to the outside environment and enable the formation of specialized compartments for organs to carry out essential functions. Barrier functions are mediated by cellular junctions that line the lateral plasma membrane between cells, principally tight junctions in vertebrates and septate junctions (SJs) in invertebrates. Over the last two decades, more than 20 genes have been identified that function in SJ biogenesis in *Drosophila*, including those that encode core structural components of the junction such as Neurexin-IV, Coracle, and several claudins, as well as proteins that facilitate the trafficking of SJ proteins during their assembly. Here we demonstrate for the first time that *Macroglobulin complement related* (*Mcr*), a gene previously implicated in innate immunity, plays an essential role during embryonic development in SJ organization and function. We show that Mcr is a core component of SJs since it colocalizes with other SJ proteins in mature ectodermally-derived epithelial cells, that it shows interdependence with other SJ proteins for SJ protein localization, and that *Mcr* mutant epithelia display a defective paracellular barrier. Tissue-specific RNA interference and clonal analysis further demonstrate that *Mcr* is required cell-autonomously for SJ organization. Finally, we show a unique interdependence between Mcr and Nrg for SJ localization that suggests a higher order organization to the SJ. This characterization of *Mcr* also highlights the functional similarity between innate immunity and epithelial barrier junctions in protecting organisms by segregating self from non-self.

Section 2.2 Introduction

Polarized epithelia play critical roles as barriers to the outside world and in providing distinct compartments for organs to carry out essential metabolic functions in all metazoans. These functions require a physiologically tight epithelium to provide a barrier to the flow of small molecules between the apical and basal sides of the epithelium. This paracellular barrier is established and maintained by tight junctions (TJs) in the epithelia of vertebrate organisms, and by septate junctions (SJs) in invertebrate organisms. TJs localize along the lateral membrane in a region apical to the adherens junction and are characterized ultrastructurally as a series of anastamosing ribbons where the plasma membranes of adjacent cells are in direct opposition (Farquhar and Palade 1963). In contrast, the pleated SJs found in invertebrate epithelia localize basal to the adherens junction and are characterized by uniformly spaced rows of electron dense septa between the plasma membranes of adjacent cells (Noirot-Timothee et al., 1978). Despite these differences in subcellular localization and ultrastructure, the functional similarity and molecular conservation of key proteins including members of the claudin and membrane associated guanylate kinase (MAGUK) families, suggest that TJ and SJ are analogous structures.

The localization of cell signaling and polarity proteins to TJs and SJs also suggests that these barrier junctions play critical roles in organizing and orchestrating basic epithelial functions during development. Mutations in SJ genes in *Drosophila* strongly support this supposition. Disruption of SJs in embryonic epithelia and glia nearly always results in embryonic lethality, with characteristic

defects in epidermal cuticle, defects in the size of the developing trachea (S. Wang et al. 2006), defects in the morphogenetic process of dorsal closure (Baumgartner et al. 1996; Fehon, Dawson, and Artavanis-Tsakonas 1994; Woods, Wu, and Bryant 1997), and embryonic paralysis due to a disrupted blood brain barrier (Baumgartner et al. 1996).

Genetic studies in *Drosophila* have identified more than twenty genes that function in the establishment or maintenance of SJs. The core constituents of the SJ include transmembrane proteins of the claudin family (Behr, Riedel, and Schuh 2003; Nelson, Furuse, and Beitel 2010; Wu et al. 2004), Neurexin IV (Nrx-IV;Baumgartner et al., 1996), Contactin (Cont) (Faivre-Sarrailh et al. 2004), Lachesin (Llimargas et al. 2004), Neuroglian (Nrg), Gliotactin and the α and β subunits of the Na+/K+ ATPase (Genova and Fehon 2003), the GPI-linked protein Melanotransferrin (also known as Transferrin 2, Tsf2) (Tiklová et al. 2010)and the cytoplasmic proteins Coracle (Cor) (Fehon, Dawson, and Artavanis-Tsakonas 1994) and Varicose (Wu et al. 2007). A second group of proteins is required for SJ assembly, but the proteins do not physically reside in the junction. This group includes several members of the Ly6 family of proteins (Hijazi et al. 2009; Nilton et al. 2010), as well as proteins that function in endocytosis and recycling such as Clathrin heavy chain, Dynamin, Rab5 and Rab11 (Tiklová et al. 2010).

The biogenesis of SJs is a multistep process involving the synthesis and secretion of membrane resident SJ proteins, followed by endocytosis and recycling of these proteins to the apical lateral plasma membrane during mid embryogenesis (Tiklová et al. 2010). The final refinement of the SJ requires that each member of the

core complex is present, suggesting that the SJ is a large, stable, and highly crosslinked protein complex. This was first appreciated when Ward et al. (1998) showed that Nrx-IV and Cor physically interact, and that correct localization of each protein to the SJ required the presence of the other protein. Other studies revealed the interdependence of additional SJ proteins in the establishment of the intact junction (for example Behr et al., 2003; Faivre-Sarrailh et al., 2004; Genova and Fehon, 2003; Paul et al., 2003; Tiklova et al., 2010). Recent experiments using Fluorescence Recovery After Photobleaching (FRAP) revealed that SJ proteins are essentially fixed in the membrane by stage 14 of embryogenesis (Laval, Bel, and Faivre-Sarrailh 2008; Oshima and Fehon 2011). Mutations in any core SJ gene increases the mobility of other SJ proteins at stage 14, further demonstrating the highly stable and interdependent nature of the SJ complex. Of particular note, Oshima and Fehon (2011) observed cells at stage 13 that showed stable SJ along a membrane with one neighbor, but dynamic SJ mobilities along a membrane with a different neighbor, suggesting that stable SJs require interactions between cells and not just in the plane of the membrane. The identity of the protein(s) that form the intercellular "glue" is currently unknown.

Here we identify a role for *Macroglobulin complement related* (*Mcr*) during SJ biogenesis. Mcr belongs to a family of thioester-containing proteins (TEPs) that are conserved in nearly all multicellular organisms, and primarily serve functions related to innate immunity (Medzhitov and Janeway 2002). There are 6 TEPs encoded in the *Drosophila* genome, of which *Mcr* is annotated as *TEP6*. Five of them, including *Mcr,* are expressed in larval hemocytes (Bou Aoun et al. 2011), suggesting

a role in innate immunity. In addition, Stroschein-Stevenson et al. (2006) identified *Mcr* in an RNAi screen of genes required for the phagocytosis of *C. albicans*. Our experiments demonstrate for the first time that a member of the TEP protein family plays an additional essential developmental role in insects. We show that *Mcr* is required for embryonic processes that require intact SJs. Consistent with this observation, *Mcr* mutant epithelial tissues have defective SJ organization and function. We demonstrate that Mcr is a core structural component of epithelial SJs as it colocalizes with other SJ proteins in ectodermal epithelial cells, and its subcellular localization is interdependent with other SJ proteins. These studies also highlight an intriguing connection between epithelial barrier function and the innate immune response in insects.

Section 2.3 Results

Identification and Characterization of *Macroglobulin complement related* (*Mcr*) mutations

We recovered an EMS-induced allele in *Macroglobulin complement related* (*Mcr*) from a genetic screen of mutations that dominantly enhanced the malformed leg phenotype associated with a hemizygous mutation in *broad* (br^1) (originally referred to as *E(br)155*, but hereafter referred to as Mcr^1; Ward et al., 2003). *Mcr* encodes a 1760 amino acid protein with α-2-macroglobulin and LDL receptor class A domains, and a predicted C-terminal transmembrane domain (amino acids 1726 and 1745, with ~90% probability according to TMHMM; Krogh et al. 2001) (Fig. 1A). The Mcr^1 allele results from a CG to TA transition at nucleotide 8,079,766 of Genbank sequence AE014134.5, generating a Ser^{282} to Leu substitution in the conserved α-2-macroglobulin N-terminal domain (Fig. 2.1A). We obtained a molecularly-defined deficiency (*Df(2L)Exel7034*) that uncovers the *Mcr* locus and a lethal *P*-element insertion that is inserted 24 nucleotides downstream of the transcription start site of *Mcr* ($P\{EPgy2\}Mcr^{EY07421}$; Fig. 1A). We generated a set of *P*-excision alleles from $Mcr^{EY07421}$, including a number of precise excisions that were adult viable indicating that there are no second-site lethal mutations on the $Mcr^{EY07421}$ chromosome. We characterized one of the imprecise excision alleles (Mcr^{Pex9}).

Lethal phase and phenotypic analyses revealed that *Mcr* is required during embryogenesis. All mutant combinations in *Mcr* display 95-100% embryonic lethality, with nearly completely penetrant defects in ventral denticle belt

deposition, deposits in the region of the salivary glands and convoluted tracheae, and lesser penetrant defects in dorsal closure (Fig. 2.1 and Supplemental Table 2.1). Ubiquitous expression of *UAS-Mcr-RNAi* (via *Actin-GAL4* and *daughterless-GAL4*) recapitulated all of the mutant phenotypes associated with the *Mcr* alleles, whereas tracheal-specific expression of *Mcr-RNAi* (using *breathless(btl)-GAL4*) recapitulated the tracheal length defects (Fig. 2.1E and data not shown). Taken together, these results indicate that loss of *Mcr* is responsible for all of these phenotypes.

Mcr is required for septate junction organization and function

As the suite of phenotypes observed in *Mcr* mutant animals is commonly found with mutations in other genes that function in the SJ (Lamb et al. 1998; Llimargas et al. 2004; Paul et al. 2003; Tiklová et al. 2010; Wu et al. 2004; Wu et al. 2007), we examined the organization and function of SJs in embryonic epithelia of *Mcr* mutant animals. In the ectodermal epithelia of stage 16 wild type embryos, the SJ is localized to the apical part of the lateral membrane in a region basal to the adherens junction, and can be visualized by the localization of core SJ proteins including Cor (Fig. 2.2A). Consistent with a defect in SJ organization, Cor is mislocalized in the salivary glands, hindguts and tracheae of *Mcr* mutant stage 16 animals (Figs. 2C–J, and data not shown). Interestingly, the mislocalization of Cor is more pronounced in the hindguts than in the salivary glands, and Mcr^{1} shows a stronger phenotype in the salivary glands than the other *Mcr* mutations (Figs. 2.2C–J). The correct localization of marginal zone (Crumbs; Figs. 2.2C, G, E and I) and adherens junction (Armadillo and α-Catenin; data not shown) proteins in *Mcr* mutant embryos indicates that *Mcr* is not required for overall apical/basal polarity.

In order to test the barrier function of the SJs, we injected a 10 kD rhodamine-labeled dextran into the hemocoel of stage 17 wild type and *Mcr* mutant embryos (Lamb et al. 1998). In wild type embryos, the SJs are physiologically tight by this stage, which prevents the infiltration of the labeled dextran into the lumen of the trachea (Fig. 2.2K'). In stage 17 Mcr^{1} mutant embryos, the dextran freely passes between tracheal cells, filling the lumen with dye (Fig. 2.2L'). Taken together, these results indicate that *Mcr* is required to establish or maintain a physiologically tight SJ in *Drosophila* embryonic epithelia.

Mcr is expressed in ectodermal epithelia and localizes to SJs

Developmental northern blot analysis revealed *Mcr* transcripts in 0-2 hour embryo lysates, suggesting a maternal contribution of *Mcr*. Subsequently, *Mcr* levels are reduced in 2-4 hour embryo lysates, but rise and peak between 4-12 hours of embryogenesis, after which transcript levels are strongly reduced (Fig. 2.3A). We generated a polyclonal antibody against a non-conserved region of Mcr (indicated in Fig. 2.1A). Consistent with the predicted molecular mass of 203 kDa, we observe an ~ 225 kDa band from embryonic and imaginal disc lysates from wild type and Mcr^{1} mutant animals that is substantially reduced in lysates derived from $Mcr^{EY07421}$, Mcr^{Pex9} and *Df(2L)Exel7034* late embryos (Supplemental Fig. 2.1A). On tissues, the antiserum recognizes a protein expressed in wild type and Mcr^{1} stage 16 embryos that is strongly reduced in $Mcr^{EY07421}$ and nearly absent in stage 16 Mcr^{Pex9} and *Df(2L)Exel7034* mutant embryos (Supplemental Figs. 2.1B-F). Taken together, these results indicate that the serum is specific for Mcr.

In wild type embryos, Mcr protein is expressed in ectodermally-derived epithelia including the epidermis, salivary glands, trachea, and fore- and hindgut, where it is associated with the plasma membrane (Figs. 2.3B–E). We first detect membrane-associated Mcr in some stage 9 embryos (data not shown), with strong expression apparent by stage 11 (Fig. 2.3B). At stage 13 Mcr is broadly localized along the basolateral membrane (Fig. 2.3C), and by stage 14 is enriched at the apical lateral membrane in the region of the SJ (Fig. 2.3D). In stage 16 epithelia, Mcr is refined to the region of the SJ, where it colocalizes with other SJ proteins including Cor (Fig. 2.3E).

Mcr protein is also strongly expressed in imaginal discs and larval hemocytes (Figs. 2.3F–H, and data not shown), consistent with the RNA expression patterns reported by Bou Aoun et al. (2011). In imaginal discs, Mcr localizes along the apical lateral membrane in disc proper cells and in the peripodial epithelium (Figs. 2.3F–H). Although the majority of Mcr co-localizes with Cor in imaginal discs, we note that Cor extends further basally than Mcr in these cells, and that Mcr is expressed in an apical domain independent of Cor (outset in Fig. 2.3H). This apical Mcr domain appears to be on the apical surface since it does not colocalize with adherens junction proteins including α-Catenin and Armadillo, but does colocalize with the apical plasma membrane protein Uninflatable (Supplemental Figs. 2.2A–C). In addition, when we incubate wing imaginal discs with antibodies against Mcr prior to fixation, we observe an apical localization of Mcr in peripodial epithelial and disc proper cells, indicating that this pool of Mcr is expressed on the cell surface and does not represent an endosomal compartment (Supplemental Figs. 2.2D, E).

In the ovary, Mcr is expressed in the germarium, the ovarian follicle cells and in germ cells. In the germarium, Mcr shows the highest level of expression in region 1, where neither Fasciclin 3 (Fas3) nor Cor are strongly expressed (Fig. 2.3I, and data not shown). Mcr is also strongly expressed in the polar follicle cells where it colocalizes with Fas3 (Fig. 2.3I). Mcr staining remains strong in the border cells as they migrate through the germ cells (data not shown). Finally, Mcr is expressed at low levels in the germ cells where Cor and Fas 3 are nearly absent.

The SJ localization of Mcr depends on other core SJ proteins

Proteins involved in SJ biogenesis typically display an interdependence, in which the loss of any SJ protein results in the mislocalization of other SJ proteins. We therefore examined the localization of Mcr in stage 16 embryonic hindguts and salivary glands from animals with mutations in several SJ genes and compared the localization to that of Cor as a readout of SJ organization (Fig. 2.4). Mcr is mislocalized in the hindguts of every mutation we examined (*Cont*^{ex956}, *cor*^{4}, *crok*^{KG06053}, *kune*^{c309}, *nrv2*^{ZCL1649}, *Nrx-IV*^{4304}, *pck*^{G0012}, *sinu*^{nwu7}, and *Tsf*^{KG01571}; Figs. 2.4B–E, and data not shown). In general the mislocalization of Mcr is coincident with a mislocalization of Cor. One notable exception is in *Tsf*^{KG01571} mutant embryos, in which Mcr is not only mislocalized along the basolateral domain, but is also strongly enriched on the apical membrane, whereas Cor is only mislocalized along the basolateral domain (Fig. 2.4E). We occasionally noticed situations in which although both proteins were mislocalized along the lateral membrane, Mcr appeared to be more enriched in the region of the SJ than Cor (for example in Fig. 2.4D, the apical lateral membrane in *Crok* mutant hindguts is red biased in the 2-color image,

whereas the basal lateral membrane is green biased). Mcr and Cor are also similarly mislocalized in the salivary glands of all these mutant animals, however the degree of mislocalization is often less extreme than in hindguts. For example, both Mcr and Cor are primarily mislocalized along the lateral membrane in *sinu*^{nwu7} mutant salivary glands, with some residual enrichment of both proteins in the region of the SJ (Fig. 2.3F), whereas Mcr and Cor show mostly correct localization in the salivary glands of *crok*^{KG06053} mutant embryos, with only a slight degree of lateral mislocalization (Fig. 2.4G), even as both proteins are more severely mislocalized in the hindguts of these animals (Fig. 2.4D, and data not shown).

We next performed fluorescence recovery after photobleaching (FRAP) analysis to examine the mobility of the core SJ protein Nrx-IV (as Nrx-IV-GFP) in the epidermis of stage 15 *Mcr*^{EY07421} mutant animals. Oshima and Fehon (2011) observed that core SJ proteins (including Nrx-IV) display extremely slow recovery kinetics when photobleached in the epidermis of wild type embryos, but show vastly increased mobility in the epidermis of embryos homozygous for most SJ mutations. As shown previously for other genes encoding core SJ components (Oshima and Fehon 2011), stage 15 *Mcr*^{EY07421} mutant embryos displayed rapid recovery of Nrx-IV-GFP after photobleaching in the epidermis (Fig. 2.4H; compare to Fig. 2.7C in Oshima and Fehon, 2011). Given the strong localization of Mcr at SJs in wild type tissues, the mislocalization of Mcr in animals with mutations in other SJ genes and the effect of Mcr loss on Nrx-IV mobility, we conclude that Mcr is a core component of epithelial SJs.

Mcr is required cell autonomously for SJ structure and function

Given the precedent of Boudin as a SJ protein that functions non cell-autonomously (Hijazi et al. 2009), and the observation that *Mcr* is secreted from S2 cells (Stroschein-Stevenson et al. 2006), we sought to determine whether *Mcr* is required cell autonomously for SJ organization by using tissue-specific RNA interference (RNAi) and clonal analysis. We expressed *Mcr-RNAi* in posterior cells in each segment of the embryonic epidermis using *engrailed(en)-GAL4* and examined stage 16 embryos for Mcr, Cor and En expression by confocal microscopy (Figs. 2.5A, B and Supplemental Fig. 2.3A). Mcr protein was strongly reduced specifically in the En^{+} cells (Supplemental Fig. 2.3), whereas Cor was expressed at wild type levels. Confocal z-sectioning revealed that Cor extended more basally along the lateral membranes in *Mcr-RNAi* cells and was less enriched apically (Fig. 2.5C), suggesting a disruption of SJ organization in these cells. We next expressed *Mcr-RNAi* in the dorsal compartment of the wing imaginal disc using *apterous(ap)-GAL4*. Consistent with the previous result, Mcr protein is strongly reduced specifically in the cells expressing *Mcr-RNAi* (Supplemental Fig. 2.3B), whereas Cor is expressed at normal levels and is not enriched in the region of the SJ (Fig. 2.5D). To examine the SJ functionally we injected 10 kDa rhodamine-dextran into the hemocoel of late 3rd instar w^{1118} and *ap>Mcr-RNAi* animals and examined the wing imaginal discs for the presence of labeled dextran. We did not observe labeled dextran in the lumen between the disc proper cells and the peripodial epithelium in the wild type discs, but the *ap>Mcr-RNAi* discs rapidly filled with dye, indicating a functional disruption of the SJ in these cells (Supplemental Fig. 2.3). The residual Mcr protein found in the *Mcr-RNAi* cells is not uniformly localized around the cell, but is instead enriched

along the border between a cell and one or two of its neighbors (Fig. 2.5D). These persistent Mcr-containing clusters are also enriched apically in the cell, typically in a region that would correspond to the SJ (Fig. 2.5E). To complement these studies, we generated $Mcr^{EY07421}$ mitotic clones in late third instar wing imaginal discs and examined Cor localization by confocal z-series to assess SJ organization. Again we observed that Cor was no longer apically enriched along the lateral membrane in the homozygous mutant tissues, but instead was evenly distributed along the lateral membrane (Fig. 2.5F). Taken together, these results indicate that Mcr is required cell autonomously for SJ organization.

Mcr requires *Nrg* for maintenance at the SJ

While conducting experiments to examine Mcr and Cor localization in imaginal discs expressing SJ-RNAi transgenes in the dorsal wing compartment, we noticed that *UAS-Dcr-2;ap>Nrg-RNAi* had a nearly identical phenotype to that observed in *UAS-Dcr-2;ap>Mcr-RNAi* (Figs. 2.6A–C; compare to Figs. 2.5C–E). Specifically, Mcr is strongly reduced and Cor loses its apical enrichment in dorsal cells expressing *Nrg-RNAi*. Interestingly, the loss of Mcr in *Nrg-RNAi* cells included both the SJ-associated Mcr as well as that expressed on the apical plasma membrane (Fig. 2.6C). The Mcr protein that was expressed in these cells aligned with membranes at the boundary of neighboring cells and was apically enriched, similar to that seen in *Mcr-RNAi* cells. To extend these observations, we examined Mcr localization in embryos mutant for a strong loss of function allele of *Nrg* (Nrg^{17}). In stage 16 Nrg^{17} embryos, we observed essentially no Mcr in any ectodermal epithelia cell (Fig. 2.6D). Examining earlier *Nrg* mutant embryos revealed that Mcr was

expressed and appeared to show some membrane localization at stage 11 (Fig. 2.6E), but by stage 15 had largely disappeared from the lateral membrane and was mainly enriched on the apical surface (Fig. 2.6F).

Section 2.4 Discussion

In this report we have identified an essential developmental role for *Macroglobulin complement related* (*Mcr*) for the establishment and/or maintenance of epithelial septate junctions. From these studies we conclude that Mcr is a core structural component of the junction, and that it is required cell autonomously for SJ organization. Since *Mcr* is expressed in larval hemocytes and has been implicated in innate immunity, we also comment on a connection between SJ biogenesis and innate immunity.

Mcr in SJ organization

Five pieces of evidence indicate that Mcr is a core component of epithelial SJs. First, Mcr localizes to the SJ in embryonic and imaginal epithelia, where its pattern of localization during embryonic development mirrors that of other core SJ proteins (Fig. 2.3). Second, loss of function mutations in *Mcr* (including RNAi) disrupt the organization of SJs as demonstrated by the mislocalization of other core SJ proteins (Fig. 2.2). Third, *Mcr* mutant animals fail to establish an effective paracellular barrier in embryonic tracheae (Fig. 2.2). Fourth, loss of function mutations in other core SJ genes results in the mislocalization of Mcr coincident with Cor (Fig. 2.4). Finally, FRAP analysis indicated that the mobility of the core SJ protein Nrx-IV in $Mcr^{EY07421}$ mutant epidermal cells is similar to that observed in mutations in other core SJ genes (Fig. 2.4).

Since Mcr has been shown to be secreted from S2 cells (Stroschein-Stevenson et al. 2006), we wondered if Mcr may be secreted from epithelial cells and thus

serve a non cell-autonomous role in SJ organization. We therefore examined SJ organization in embryonic and imaginal epithelia in which we could experimentally create a sharp boundary of Mcr expressing and non-expressing cells. Using both RNA interference and clonal analysis, we observed that Cor was mislocalized in all *Mcr* mutant cells (Fig. 2.5), indicating a cell-autonomous role for Mcr in SJ organization. At the dorsal-ventral boundary we noted that Mcr expression was substantially reduced in many wild type cells just at the membrane in contact with *Mcr-RNAi* cells (Fig. 2.5), suggesting that the disrupted SJ in the *Mcr-RNAi* cells had a non-cell autonomous effect on the wild type cells. A similar observation was made by Genova and Fehon (2003), who noticed that Nrx-IV is strongly reduced in wild type cells at the membrane in contact with cor^{5} mutant cells in wing imaginal disc clones.

Mcr was not completely absent from cells expressing *Mcr-RNAi*. Rather, the majority of residual Mcr accumulated at high levels along distinct cell-cell contacts, and maintained an apical enrichment in a region that would correlate with the SJ (Fig. 2.5), raising the possibility of a residual SJ complex or subcomplex at these membranes. This may not be surprising in light of FRAP analyses in imaginal discs showing that SJ complexes persist even in cells undergoing mitosis (Oshima and Fehon 2011), and so it may take considerable time for an established junction to completely disintegrate. Alternatively, Mcr may play a role in the initial establishment of SJ and the residual Mcr found in these cells (likely via incomplete RNA interference) may represent an attempt to organize the remaining SJ proteins into a junction.

The results presented here also highlight a unique interdependence between *Mcr* and *Nrg* for proper SJ localization of each other. Mcr is localized both at the SJ and on the apical membrane (Supplemental Fig. 2.2), and mutations in *Nrg* alter the relative distribution of Mcr to these locations. Specifically, Mcr can be found at the lateral membrane in stage 11 *Nrg* mutant embryos, but is predominantly apical localized in the epithelia of animals through stage 15, after which it largely disappears (Fig. 2.6). Nrg is also expressed on both the apical plasma membrane and the SJ (as indicated by the GFP protein trap line Nrg^{G00305}, S. Hall and R. Ward, unpublished). Bätz et al. (submitted) observed a similar alteration of Nrg distribution in *Mcr* mutant animals, in which Nrg is predominately at the apical domain at the expense of its SJ localization. We also noted that Mcr was enriched apically in *Tsf2* mutant embryos, whereas Cor was only mislocalized along the lateral domain (Fig. 2.4), and have recently observed that Nrg is also apically enriched in *Tsf2* mutant embryos (S. Hall and R. Ward, unpublished), raising the possibility that *Mcr*, *Nrg* and *Tsf* may all work together to ensure proper localization of Mcr and Nrg. Further experiments are necessary to understand how these genes interact to ensure correct distribution of each protein to the SJ.

These studies also indicate that the SJ may not be as monolithic as previously thought with every protein completely dependent upon each other for proper localization. Rather, the SJ may be composed of subcomplexes that may show remarkable interdependence among their members, but less dependence on other subcomplex members. In this regard we noted situations in which Cor was more strongly mislocalized than Mcr (Fig. 2.4) indicating that they may be in distinct

subcomplexes. Similar suggestions about the organization of SJ have been made in the past (Nelson, Furuse, and Beitel 2010).

Mature SJs are composed of more than a dozen membrane and cytoplasmic proteins that appear to form a highly stable and crosslinked structure in the plane of membrane. FRAP analyses by Oshima and Fehon (2011) indicated that stable SJs require interactions between cells and not only within the plane of the membrane. The nature of the extracellular "glue" that holds SJ complexes together between cells is unknown. We propose that Mcr may function to organize the extracellular components in the SJ, potentially even as this intercellular "glue". Four lines of evidence motivate this speculation. First, the potential cytoplasmic domain of Mcr is only 15 amino acids and has no conserved protein motifs, reducing the possibility that it interacts with other core SJ proteins. Second, the plasma membrane in wild type cells at the boundary between Mcr expressing and non-expressing cells often has substantially reduced Mcr expression (Fig. 2.5). Third, we noticed strong residual Mcr protein expression in *Mcr-RNAi* cells at the boundary between two cells (Fig. 2.5), raising the possibility that some form of intact SJ complex or subcomplex has been retained at this cell-cell contact. Finally, biochemical analysis indicates that α-2-macroglobulin proteins can form homodimers and homotetrameres. In vertebrate and some invertebrate organisms, α-2-macroglobulins exist as a homotetramer consisting of two noncovalently attached cysteine-bridged homodimers (Bender and Bayne 1996; Sottrup-Jensen et al. 1989), while in many invertebrates the serum soluble form is a homodimer (Quigley and Armstrong, 1994). Interestingly, Mcr^{1} encodes a full-length protein that is membrane associated,

but is defective in SJ organization. *Mcr*^{1} produces a Ser^{282} to Leu substitution in the α-2-macroglobulin N-terminal domain. Ser^{282} is highly conserved in all insect species, even as adjacent amino acids are divergent. There are four positively charged amino acids within 10 residues on either side of Ser^{282}. It is possible that ionic interactions between the A2M_N domains of Mcr proteins linked to opposing cells may facilitate the adhesion of SJ complexes between cells. Additional experiment will be necessary to test this idea.

Mcr in innate immunity

Protein sequence analysis places Mcr in the thioester-containing protein (TEPs) family. In vertebrates, TEPs include complement proteins that serve innate immune functions (Medzhitov and Janeway 2002) as well as α-macroglobulins, which function as broad range protease inhibitors (Armstrong and Quigley 1999). There are 6 TEPs encoded in the *Drosophila* genome, five of which (including *Mcr*) are expressed in larval hemocytes (Bou Aoun et al. 2011), suggesting a role in innate immunity. We confirmed that Mcr is expressed in larval hemocytoes (S. Hall and R. Ward, unpublished). The thioester motif conserved in nearly all TEPs is a four amino acid sequence (CGEQ) that can form a covalent attachment to microbes. Curiously, Mcr contains a serine in place of the cysteine in the conserved thioester motif suggesting a novel function for Mcr. Nevertheless, using an S2 cell assay with GFP-labeled *Candida albicans*, Stroscheim-Stevenson et al. (2006) identified *Mcr* in an RNAi screen of genes required for the phagocytosis of *C. albicans*. The authors also demonstrated that Mcr is secreted from S2 cells (which have a hemocyte origin).

Recently, Mudiganti et al. (2010) conducted a genome-wide expression analysis on S2 cells infected with the alphavirus Sindbis and found that both *TEP II* and *Mcr* were significantly upregulated five days post infection. Together, these observations suggest a role for *Mcr* in innate immunity. Perhaps Mcr expressed in hemocytes plays a primary role in the surveillance of pathogens in the hemocoel, which is in contact with the basal surfaces of all ectodermal epithelia, whereas Mcr expressed on the apical plasma membrane of ecdotermal cells can provide a similar function in those compartments in direct contact to the outside world.

The encapsulation response of larval hemocytes suggests another connection between *Mcr* and innate immunity. Larval hemocytes are remarkably versatile cells in the innate immune response (reviewed in Williams, 2007). They circulate through the hemolymph, recognizing and engulfing invading microorganisms, and secrete anti-microbial peptides to further protect the animal. When they encounter a foreign invader that is too large to engulf, for example a parasitic wasp egg, they initiate an encapsulation program to protect the larva. Encapsulation involves the coordinated assembly of adherent hemocytes into a polarized epithelium around the invading organism, followed by degranulation of crystal cells into the encapsulated compartment (Russo et al., 1996). The encapsulation epithelium expresses SJ proteins including Nrg and Cor (Williams, 2009; Williams et al., 2005), and has ultrastructural characteristics of a fully formed SJ (Russo et al., 1996). Although it has not been demonstrated to be physiologically tight, the ultrastructure strongly suggest that it provides a paracellular barrier to the epithelium, presumably to protect the larval internal organs from collateral damage from

destructive agents secreted onto the invading organism. Thus larval hemocytes can be thought of as “pro-epithelial” cells, capable of a mesenchymal to epithelial transition. Ultimately this pro-epithelial function of hemocytes is similar to that of the ectodermally derived epithelia of the embryo (all of which are all in contact with the outside world) in physiologically partitioning self from non-self, highlighting an interesting evolutionary connection between epithelial biology and innate immunity.

Section 2.5 Materials and Methods

Drosophila strains

Mcr^{1} is an EMS induced mutation on the *E(br)155* chromosome reported in (Ward et al., 2003). We recombined *PBac{PB}CG43322*^{c06748} onto the *Mcr*^{1} chromosome in order to remove the linked *uif*^{1} allele (Zhang and Ward, 2009). *P{EPgy2}*^{EY07421} (hereafter *Mcr* ^{EY07421}) was obtained from the Bloomington *Drosophila* Stock Center (Bloomington, IN). The *P* element in *Mcr* ^{EY07421} was mobilized by crossing to *TM3, ry Sb Ser Δ2-3/Df(3R)C7, ry* and precise and imprecise excisions were obtained and balanced over *CyO, P{w*$^{+}$*, Dfd-EYFP}* (Le et al., 2006). One imprecise excision, *Mcr*^{Pex9}, was used for subsequent lethal phase and phenotypic analyses. *UAS-Mcr-RNAi* (v100197) and *UAS-Nrg-RNAi* (v107991) strains were obtained from the Vienna *Drosophila* RNAi Center (VDRC, Vienna, Austria; Dietzl et al., 2007). *Df(2L)Exel7034*, *breathless*(*btl*)-*Gal4*, *apterous*(*ap*)-*Gal4*, *daughterless*(*da*)-*Gal4*, *engrailed*(*en*)-*Gal4*, *actin*(*act*)-*Gal4*, *UAS-Dcr-2* (on the X chromosome), *crok*^{KG6053}, *kune*^{c309}, *Nrg*^{17}, *Nrx-IV*^{4304}, *nrv2*^{ZCL1649}, *pck*^{G0012}, *sinu*^{nwu7}, and *Tsf*^{KG01571} were obtained from the Bloomington *Drosophila* Stock Center. *Cont*^{ex956} was obtained from M. Bhat (University of North Carolina, Chapel Hill, North Carolina). *Mcr*^{1}, *Mcr*^{EY07421}, *Mcr*^{Pex9}, *nrv2*^{ZCL1649}, *actin-Gal4*, *ap-Gal4*, *btl-Gal4*, *en-GAL4* and *Df(2L)Exel7034* were balanced with *CyO, P{w*$^{+}$*, Dfd-EYFP}* and *Nrx-IV*^{4304} was balanced with *TM6B, P{w*$^{+}$*, Dfd-EYFP}* to allow for unambiguous identification of embryos. *Tsf*, *crok*, *kune*, *pck*, and *sinu* mutant embryos were identified by convoluted tracheae and mislocalization of Cor in hindguts. *Nrg*^{17} was identified by absence of immunostaining by Nrg specific antibodies. All *Drosophila* stocks were

maintained on media consisting of corn meal, sugar, yeast, and agar in incubators maintained at a constant temperature of 21°C or in a room that typically fluctuated between 21°C and 22.5°C. Genetic experiments were conducted in incubators controlled at a constant temperature of 25ºC.

Phenotypic analyses

Non-hatched embryos from the lethal phase analyses were mounted on microscopes in Hoyer's medium. Photomicrographs of the cuticle preparations were collected on a Nikon Eclipse 80*i* compound microscope equipped with a Photometrics CoolSNAP *ES* high performance digital CCD camera, and adjusted for brightness and contrast with Adobe Photoshop (versions CS3-6, San Jose, CA). Figures were compiled in Adobe Illustrator (version CS6, San Jose, CA).

Generation of anti-Mcr antibodies

We amplified nucleotides 1101 to 2091 of LD23292 (representing amino acids 321-650 of Mcr) by PCR with primers containing 5' NdeI and 3' XhoI linkers, and cloned them into an NdeI/XhoI cut pDZ1 plasmid (Estrada et al., 2009). The plasmid was transfected into *E.Coli* BL21 (DE3) cells from which the protein was overexpressed. The His-tagged Mcr protein was solubilized in binding buffer (20mM Tris-HCl pH8.0 500mM NaCl, 5mM Imidazole) with 6M urea, and purified through Ni^{2+} affinity chromatography. Purified protein (which formed a precipitate upon dialysis in PBS) was used for antibody generation in guinea pigs and rats at the Pocono Rabbit Farm and Laboratory Inc. (PRF&L, Canadensis, PA).

Immunostaining, dye exclusion experiments and FRAP analysis

Embryos and imaginal discs were fixed and processed for antibody staining as described (Fehon et al., 1991). Embryonic staging was determined by gut morphology. The following primary antibodies were used at the given dilutions for immunostaining: guinea pig anti-Mcr (described above) 1:400, mouse anti-Cor (clones C556.9 and C615.16 from the Developmental Studies Hybridoma Bank at the University of Iowa, Iowa City, IA) 1:50, guinea pig anti-Cor 1:2,000, mouse anti-Crb (clone Cq4 concentrate, DSHB) 1:100, mouse anti-Fasciclin 3 1:300 (clone 7G10, DSHB), mouse anti-Nrg (clone BP 104, DSHB) and rabbit anti-GFP (Clontech, Mountain View, CA) 1:1000. Rhodamine-labeled wheat germ agglutinin (WGA; Molecular Probes/Life Technologies) was used at 1:400. Secondary antibodies were obtained from Jackson ImmunoResearch Laboratories (West Grove, PA) and used at 1:800. Confocal images were acquired either on an Olympus FV1000 confocal microscope (Olympus America, Inc, Center Valley, PA) equipped with Fluoview software or a Zeiss LSM510 Meta Laser Scanning Confocal Microscope (Carl Zeiss Inc, Thornwood, NY). Photomicrographs were cropped and rotated, and x-z renderings of confocal z-series stacks were performed in ImageJ (Schneider et al., 2012). Figures were compiled in Adobe Illustrator (version CS6). Dye exclusion experiments to test the integrity of tracheal septate junctions were performed as described (Lamb et al., 1998). Fluorescence Recovery After Photobleaching was performed as described (Oshima and Fehon, 2011).

Section 2.6 Figures

Figure 2.1

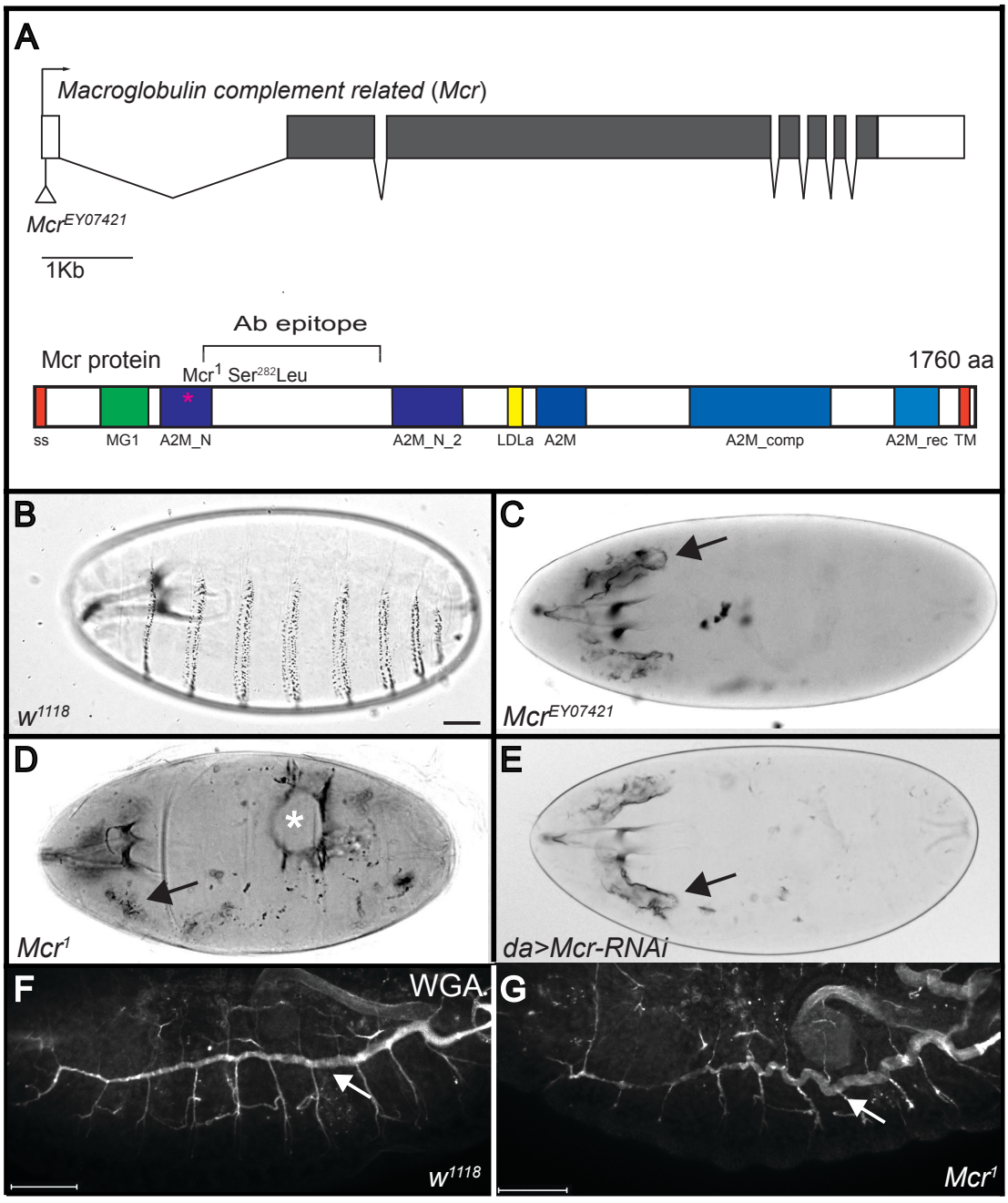

Figure 2.1 Mutations in *Mcr* are embryonic lethal with phenotypes associated with SJ defects. (A) Schematic of the Mcr gene and Mcr protein. The insertion site of $Mcr^{EY07421}$ and the amino acid substitution in Mcr^{1} are shown. The region of Mcr used for antibody generation is indicated by a bracket. Ss, signal sequence; MG1, alpha-2macroglobulin MG1 domain; A2M_N, MG2 domain; A2M_N_2, alpha-2-macroglobulin family N-terminal region; LDLa, low-density lipoprotein receptor A domain; A2M, alpha-2-macroglobulin family; A2M_comp, alpha-2-macroglobulin receptor; TM predicted transmembrane domain. (B-E) Cuticle preparations of a w^{1118} (wild-type) late embryo (B) and $Mcr^{EY07421}$ (C), Mcr^{1} (D) and *da-GAL4>UAS-Mcr-RNAi* (E) mutant embryos. Anterior is left and dorsal is up or facing. Note the dorsal hole in the Mcr^{1} embryo (asterisk in D) and the ectopic salivary gland deposition in mutant animals (arrows in C-E). (F,G) Confocal optical sections of stage 17 w^{1118} (F) and Mcr^{1} mutant (G) embryos stained with Rhodamine-labeled wheat germ agglutinin (WGA), showing a highly convoluted trachea (arrows) in the Mcr^{1} animal. Scale bars: 100um.

Figure 2.2

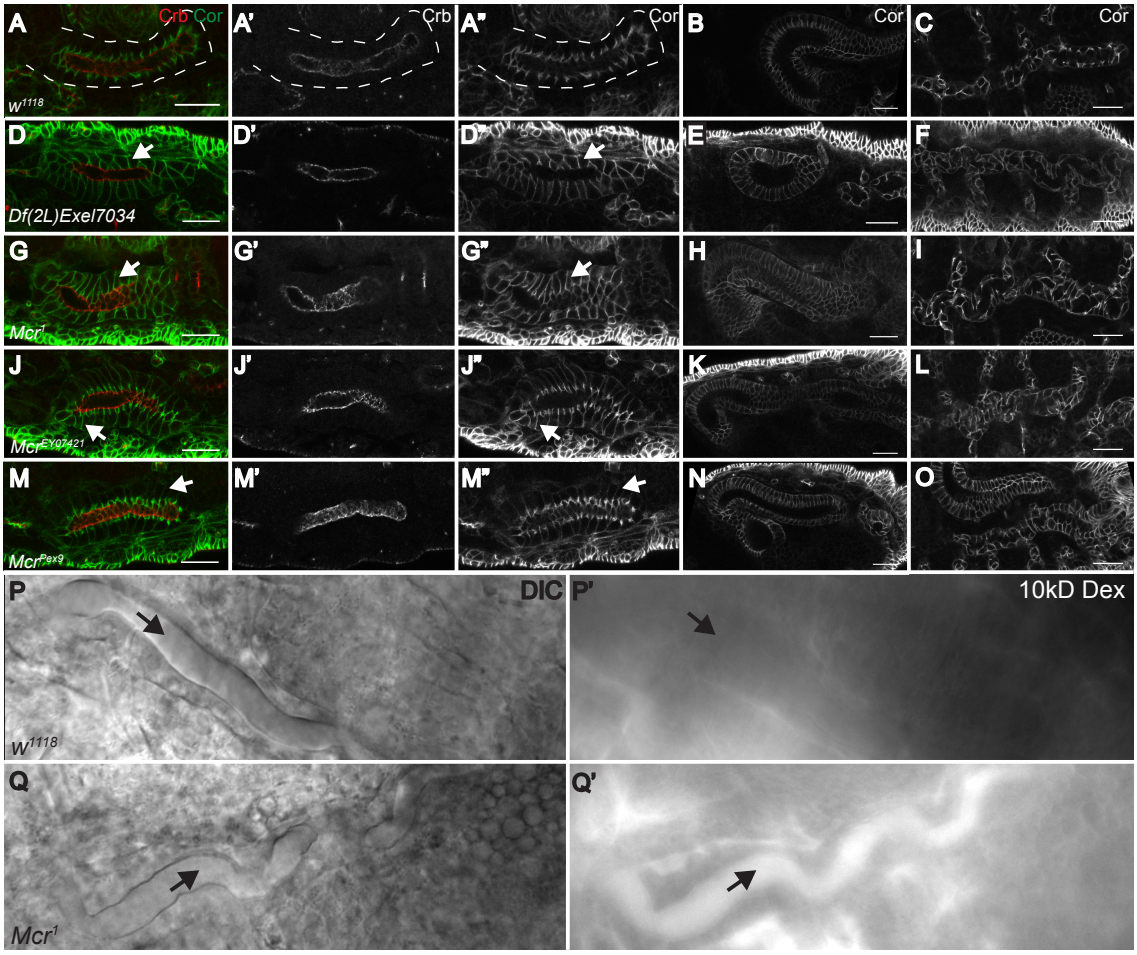
A
Crb Cor
w1118
A'
Crb
A"
Cor
B
Cor
C
Cor
D
Df(2L)Exel7034
D'
D"
E
F
G
Mcr1
G'
G"
H
I
J
McrEY07421
J'
J"
K
L
M
McrPex9
M'
M"
N
O
P
DIC
w1118
P'
10kD Dex
Q
Mcr1
Q'

Figure 2.2 *Mcr* is required for SJ structure and paracellular barrier function. (A-O) Confocal optical sections of salivary glands (A, D, G, J, M) stained with antibodies against Crb (red, and in A', D', G', J', M') and Cor (green, and in A", D", G", J", M"), and hindguts (B,E,H,K,N) and trachea (C,F,I,L,O) from stage 16 w^{1118} (A-C), *Df(@L)Exel7034)* (D-F), Mcr^{1} (G-I), $Mcr^{EY07421}$ (J-L) and Mcr^{Pex3} (M-O) embryos. The salivary gland in G is from the same animal as the hindgut in H, as are the salivary gland and hindgut shown in J and K. Apical surfaces face the lumen of the gland. The wild-type salivary gland epithelium is outline by a dashed line in A. Note that Cor is mislocalized along the lateral membrane in *Mcr* mutant salivary glands (arrows), whereas Crb is unaffected. (P-Q') Differential interference contrast (P,Q) and fluorescence (P',Q') photomicrographs of the tracheal dorsal trunk in stage 17 w^{1118} (P) and Mcr^{1} (Q) embryos that had been injected with a 10kDa Rhodamine-labeled dextran. The labeled dextran does not cross the tracheal epithelium and enter the lumen in the wild-type embryo, but does in the Mcr^{1} mutant embryo (arrows). Scale bars: 20um.

Figure 2.3

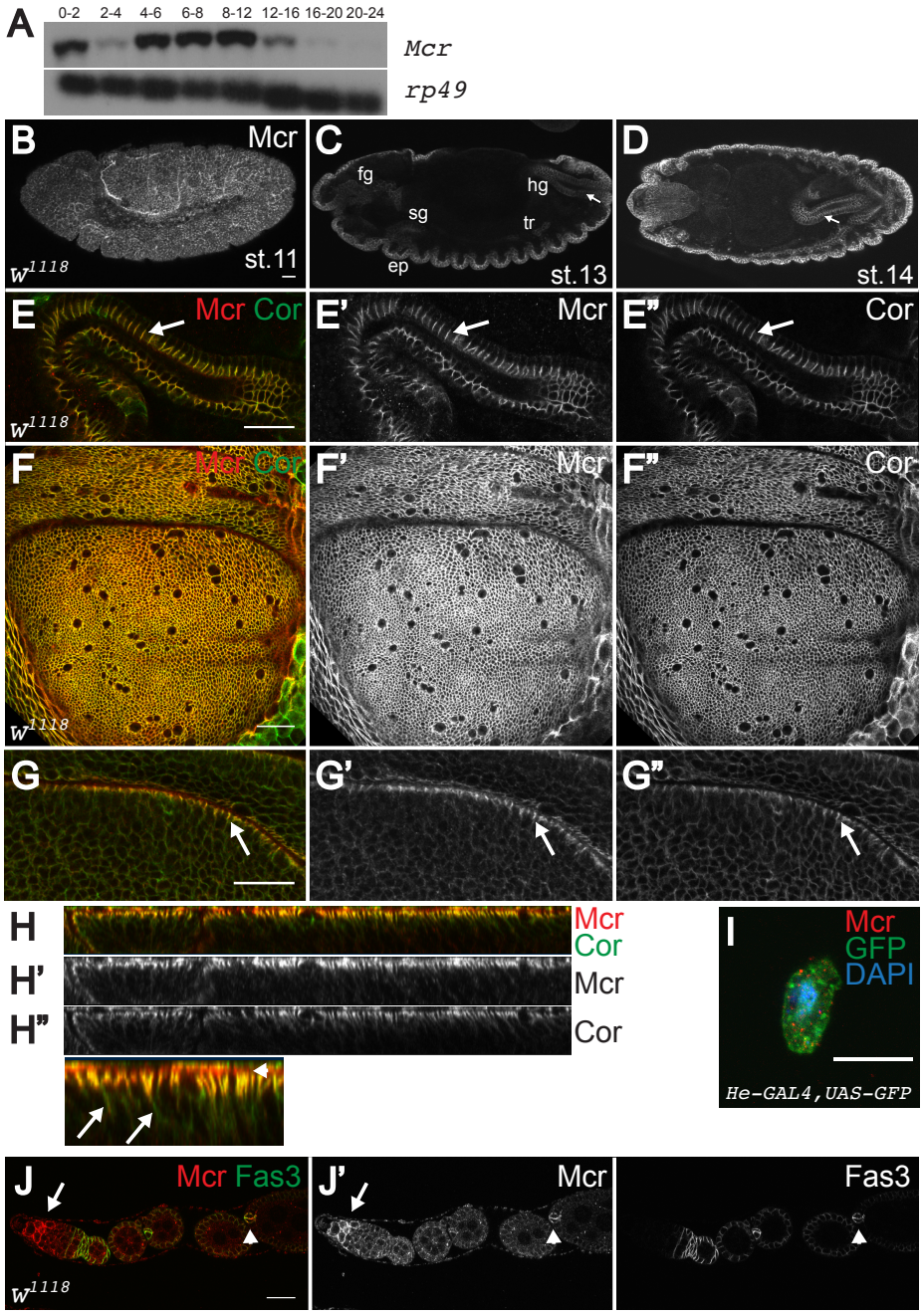
A
0-2 2-4 4-6 6-8 8-12 12-16 16-20 20-24
Mcr
rp49
B
Mcr
w1118
st.11
C
fg
hg
sg
tr
ep
st.13
D
st.14
E
Mcr Cor
E'
Mcr
E"
Cor
F
Mcr Cor
F'
Mcr
F"
Cor
G
G'
G"
H
Mcr
Cor
H'
Mcr
H"
Cor
I
Mcr
GFP
DAPI
He-GAL4,UAS-GFP
J
Mcr Fas3
J'
Mcr
Fas3

Figure 2.3 *Mcr* transcript expression and Mcr protein expression and localization during development. (A) Northern blot analysis of total RNA isolated from staged w^{1118} embryos probed for *Mcr* expression. Numbers refer to hours after egg laying. Hybridization to rp49 (RpL32) was used as a control for loading and transfer. (B-J) Confocal optical sections of w^{1118} embryos (B-E), w^{1118} third instar larval wing imaginal disc (F-H), *He-GAL4, UAS GFP* third instar larval hemocyte (I) and w^{1118} ovariole (J) stained with antibodies against Mcr alone (B-D), or co-stained with antibodies against Mcr (red, and in E′-J′) and Cor (green, and in E″-H″), GFP (green in I) or Fas3 (green in J, and in J″). (B-E) Mcr is associated with the membrane in stage 11 embryos (B) and by stage 13 is obviously expressed in ectodermally derived epithelia including the epidermis (ep), foregut (fg), hindgut (hg), salivary gland (sg) and trachea (tr) (C). In stage 14 embryos (D), Mcr is enriched at the apical lateral region of the membrane, but is also expressed more basolaterally (arrow). By stage 16 (E; in the hindgut), Mcr colocalizes with Cor in the region of the SJ. In third instar wing imaginal discs (F-H), Mcr colocalizes with Cor in the apical region of the lateral membrane of the disc proper cells, which can be seen in deeper sections (G) where lateral membranes lie adjacent to the folds in the epithelium (arrow), and by rendering an xz transverse section from a confocal z-series (H). A higher magnification view (outset in H) shows that Cor localization extends more basally than Mcr (arrows), and that Mcr is also expressed on the apical surface in a domain independent of Cor (arrowhead; note that staining in the peripodial epithelium can be seen above this line). (I) Confocal optical section of a *He-GAL4, UAS-GFP* hemocyte stained with antibodies against Mcr (red) and GFP

(green) and with DAPI (blue). Mcr is expressed in larval hemocytes, but is largely found inside the cell. (J) In the ovary, Mcr is most strongly expressed in stage 1 of the germarium (arrow) and in polar follicle cells (arrowhead), where it colocalizes with Fas3. Mcr is also expressed at lower levels in the follicle cells and at the membrane in the germ cells. Scale bars: 20um.

Figure 2.4

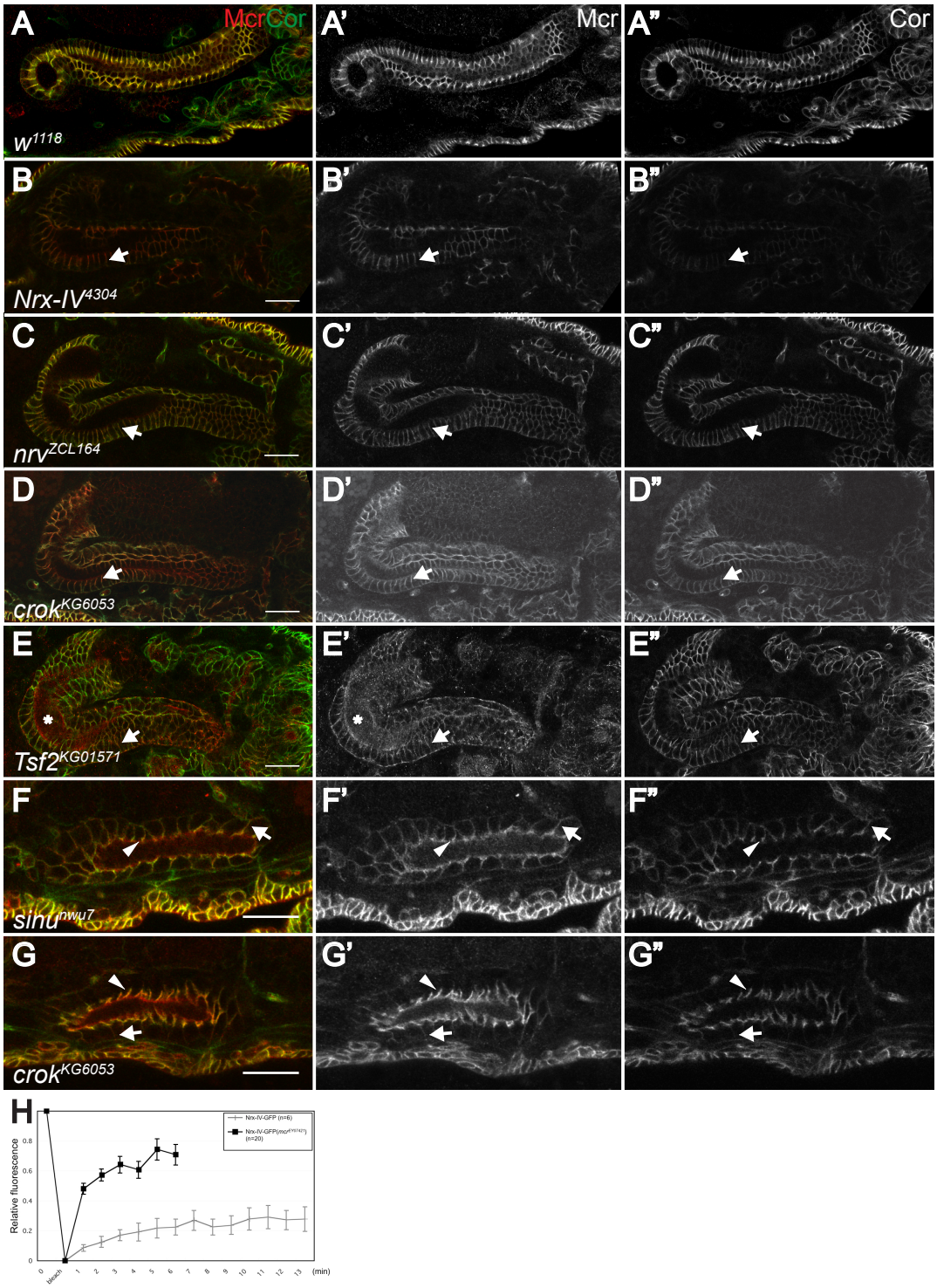
A
Mcr Cor
w1118
A'
Mcr
A"
Cor
B
Nrx-IV4304
B'
B"
C
nrvZCL164
C'
C"
D
crokKG6053
D'
D"
E
Tsf2KG01571
E'
E"
F
sinunwu7
F'
F"
G
crokKG6053
G'
G"
H
Relative fluorescence
0
0.2
0.4
0.6
0.8
bleach
1
2
3
4
5
6
7
8
9
10
11
12
13
(min)

Figure 2.4 Mcr is mislocalized in the hindguts of SJ mutant embryos. (A-G) Confocal optical sections of hindguts (A-E) and salivary glands (F,G) from stage 16 w^{1118} (A), $Nrx\text{-}IV^{4304}$ (B), $nrv2^{ZCL164}$ (C), $crok^{KG6053}$ (D,G), $Tsf2^{KG01571}$ (E) and $sinu^{nwu7}$ (F) embryos stained with antibodies against Mcr (red, and in A′-G′) and Cor (green, and in A″-G″). Mcr is mislocalized along the basolateral domain in the hindgut epithelia coincident with Cor in all of these embryos (arrows), and also shows strong mislocalization on the apical plasma membrane of $Tsf2^{KG01571}$ embryos (E) that is independent of Cor (asterisks). Scale bars: 20 μm. (H) Plot of average fluorescence recovery after photobleaching (FRAP) of Nrx-IV-GFP in the epidermis of stage 15 wild-type (gray line) and $Mcr^{EY07421}$ mutant (black squares) animals. Error bars indicate s.e.m.

Figure 2.5

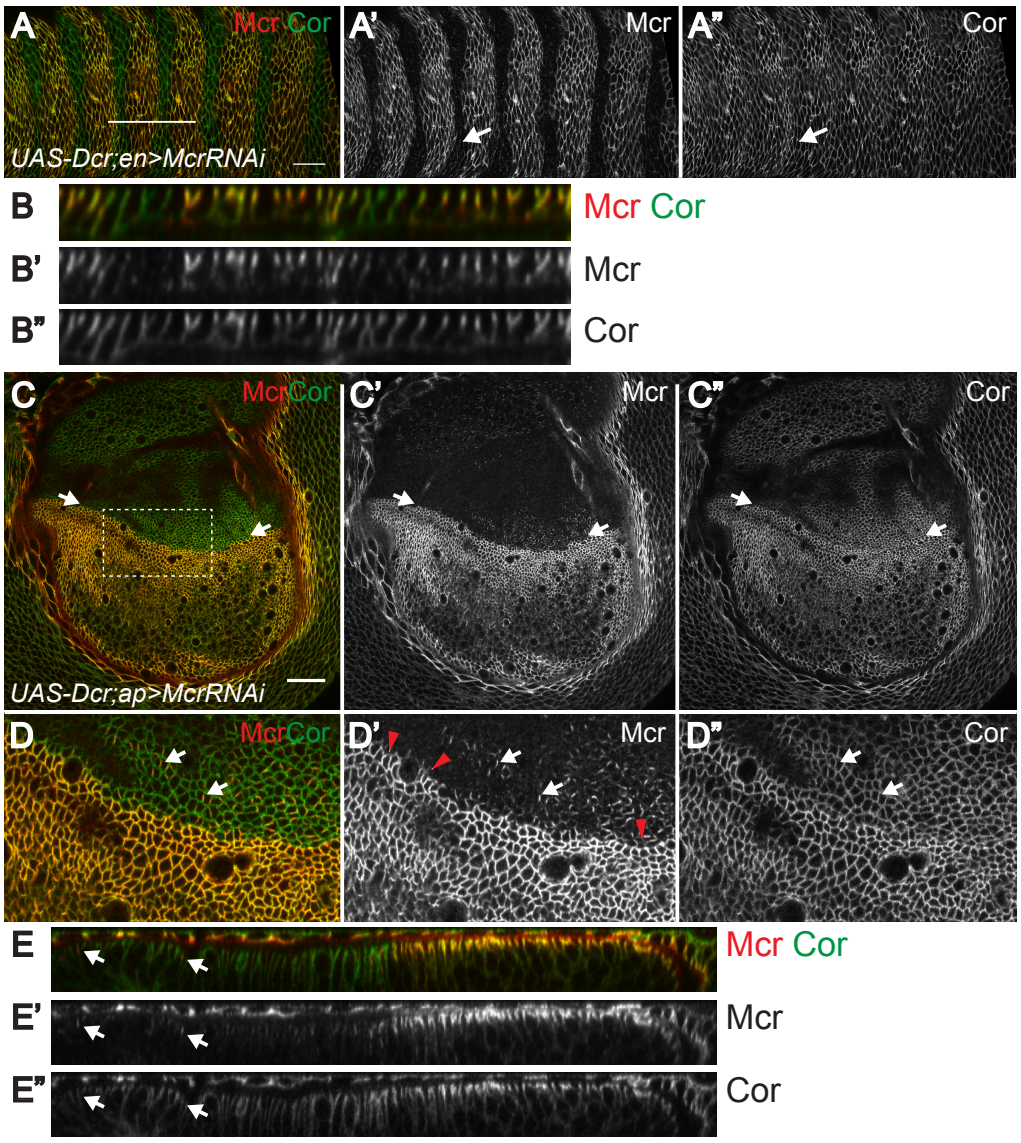
A
Mcr Cor
A'
Mcr
A"
Cor
UAS-Dcr;en>McrRNAi
B
Mcr Cor
B'
Mcr
B"
Cor
C
McrCor
C'
Mcr
C"
Cor
UAS-Dcr;ap>McrRNAi
D
McrCor
D'
Mcr
D"
Cor
E
Mcr Cor
E'
Mcr
E"
Cor

Figure 2.5 *Mcr* is required cell-autonomously for SJ organization in embryonic epithelia and larval wing imaginal discs. (A,B) Confocal optical sections (A) and xz rendering from a confocal z-series (B) of the epidermis of a stage 16 *UAS-Dcr-2; en-GAL4/UAS-Mcr-RNAi* embryo stained with antibodies against Mcr (red, and in A',B') and Cor (green, and in A",B"). The xz rendering is along the white line in A. Mcr expression is strongly reduced in the posterior cells, although the majority of the remaining protein appears to be membrane associated (arrow in A′ , compared with Cor localization in A″). Note that Cor is not as enriched in the apical regions of *Mcr- RNAi* cells, indicating a disorganization of the SJ junction (B). (C-E) Confocal optical section and xz rendering from a confocal z-series from a late third instar *UAS-Dcr-2; ap- GAL4/UAS-Mcr-RNAi* wing imaginal disc stained with antibodies against Mcr (red, and in C′ -E′) and Cor (green, and in C″ -E″). Dorsal is to the top in C and D and to the left in E, and the dorsal-ventral boundary is indicated by arrows in C. D is a higher magnification of the boxed region in C. Mcr is strongly reduced in the dorsal compartment of *Mcr-RNAi* wing discs, but the residual Mcr appears to align with Cor at the boundary between adjacent cells (arrows in D) and is apically enriched in the lateral membrane (arrows in E). Wild-type cells at the dorsal-ventral boundary have reduced Mcr expression along the membrane in contact with *Mcr-RNAi* cells (red arrowheads in D'). Scale bars: 20um.

Figure 2.6

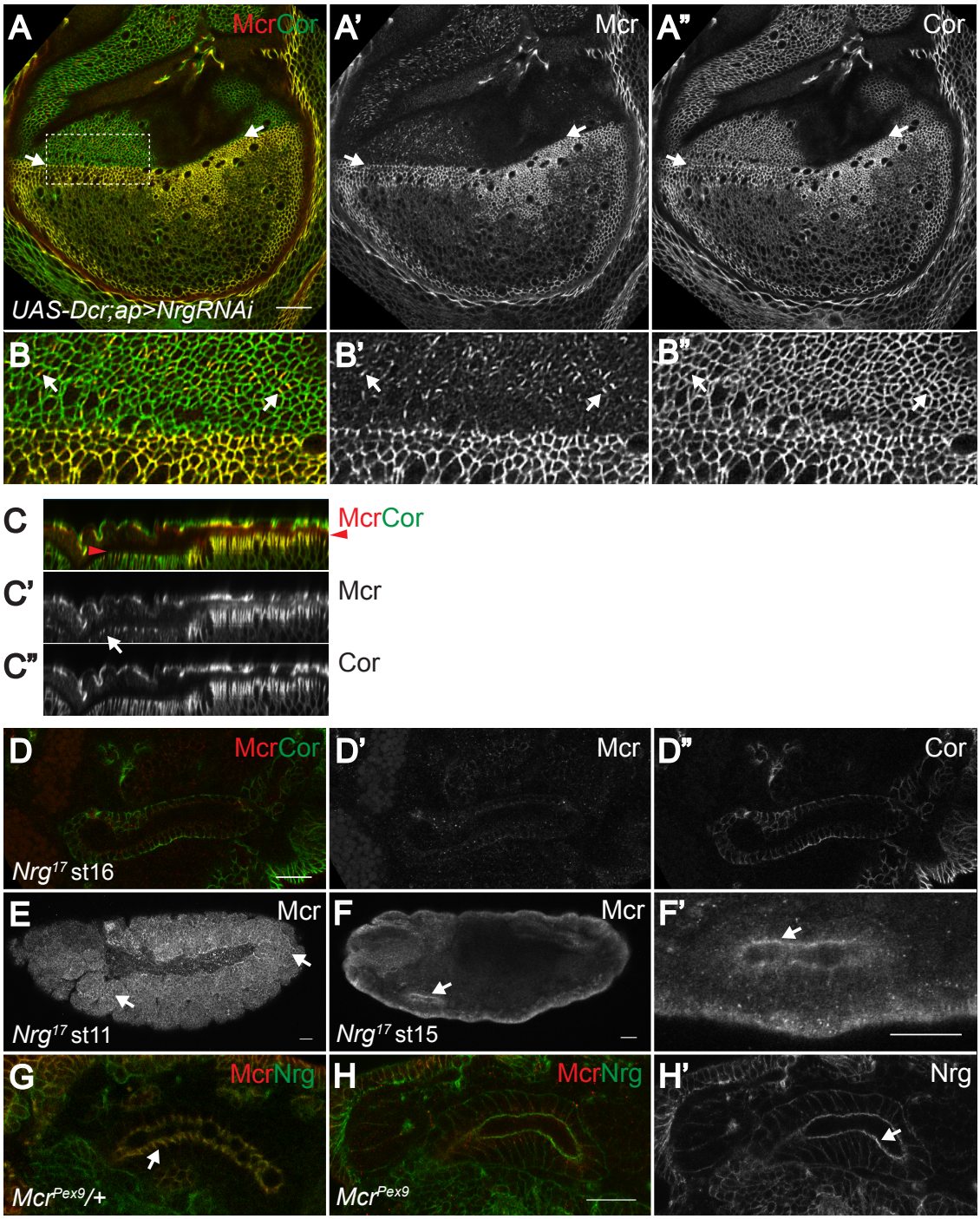
A
McrCor
A'
Mcr
A"
Cor
UAS-Dcr;ap>NrgRNAi
B
B'
B"
C
McrCor
C'
Mcr
C"
Cor
D
McrCor
Nrg17 st16
D'
Mcr
D"
Cor
E
Mcr
Nrg17 st11
F
Mcr
Nrg17 st15
F'
G
McrNrg
McrPex9/+
H
McrNrg
McrPex9
H'
Nrg

Figure 2.6 The SJ localization of Mcr and of Nrg depend upon each other. (A-C) Confocal optical section and xz rendering from a confocal z-series of a third instar *UAS-Dcr-2; ap- GAL4/UAS-Nrg-RNAi* wing imaginal disc stained with antibodies against Mcr (red, and in A′-C′) and Cor (green, and in A″-C″). Dorsal is to the top in A and B and to the left in C, and the dorsal-ventral boundary is indicated by arrows in A. (B) Higher magnification of the boxed region in A. Mcr is strongly reduced in *Nrg-RNAi* cells, but appears to colocalize with Cor along the boundary between adjacent cells (arrows in B), and is apically enriched in the lateral membrane (arrow in C′). Note that the apical plasma membrane expression of Mcr is also eliminated in the *Nrg-RNAi* cells (red arrowheads). (D) Confocal optical section of the hindgut from a stage 16 Nrg^{17} embryo stained with antibodies against Mcr (red, and in D′) and Cor (green, and in D″). Whereas Cor is mislocalized along the lateral membrane in the hindgut of the Nrg^{17} embryo, Mcr is nearly absent from the lateral membrane. (E-F′) Confocal optical sections of a stage 11 (E) and stage 15 (F) Nrg^{17} embryo stained with antibodies against Mcr. A higher magnification view of the salivary gland in F is shown in F′. Note that Mcr is expressed and shows some membrane localization in the stage 11 Nrg^{17} embryo (arrows in E), but is largely lost from the lateral membrane at the expense of the apical plasma membrane by stage 15 (arrows). (G,H) Confocal optical sections of salivary glands from a stage 16 $Mcr^{EY07421}$ heterozygous (G) and homozygous (H) animal stained with antibodies against Mcr (red) and Nrg (green, and in H′). Mcr and Nrg colocalize at the SJ in the heterozygous animal (arrow in G), whereas Nrg predominantly localizes to the apical surface in the *Mcr* mutant animal (arrow in H'). Scale bars: 20um.

Supplementary Figure 2.1

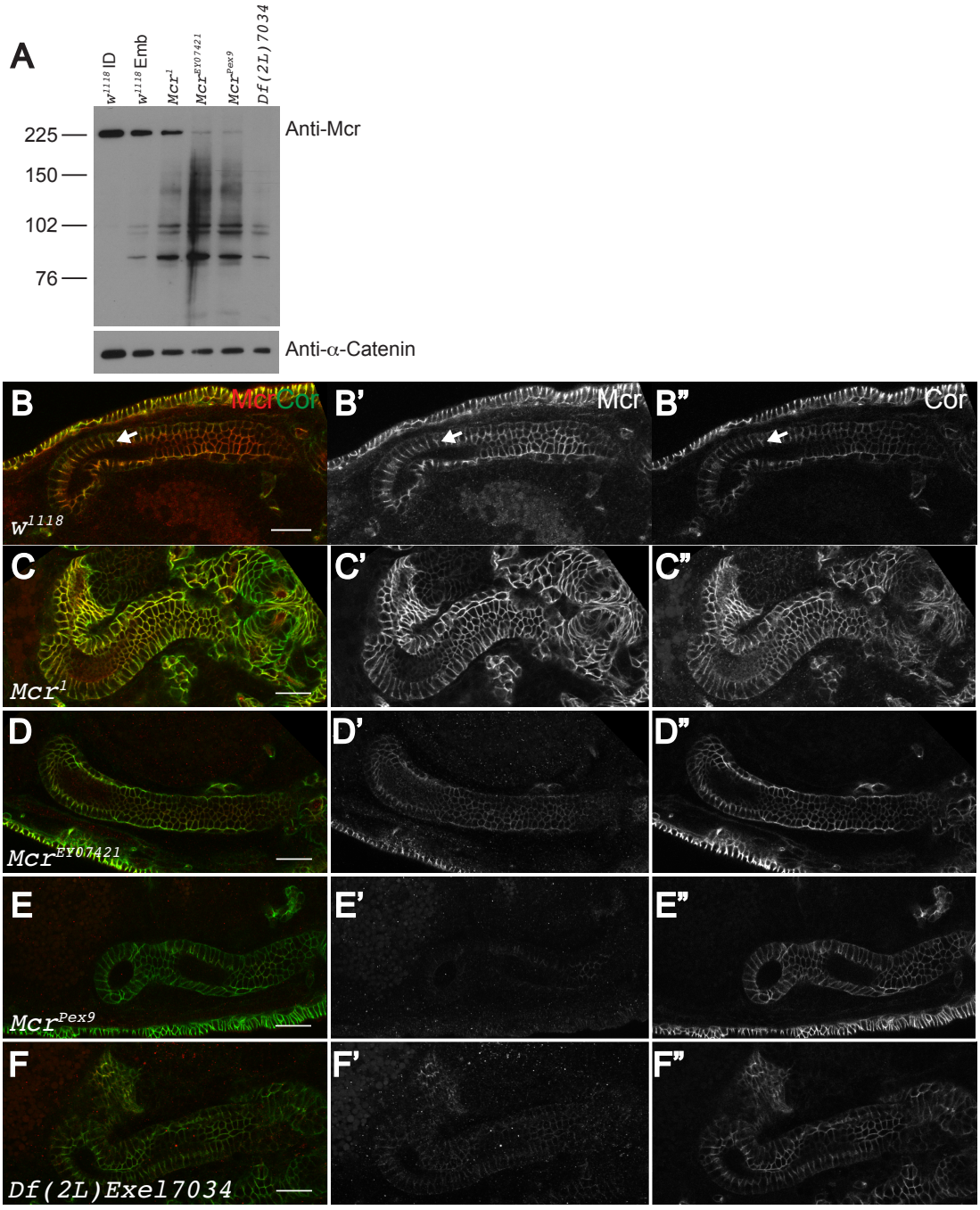

Supplemental Figure 2.1 Specificity of the anti-Mcr antibody (A) Western blot of lysates from w^{1118} third instar wing imaginal discs, and w^{1118}, Mcr^{1}, $Mcr^{EY07421}$, Mcr^{Pex3}, and *Df(2L)Exel7034* late embryos (17-22 hours after egg laying) probed with antibodies against Mcr and alpha-Catenin. (B-F) Confocal optical sections showing the hindguts of stage 16 w^{1118} (B), Mcr^{1} (C), $Mcr^{EY07421}$ (D), Mcr^{Pex3} (E), and *Df(2L)Exel7034* (F) mutant embryos stained with antibodies against Mcr (red and in panels B'-f') and Cor (green, and in panels B"-F"). In the w^{1118} hindgut, Mcr co-localizes with Cor in the region of the SJ (arrow), whereas Mcr is strongly expressed but mislocalized coincidently with Cor in the Mcr^{1} mutant hindgut (C). mcr levels are reduced and Cor is mislocalized in the hypomorphic allele Mcr^{Pex3} (E). Mcr protein is strongly reduced in $Mcr^{EY07421}$ mutant hindguts (D), and is nearly absent in *Df(2L)Exel7034* mutant hindguts (F), whereas Cor is mislocalized in both of these embryos. Preimmune serum fails to recognize the ~225kDa protein on westerns of wild type lysates, and shows no immunoreactivity on wildtype embryos or imaginal discs (data not shown). Scale bars = 20um.

Supplementary Figure 2.2

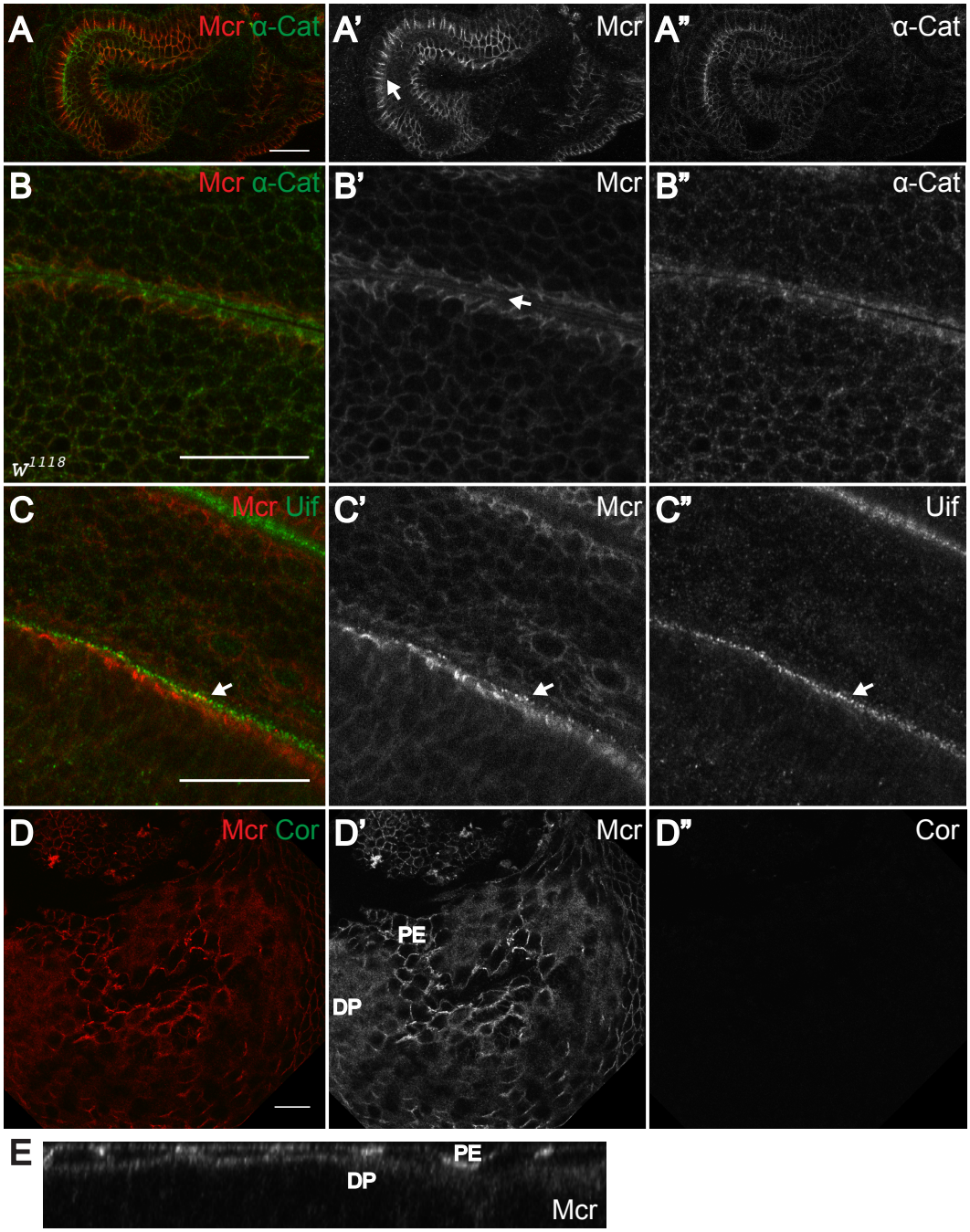

Supplemental Figure 2.2 Mcr's localization is distinct from the adherens junction, but does include the apical plasma membrane. (A,B) Confocal optical sections from a stage 16 hindgut (A) and an epithelial fold in a w^{1118} third instar wing imaginal disc (B) stained with antibodies against Mcr (red, and in panels A' and B') and alpha-Catenin (green, and in panels A" and B"). In the fold of the wing disc the apical surfaces face each other and the lateral membranes can be readily observed. Note that Mcr and alpha-Catenin do not overlap in the embryonic hindgut or imaginal disc. The apical plasma membrane expression of Mcr can be observed in both tissues (arrows). (C) Confocal optical section from an epithelial fold in a w^{1118} third instar wing imaginal disc stained with antibodies against Mcr (red, and in panel C') and Uninflatable (green, and in panel C"). Note that Mcr and Uif puncta are intermingled in the deepest part of the fold (representing the apical surface; arrow). (D, E) Confocal optical section and xz rendering from a w^{1118} third instar wing imaginal disc that has been incubated with antibodies against Mcr (red, and in panel D') and Cor (green, and in panel D") prior to fixation and further processing so that only surface exposed epitopes can be stained. In this section parts of both the peripodial epithelium (PD) and the disc proper (DP) can be observed. Note that Mcr is exposed on the apical surface of both the PE and the DP and that the Mcr antibody was able to reach the lateral membrane in the PE during the 20-minute incubation, whereas the cytoplasmic protein Cor was not accessible. Scale bars = 20um.

Supplementary Figure 2.3

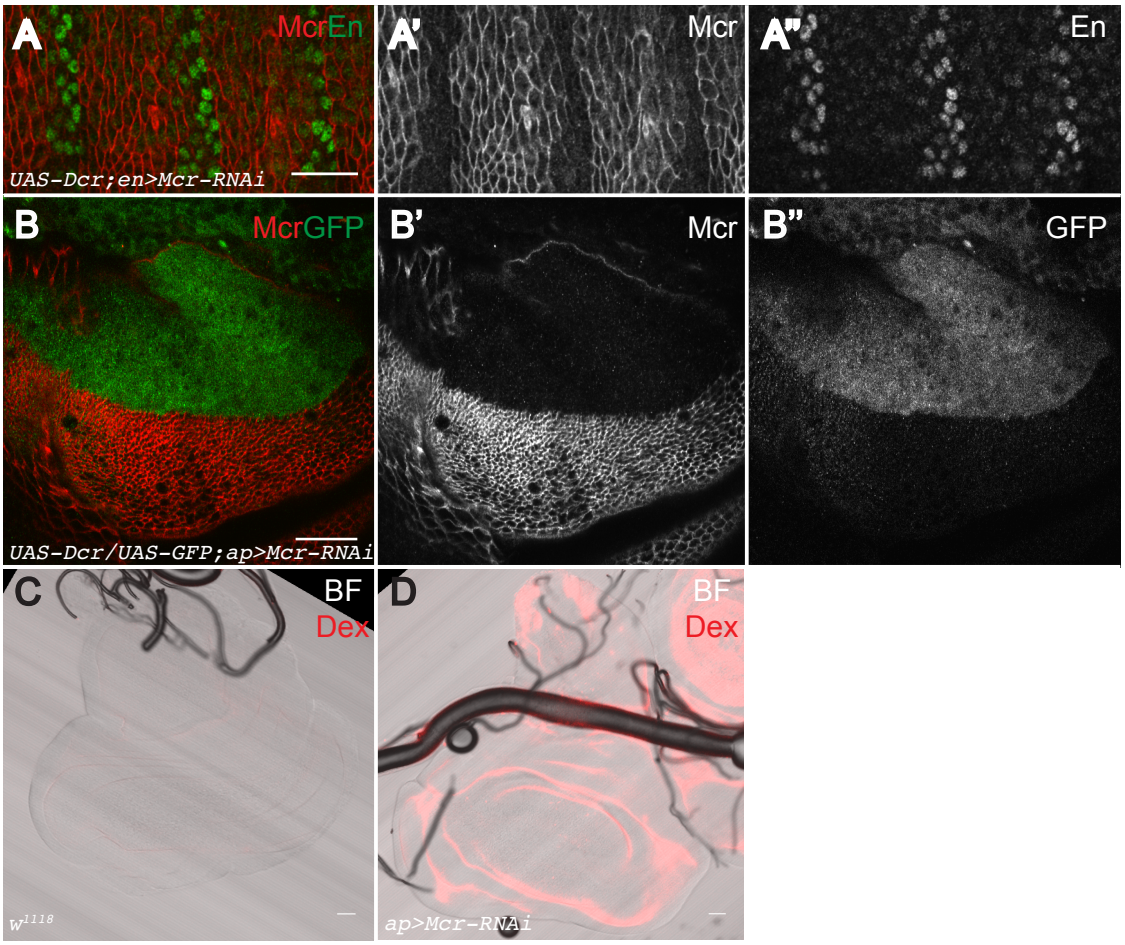

Supplemental Figure 2.3 Control experiments showing the specificity of *Mcr-RNAi* in the *en-GAL4* and *ap-GAL4* expression domains, and the functional disruption of the paracellular barrier in *ap>Mcr-RNAi* discs. (A) Confocal optical section from the epidermis of a stage 16 *UAS-Dcr;en-GAL4/Mcr-RNAi* embryo stained with antibodies against Mcr (red, and in panel A') and En (green, and in panel A"). (B) Confocal optical section of the wing imaginal disc from a *UAS-Dcr/UAS-GFP;ap-GAL4/Mcr-RNAi* animal. Note that in both tissues, Mcr is substantially reduced specifically in the cells expressing *Mcr-RNAi*. (C,D) Brightfield/fluorescence micrographs of late third instar w^{1118} (C) and *ap>McrRNAi* (D) wing imaginal discs from animals that had been injected with 10kDa rhodamine-labeled dextran prior to dissection. Note that the labeled dextran fills the space between the disc proper and peripodial epithelim and can be seen pooling in the folds of the *ap>McrRNAi* disc, whereas very little dextran has infiltrated the wild type disc. Scale bars = 20um.

Supplemental Table 1 Lethal phase and terminal phenotypic analysis of *Mcr* mutations

Genotype	% Embryonic lethality[a] (n)[b]	% Faint denticle belts	% Deposits in salivary glands	% Dorsal closure defect
Mcr[1]	100 (290)	99 ± 1	92 ± 3	20 ± 1
Mcr[EY07421]	100 ± 1 (304)	100	76± 7	0
Mcr[Pex3]	90 ± 8 (285)	100	53 ± 11	11 ± 4
Mcr[1]/Df(2L)Exel7034	99 ± 1 (361)	97± 3	51 ± 10	7 ± 1
Mcr[EY07421]/Df(2L)Exel7034	100 (385)	100	96 ± 1	1 ± 1
Mcr[Pex3]/Df(2L)Exel7034	100 (273)	100	79 ± 5	4 ± 1
Mcr[1]/Mcr[EY07421]	100 (288)	99 ± 1	61 ± 6	3 ± 1

[a]Mean ± s.e.m. from 3-5 independent experiments.
[b]Total umber of animals of indicated genotype that were scored.

Chapter III

Septate junction proteins are required for proper cell shape changes and cell rearrangements during morphogenesis

Section 3.1 Abstract

Organismal development depends upon highly regulated cellular rearrangements and cell shape changes. These morphological processes require signaling pathways that regulate actin dynamics to propagate forces through tissues, and stabilization of these effects is mediated by the lateral membrane. Our lab conducted a screen for genes that regulate imaginal disc morphogenesis during metamorphosis in *Drosophila*. From this screen we identified *Macroglobulin complement related (Mcr*). During the characterization of *Mcr*, we found that it serves an essential role in the establishment of septate junctions (SJs). Similar to vertebrate tight junctions, SJs are occluding junctions along the lateral membranes of epithelial cells that allow for the separation of chemically distinct organ compartments. Previous work indicated that a few SJ genes play a role in morphogenesis, including *coracle* and *Neurexin-IV* in dorsal closure, and *Gliotactin* and *Coracle* in imaginal disc morphogenesis. To determine whether the SJ as a complex functions in morphogenesis, or if only a few individual SJ genes have additional roles in regulating morphogenesis, we conducted an analysis of nine SJ mutations in coordinating complex morphogenetic processes during embryonic development. Using salivary gland organogenesis and dorsal closure as models, we identified that SJ components contribute to morphogenesis by regulating cell shape changes and cell rearrangements. From this analysis, we identified that each SJ component examined has an essential role in regulating morphogenesis during

development and that the SJ components have a novel, essential role in morphogenesis prior to their assembly into the occluding junction.

Section 3.2 Introduction

Morphogenesis is a highly coordinated process that requires the integration and regulation of tissue and cellular level events, including cell signaling, cell intercalation, and force distribution. Laying at the foundation of these mechanisms is a requirement for cell-cell contacts established between lateral membranes. A substantial amount of work has revealed the importance of the adherens junction (AJ) in maintaining cell contacts (Langevin et al. 2005; Georgiou et al. 2008; Gumbiner 2005), regulating cell signaling (De Matos Simões, Mainieri, and Zallen 2014; Géminard et al. 2014), facilitating trafficking (Shaye, Casanova, and Llimargas 2008; Shindo et al. 2008; Li, Satoh, and Ready 2007), and organizing apical constriction and expansion (Takeichi 2014; Y.-C. Wang et al. 2012) during complex morphogenetic events (reviewed in Wirtz-Peitz and Zallen 2009) yet, current models cannot fully account for the distribution and cellular stabilization of forces using the AJ as the sole stabilizing factor along the lateral membrane (Polyakov et al. 2014). A good way to discover these unknown mechanisms that contribute to morphogenesis is through open-ended genetic screens.

To identify genes involved in regulating morphogenesis, our lab conducted three screens, a deficiency kit screen, a screen to identify dominant modifiers of *Rho1*, and an EMS modifier screen using a hypomorphic allele of *broad (br)* that had a low penetrance of morphogenesis defects (Ward, Evans, and Thummel 2003; Patch et al. 2009). *br* is a zinc-finger transcription factor that regulates morphogenesis. Using this hypomorpic allele, we identified second-site mutations that add to these morphogenetic defects due to their interaction with *br*. We

identified all of the modulators of the actin cytoskeleton such as *Rho1*, *zipper,* and *myosin light chain,* among others. What stood out was that all of the genes identified fit together into a group due to their role in modulating the actin cytoskeleton. However, we also identified a number of other genes that did not fit into this pathway yet. By cloning some of these genes, we sought to gain a better understanding of the events between the upstream component *Rho1* and the direct regulator of the cytoskeleton. One of these genes we characterized was *Macroglobulin complement related (Mcr)* (S. Hall et al. 2014).

Mutations in *Mcr* are embryonic lethal and exhibit defects in morphogenesis including defects in dorsal closure (DC) and convoluted trachea (S. Hall et al. 2014). Our work revealed that *Mcr* is required for the organization and function of the septate junction. The SJ serves as an occluding junction to provide the isolation of functional organ compartments and the outside environment and is functionally analogous to the vertebrate tight junction. The SJ is a large protein complex, composed of over twenty proteins, that spans the intermembrane space between adjacent lateral membranes of epithelial cells. The majority of these proteins are transmembrane adhesion molecules, including three claudin family proteins, Contactin, Neurexin-IV, Neuroglian, and nervana2, among others.

The SJ assembles between stages 12 and 16 of embryogenesis. The details of SJ biogenesis were elegantly demonstrated by Tiklová et al. (2010) and involve an initial broad localization of SJ proteins along the length of the lateral membrane at stage 12. These proteins are then endocytosed and recycled at stages 13-14 where they are then refined to the region of the SJ at stage 15. Final maturation of the SJ

occurs at stage 16 through an unexplained process. The ultrastructure of the SJ, at stage 16, appears as ladder-like electron-dense arrays that span the 15nm space between epithelial cells. It is the formation of these electron dense structures that provide the occluding function. SJ proteins are highly interdependent for their assembly and occluding function where the absence of a single core component of the SJ results in the mislocalization of all other SJ components along the lateral membrane. This dynamic process of endocytosis and recycling occurs during a period where critical morphogenetic events are taking place. The identification of a SJ gene in a screen for morphogenesis combined with findings in the literature suggesting a requirement for the larger lateral membrane in regulating morphogenesis and the observations of mutations in the core SJ components *coracle (cor)* and *Neurexin-IV (Nrx-IV)* leading to defects in dorsal closure (DC) (Fehon, Dawson, and Artavanis-Tsakonas 1994; Baumgartner et al. 1996) raises questions regarding the possibility of SJ proteins playing a novel role in regulating morphogenesis, independent of their occluding function.

To investigate this whether SJ proteins are involved in the regulation of morphogenesis, we assembled a large collection of loss-of-function mutations in SJ genes representing the adhesion molecules, claudins, and cytoplasmic proteins, and examined several distinct morphogenetic developmental events by examining cuticles and by immunostaining. Cuticle phenotypes revealed penetrant defects in head involution and dorsal closure with many embryos showing no cuticle. Immunostaining revealed embryos arresting development prior to the completion of germband retraction and defects in salivary gland organogenesis. We focused our

attention on dorsal closure and salivary gland morphogenesis. Our findings, presented here, demonstrate that the zygotic loss of SJ genes results in defects in cell shape changes and rearrangements.

Section 3.3 Results

Loss of zygotic expression of SJ genes results in head involution and dorsal closure defective phenotypes

Given our observations and evidence in the literature that *cor*, *Nrx-IV*, and *Mcr* are required for DC (Fehon, Dawson, and Artavanis-Tsakonas 1994; Baumgartner et al. 1996; Ward, Lamb, and Fehon 1998; Hall et al. 2014), a major morphogenetic event, we felt it would be instructive to survey SJ mutant lines for defects in DC and head involution (HID) to determine if this is a general requirement of this group of lateral membrane proteins or a pleiotropic effect of a few. For this analysis, we relied on the ability to determine developmental patterning and cell fates using the cuticle morphology of mutant animals that failed to crawl away forty-eight hours after egg lay.

To begin this investigation, we used alleles for nine SJ genes that have been well characterized in the literature to result in defects in SJ organization. Our analysis revealed that each line examined showed clear examples of defects in these two fundamental development events (Fig. 3.1, Table 3.1). We also observed variation among cuticles displaying HID (Fig. 3.1E, H, and M). Our results suggest two phenotypic classes: inability to invert the head structure (Fig. 3.1E and M) and abnormal head skeleton morphology (Fig. 3.1H).

Similar variation exists within the population of cuticles displaying defects in DC, where there are changes in the location and size of the dorsal hole (compare Fig. 3.1B, J, and N). Some of the variation in the placement of the hole appears to be linked to abnormal germband retraction, which was observed in many SJ mutant

lines using posterior spherical positioning. Quantification of the germband retraction phenotype was not possible due to poor cuticle formation in the mutant animals. DC defects were less penetrant among our mutant animals, compared to HID, but were observed in each line (Table 3.1). To ensure that the phenotypes were due to the loss of the SJ genes and not second site mutations, we used a combination of multiple alleles, ubiquitous RNAi, and hemizygous deficiencies. These experiments resulted in a recapitulation of the DC and HID phenotypes, suggesting that there is not a second site mutation influencing these phenotypes (Fig. 3.1C, E, G, I, and M). In addition, the penetrance of DC defects in cor^{4} mutant animals of 27.6% $\pm$ 2.9 is consistent with those published by (Ward, Lamb, and Fehon 1998).

During our analysis, we also observed a number of prepared lethal cuticles that did not have any observable cuticle morphology (Fig. 3.1G). To determine if this empty phenotype was due to an absence of cuticle alone or an early arrest of development, we prepared one-hour collections and aged them for 17 hours. Using a YFP balancer to unambiguously distinguish between mutants and the heterozygous siblings, we scored individual embryos for the stage at which development was arrested (Fig. 3.2) using gut and/or other morphological characteristics. Our results revealed that in $cont^{ex956}$, Mtf^{P}, nrg^{14}, and $Nrx\text{-}IV^{4304}$ animals, a number of individuals fail to develop to stage 16, when cuticle secretion would occur and also when a functional occluding junction would be required (Fig. 3.2B, C, and D, Table 3.2).

Our observations of an earlier requirement for SJ components raised the question of whether these proteins are expressed during these early stages of development. Typically, SJ genes are characterized and closely examined between

stages 12 and 16, when SJ biogenesis occurs. To identify the early expression and localization of this group of proteins, we used immunohistochemistry. These experiments revealed that most SJ proteins are present at stage 10 of embryogenesis where they are observed associated with the membrane (Fig. 3.3).

Taken together, these analyses indicate that SJ genes are expressed early in embryogenesis and are required for early developmental events that occur prior to the formation of the SJ, which implies an alternative functional role for this large collection of lateral membrane proteins. Therefore, it is important to understand how these lateral membrane proteins regulate development and not the role of the barrier in regulating development.

Salivary gland organogenesis requires SJ proteins for correct cell shape and rearrangements

Observations have been noted in the literature that mutations in the SJ genes *Nrv2, Atpα, Nrg, cor* and *Nrx-IV* lead to abnormal salivary gland morphology (Lamb et al. 1998; Genova and Fehon 2003) however a detailed description of the phenotype has not been described. Similar to the major developmental events of head involution and dorsal closure, salivary gland (SG) organogenesis involves the coordinated movement and reorganization of cells within the tissue without undergoing division. The SG is an epithelial tube that creates a single lumen for its function. The formation of the lumen begins at stage 10 when primordial cells invaginate from the ventral surface (Myat 2005) and undergo apical membrane expansion (Myat and Andrew 2002). The lumen is elongated through a process of collective cell migration where the distal tip cells extend protrusions, facilitating

migration over the visceral mesoderm (Bradley et al. 2003; Vining et al. 2005). The cells proximal to the tip change from a columnar shape to cuboidal (Na Xu, Keung, and Myat 2008). These coordinated processes allow the tissue and lumen to elongate, reaching full extension by stage 15. Currently, there is not a complete understanding of the mechanisms that control cell rearrangements and lumen diameter and structure in the developing SG.

Using immunohistochemistry, we examined animals mutant for one of four SJ genes: *Nrg, Mcr, Cont,* or *Kune* and determined that SJ mutant salivary glands invaginate, migrate, and contain a wild type number of cells, yet they exhibit abnormal morphology at stage 16 that results in SGs that appear short and fat (Fig. 3.4). In $Kune^{C309}$ (Fig. 3.4C) and Mcr^{1} (Fig. 3.4D) mutant animals, the most notable phenotype was an abnormal broad morphology of the lumen. In addition to abnormal lumen morphology, $Cont^{ex956}$, Mcr^{1}, and $Kune^{C309}$ glands often display incomplete migration. Of these, $Cont^{ex956}$ glands are the most abnormal, often folding upon themselves (Fig. 3.4B). Using *fkh*-Gal4 we knocked down *Mcr* and *Kune* expressing RNAi specifically in the salivary gland and recapitulated each of the resulting phenotypes suggesting that the SG phenotypes are due to loss of *Mcr* and *Kune* specifically in the SG (Fig. 3.4F and Fig. 3.5F andTable 3.3).

To begin to understand the cellular defects behind these phenotypes we collected confocal Z-series of salivary glands from ten individuals of the following genotypes: w^{1118}, Nrg^{14}, Mcr^{1}, *fkh-GAL4>McrRNAi,* $Kune^{C309}$, *fkh-GAL4>KuneRNAi* and $Cont^{ex956}$. Using these images, we determined that the overall proximal/distal (P/D) and dorsal/ventral (D/V) dimensions of the mutant glands are not dramatically

different from wild type suggesting that overall organ size is normal in the absence of these SJ proteins and is not the cause of the gross morphological abnormalities (Fig. 3.5,Table 3.3).

SG organogenesis depends on the ability of cells to rearrange and change position with their neighbors. Xu et al (2011) determined that cell rearrangements that occur between stages 11 and 13 cause the number of nuclei in a cross section of the lumen to decrease by half. Using 3-dimensional reconstructions of our confocal z-series, we counted the number of cells surrounding the lumen at three points through each gland as a readout of cell rearrangements. We observed that *Mcr^{1}, $Kune^{C309}$, $Cont^{ex956}$, and Nrg^{14}* mutants have a statistically different number of nuclei on average per cross-section than wild type (Fig. 3.5A-F, Table 3.3). This data suggests that these lateral membrane components of the SJ are required for cell rearrangements in salivary gland organogenesis.

During our analysis of cellular rearrangements, we observed the broad lumen phenotype was due to flattening of the lumen that often results in a minimal or absent luminal expansion. In addition to the flat lumen phenotype, we observed inconsistent diameters along the length of the lumen that ranged between narrow, broad, and flat. Glands that contained variation in lumen diameter appear convoluted, leading to glands that bend and turn through focal planes, giving them a short fat appearance when observed on a single focal plane. This variable lumen diameter was not observed in *Nrg^{14}* mutants or *$Cont^{ex956}$* glands. *Nrg^{14}* glands (Fig. 3.5E) maintain a wild type appearing lumen whereas *$Cont^{ex956}$* glands (Fig. 3.5B) have large cystic-like lumen segmented by areas of constriction.

Defective apical membrane expansion along the P/D axis of the developing gland has been shown to contribute to defects in lumen size (Pirraglia, Walters, and Myat 2010). Apical constriction in SG cells results in a cell shape change from cuboidal to columnar followed by a change to pyramidal that allows for correct invagination and coordinated migration (Maruyama and Andrew 2012). These previous findings raised the possibility that our lumen morphology could be due to defects in apical membrane length. To examine this idea more closely, we measured the length of two lateral membranes per cell and the intervening apical membrane for a total of ten cells per gland for ten individuals of each genotype. From this, we found that the length of the lateral membrane is dramatically increased in Mcr^{1} and $Kune^{C309}$ mutant salivary glands and the apical membrane length is reduced compared to wild type (Fig. 3.5,Table 3.3). Since proper E-cadherin localization was identified to be involved in regulating the apical membrane, we examined E-Cadherin in Mcr^{1} and $Kune^{C309}$ mutant SGs and found no obvious changes in localization (data not shown). In addition, we examined the localization of Crumbs, Uif, and Pio to determine if the decrease in apical membrane was due to a general inability to traffic apical membrane and found localization of each protein to be normal, indicating that failure to fully elongate the apical membrane is not due to loss or reduction in E-cad or abnormal A/B polarity.

Dorsal Closure

Our identification of defective cell rearrangements during SG organogenesis caused us to question if defective cell rearrangements were also contributing to our

DC defects. DC is a dynamic process that requires extensive cell shape changes, cell signaling, force stabilization, and force propagation. During *Drosophila* development, the dorsal epidermis of the embryo is discontinuous; spanning the region between the two lateral sides of the epidermis is the amnioserosa (AS), which acts as a transient epithelium. These epithelial sheets spread and fuse to form a continuous epithelium that encloses the embryo. This process is initiated at stage 13 by the activation of the Jun-N-terminal (JNK) signaling cascade and the elongation of the dorsal most epidermal cells (DME) (Kaltschmidt et al. 2002; Jankovics and Brunner 2006; VanHook and Letsou 2008). Initiation is followed by the dorsal ward movement of the epidermis, which requires the coordinated pulsing generated by contractile forces and programmed cell death within the AS (Solon et al. 2009; Blanchard et al. 2010; David, Tishkina, and Harris 2010) and the assembly of an actomyosin cable at the leading edge that aids in the coordination of lateral epithelial sheet migration (Peralta et al. 2007; Hutson et al. 2003). As the DME migrates over the AS toward the midline, it extends filopodia, ensuring the final stages of closure results in proper alignment of cells on the opposing epidermal sheets (Jacinto et al. 2000; Hutson et al. 2003; Peralta et al. 2007; Millard and Martin 2008). Defects originating in either the AS or epidermis that alter this highly coordinated interaction lead to the inability to fuse the dorsal epithelium.

SJ mutant animals exhibit defects in dorsal closure that range from small dorsal holes, often observed in Mcr^{1} mutants (Fig. 3.1J), and large dorsal holes as seen in cor^{4} and $Nrx\text{-}IV^{4304}$ mutants (Fig. 3.1B and N). To follow-up on our observation of DC defects, we used immunohistochemistry to examine the

morphology of the two main tissues involved in the successful progression and completion of DC. Confocal imaging of *cor, Nrx-IV,* and *Mcr* mutant animals stained with antibodies to Sqh, a readout of myosin organization, and to DE-Cadherin, to outline the cells, revealed abnormal cell morphology within the AS (Fig. 3.6, compare A" and B"). These cells become positively labeled with acradine orange (data not shown), which suggests that the cells are undergoing apoptosis. This apoptosis could be due to abnormal cell signaling or cellular stress due to loss of tissue integrity. We also observed a small number of individual cells in cor^{4} mutants that appear to have decreased levels of Sqh, suggesting that myosin organization is abnormal in some AS cells (Fig. 3.6B' asterisk). The assembly of actomyosin complexes is important for regulating the pulsating contractile forces that originate in the AS to move the AS downward into the body cavity of the embryo as the DME elongates and migration progresses toward the midline. These processes happen simultaneously and loss of either chemical or mechanical components in either tissue leads to failure in dorsal closure. Consistent with this interdependence, we observed defects in Sqh organization in the DME of cor^{4} and $Nrx\text{-}IV^{4304}$ mutants indicating that assembly of the actomyosin cable is disrupted (Fig. 3.6 compare A' with B' and D'') We also observed a scalloped leading edge of the DME (Fig. 3.6, arrowheads) suggesting that the loss of SJ proteins along the lateral membrane leads to decreased tension within the DME. These findings indicate that there is disorganization of both the AS and the epidermis in SJ mutant animals suggesting a role for SJ proteins in maintaining the integrity of the AS and DME during DC.

Identifying a defect arising within the AS was surprising since SJ proteins have not been identified as being expressed within this tissue. Using antibodies targeting Cor, Nrx-IV, Mcr, Nrg, Kune, and Cont, we determined that each of these proteins is present in the AS at stage 13, the start of DC (Fig. 3.7). Mcr, Kune, and Nrx-IV(Fig. 3.7A", B', and C') have the strongest staining followed by Nrg and Cont (Fig. 3.7C", B") and all localize to the membrane. Cor was observed at low levels and remains diffuse throughout the cytoplasm (Fig. 3.7A')

Using immunohistochemistry we examined the activation of JNK signaling in the DME in a puc^{E69} enhancer trap line with a LacZ reporter in the endogenous *puc* gene, as a readout (Martín-Blanco 1998). In puc^{E69} expressing animals, we see that Puc is expressed indicating that JNK signaling is activated (Fig. 3.8). In stage 13 and 16 wild type animals, we see the Puc positive cells are ordered and regularly spaced (Fig. 3.8A and B). In the wild type animals and the SJ mutants $Nrx\text{-}IV^{4304}$ and *Melanotransferrin2* ($Tsf2^{KG01571}$) we see that *puc* expression is active in DME cells (Fig. 3.8, C-F). In the stage 16 images, we chose animals that did close the dorsal hole, which by cuticle prep would not be scored as DC defective due to the absence of a large dorsal opening, however the process is still disrupted. In wild type, these cells align directly across from each other but the SJ mutants are disorganized where Puc positive cells are observed lining up behind each other (Fig. 3.8C-F). This result could be due to bunching of the epidermis, abnormal cell shapes, or irregular cell rearrangements.

To eliminate any secondary effects due to the use of the puc^{E69} line, we immunostained cor^{4} and Mcr^{1} embryos with their heterozygous siblings using Mcr

to outline the cells and Engrailed (En) to label the posterior cells of each segment of the lateral epidermis and looked for changes in the number of En positive and negative cells within each segment (Fig. 3.9). In the heterozygous siblings, we observed on average, three En positive cells per segment in the DME at stage 13 (Fig. 3.9A and C). SJ mutants exhibited an abnormal number of En positive cells in the DME (Fig. 3.9B and D). The changes in *Mcr*^{1} animals (Fig. 3.9D) typically resulted in one or two additional En positive cells whereas; *cor*^{4} mutants (Fig. 3.9B) exhibited much larger disruptions. *cor*^{4} mutants also have abnormal cell shapes throughout the epidermis, raising the possibility that in the absence of Cor, epithelial cells cannot acquire or maintain the proper shape. This data suggests that these cells are unable to maintain their correct position in relationship to their neighbors, indicating that the cells do not follow normal rearrangements during morphogenesis.

Section 3.4 Discussion

We identified an essential developmental role for a large group of lateral membrane proteins in regulating morphogenesis that eventually mature to form the SJ at stage 16 of embryogenesis. We base this conclusion on our observation of terminal cuticle phenotypes that show clear defects in two early developmental events, dorsal closure and head involution, and a large number of animals that appear to lack any cuticle. Using immunohistochemistry, we identified that a number of mutant embryos arrest their development prior to the formation of a functional occluding junction. In addition, we have documented that these SJ proteins are expressed during this period of embryonic development and that the zygotic loss of SJ proteins leads to arrested development prior to the formation of the SJ. It is likely that these results actually underrepresent the effect of the loss of SJ genes due to maternally contributed RNA, identified by modENCODE. The temporal expression of SJ proteins and the effect of their loss on morphogenesis support the idea that these proteins regulate essential cellular level mechanisms that facilitate the execution of morphogenetic processes prior to their role as an occluding junction.

SJ proteins regulate morphogenesis throughout the life cycle of the fly. Our evidence clearly shows that every SJ gene is required for head involution and many also contribute to DC. It is also likely that SJ genes are involved in imaginal disc morphogenesis. We previously found that loss of *Mcr,* when combined with a hypomorphic allele of *br,* results in defects in leg elongation (Ward, Evans, and Thummel 2003). This process of leg elongation is driven by changes in cell shape

and rearrangements that are regulated by modulating the actin cytoskeleton (Ward, Evans, and Thummel 2003). Additionally, during prehair extension in the pupal wing, there is a transient polarization of the tricellular junction protein Gliotactin and of Cor (Venema, Zeev-Ben-Mordehai, and Auld 2004). This polarization results in the alignment of these two junctional proteins along the A/P cell boundaries. Prior to and immediately following this event, they appear stably localized to the SJ, similar to their localization at stage 16 of embryogenesis. Loss of either Cor or Gli during this developmental event results in abnormal alignment of the wing bristles (Venema, Zeev-Ben-Mordehai, and Auld 2004). Our findings combined with evidence in the literature support the idea that SJ proteins are involved in morphogenesis throughout development by regulating cell shape changes, cell rearrangements, and planar polarity.

Our study of salivary gland organogenesis has further supported the finding that SJ genes contribute to cell shape changes and cell rearrangements. Loss of Mcr, Kune, and Cont leads to abnormal organ and lumen shape (Fig. 3.4). These phenotypes are due to defects in cell shape and cell rearrangements in the developing SG (Fig. 3.5, Table 3.3). Of the SJ mutant animals we examined, we observed a decrease in apical and increase in lateral membrane lengths associated with abnormal gland morphology (Table 3.3).

Currently, two genes have been identified as being involved in regulating apical membrane length during SG organogensis, *Pak1* and *Rho1*. Defects in these genes results in abnormal SG lumen size and shape (Pirraglia, Walters, and Myat 2010; N. Xu et al. 2011). *Pak1* was shown to regulate the size of the apical

membrane along the P/D axis of the SG by regulating the stabilization and localization of E-cadherin at the AJ (Pirraglia, Walters, and Myat 2010). In the absence of Pak1, endocytosis is disrupted leading to an inability to decrease the apical membrane domain during cell rearrangements resulting in an increase in apical surface to more than twice normal size (Pirraglia, Walters, and Myat 2010). This phenotype is different from that of *Rho1* mutants, which exhibit a failure to elongate the apical membrane along the P/D length of the gland (N. Xu et al. 2011). Our observations, taken together with the data presented by Pirraglia et al, (2010) and Xu et al., (2011) raise the possibility that a subset of SJ proteins may function along the lateral membrane to regulate cross talk between the *Rho1* and *Pak1* pathways during SG organogenesis to regulate cell shape changes that facilitate cellular rearrangements. It will be informative to examine vesicle trafficking during salivary gland organogenesis to determine if a group of SJ proteins contribute to trafficking, in a manner similar to SJ biogenesis.

We identified that defective cellular rearrangements is not isolated to the loss of SJ proteins in SG organogenesis but also DC in cor^{4} and Mcr^{1} mutant animals. Upon close examination, we identified that JNK signaling is active in SJ mutants but the actomyosin cable appears less organized raising the possibility that Dpp signaling may be attenuated in SJ mutants (Fig. 3.8). Additionally, we identified premature clusters of apoptotic cells and abnormal myosin organization in the AS of cor^{4} mutants (Fig. 3.6). This observation led us to conclude that SJ proteins are broadly expressed within the AS during DC. Myosin organization was also disrupted in the DME of $Nrx\text{-}IV^{4304}$ and cor^{4} animals. This disorganization likely contributes to

the scalloping observed in the DME. It is unclear at this time which of these phenotypes, or tissues, is causative of defective DC or if it is an accumulation of these abnormalities that leads to failure. To follow up on these findings and gain further understanding of the role of SJ genes in DC, it will be important to examine the loss of these SJ components in a tissue-specific manner using the GAL4-UAS system. Additionally, it will be informative to carefully examine Dpp signaling because a decrease in Dpp signaling would contribute to weak actomyosin cable assembly in the DME in addition to altering the pulsating contractions in the AS.

The process of dorsal closure is highly coordinated and requires communication between the AS and epithelium that leads to pulsing and ratcheting behaviors of the AS cells. These physical changes result in the propagation of forces throughout the AS that drives the tissue down into the embryo while the epithelium coordinately migrates toward the dorsal midline (Peralta et al. 2007; Blanchard et al. 2010; Millard and Martin 2008; Jacinto et al. 2000). This propagation of force must be stabilized at the lateral membrane to preserve the integrity of tissue. Similarly, during SG migration and cell rearrangement, cells must maintain contact and properly distribute cellular tension to facilitate cell movement. We hypothesize that SJ proteins function as cell adhesion molecules that extend along the lateral membrane of AS cells during DC and SG organogenesis to stabilize cell-cell contacts, allowing for a uniform and stable propagation of forces within the tissue. In the absence of these proteins, cells adjacent to highly dynamic cells would experience abnormal stress, in turn undergoing apoptosis or migrating abnormally. An

examination of the AS, using targeted laser ablation will provide insight into the role of SJ proteins in stabilizing cell-cell contacts and force propagation during DC.

It is important to note that there appears to be differences in the response to the loss of specific SJ proteins. In the SG, *Cont^{ex956} and Nrg^{14}* mutants do not display defects in lateral or apical membrane lengths as *Mcr^{1}* and *Kune^{C309}* mutants. (Table 3.3). However, they all have defects in cellular rearrangements, suggesting these groups regulate different mechanisms that contribute to cellular rearrangements during SG organogenesis (Table 3.3). Our cuticle data examining head involution and DC also shows variation in the penetrance of each phenotype among the different lines examined, for example 27.6% of *cor^{4}* mutants were found to be defective in DC compared to 5.1% of animals mutant for *Kune^{C309}* (Table 3.1). These differences clearly show that there is not simply one clear phenotype that applies to each and every mutant line. This variation could be due to maternal contribution, as stated earlier, or it could suggest that SJ proteins function in subcomplexes during different developmental time points. While SJ proteins are highly stable and localized to the region of the SJ late in embryogenesis, they exhibit a broad localization along the lateral membrane prior to SJ biogenesis. At the start of the assembly of the SJ, these proteins are dynamically trafficked within the cell while morphogenetic events such as DC, head involution, and SG organogenesis are taking place, prior to localizing to the junction. We propose that prior to the formation of the junction and later in development, SJ proteins are deployed as subcomplexes to carry out specific functions such as cell signaling, vesicle trafficking, and planar polarity.

The developmental events we examined all occur prior to the formation of a functional occluding junction. Therefore, the function of SJ proteins in morphogenesis is independent of their role in the occluding junction. These findings open interesting lines of questioning for the field regarding the fundamental cell biological role of this large group of lateral membrane proteins that coalesce into the SJ. After examining our results, it is interesting to step back and examine the frame in which the occluding junctions of vertebrates and invertebrates have been compared. These structures are functionally analogous and have some molecular components that are conserved; yet they are not equivalent. If we expand our thinking of the role of these proteins as having a larger function in regulating cellular and tissue events along the entire lateral membrane, it is possible that we will uncover a conserved function of these lateral membrane proteins that extend beyond their occluding function. It will be interesting to examine vertebrate orthologs of SJ proteins to test if this control of morphogenesis is conserved.

Section 3.5 Materials and Methods

Drosophila strains

Our analysis included the use of the following SJ mutant strains: cor^{4} (Ward, Lamb, and Fehon 1998), cor^{5} (Ward et al. 2001), $fasIII^{E25}$, $kune^{C309}$ (Nelson, Furuse, and Beitel 2010), Lac^{G00044}, $P\{EPgy2\}^{EY07421}$ (hereafter $Mcr^{EY07421}$), Nrg^{14} (S. G. Hall and Bieber 1997), Nrg^{17} (Paul et al. 2003), $nrv2^{ZCL1649}$ (Buszczak et al. 2007), $Nrx\text{-}IV^{4304}$ (Baumgartner et al. 1996), $Tsf2^{KG01571}$ (Tiklová et al. 2010), w^{1118}, *apterous (ap)-Gal4, daughterless (da)-Gal4*, *actin (act)-Gal4, UAS-Lach RNAi* (38895), *UAS-NrvRNAi* (28666), *UAS-SinuRNAi* (38258), *UAS-ContRNAi* (28923), all received from the Bloomington *Drosophila* Stock Center (BDSC), Bloomington, IN, USA, Mcr^{1} (Hall et al., 2014), $Cont^{ex956}$ (Faivre-Sarrailh et al. 2004) obtained from Manzoor Bhat (University of North Carolina, Chapel Hill, NC, USA). *Nrg-GFP* FlyTrap line G00305 and *Nrx-IV-GFP* FlyTrap line CA06597 were obtained from the FlyTrap consortium (Yale University School of Medicine, New Haven, CT, USA) (Morin et al. 2001). *fkh-GAL4*, *UAS-GFP* (L. Wang et al. 2008) was obtained from Arash Bashirullah (University of Wisconsin, Madison, WI, USA). *UAS-Nrg-RNAi* (v107991), *UAS-NrxRNAi* (v8353), *UAS-CorRNAi* (v9787), *UAS-Mcr-RNAi* (v100197), *UAS-AtpaRNAi* (v100619), *UAS-KuneRNAi* (v3962), *UAS-VariRNAi* v24156), were all obtained from Vienna *Drosophila* RNAi Center (VDRC), Vienna, Austria (Dietzl et al. 2007)

Immunohistochemistry and Immunoblotting

Embryos were prepared for antibody staining following methods described by Fehon et al., (1991). Embryonic staging was determined using DAPI,

morphological markers including formation of the gut, ventral furrow, segmental grooves, and head development. Immunostaining was completed using the following primary antibody dilutions: rat anti-α-Catenin (clone Dcat1, DSHB) 1:10, mouse anti-α-Spectrin (clone 3A9, DSHB) 1:16, mouse anti-Atpα (clone a5, DSHB) 1:50, mouse anti-Cor (clones C556.9 and C615.16, DSHB) 1:50, mouse anti-Crb (clone Cq4 concentrate, DSHB) 1:50, rat anti-DE-Cadherin (clone DCAD2, DSHB) 1:16, mouse anti-Dlg (clone 4F3, DSHB) 1:10, mouse anti-Fasciclin 3 (clone 7G10, DSHB) 1:100, mouse anti-Nrv (clone Nrv5F7, DSHB) 1:50 from the Developmental Studies Hybridoma Bank (DSHB) at the University of Iowa. Rabbit anti-Cont [(Faivre-Sarrailh et al., 2004) 1:1600 and mouse anti-Nrx-IV 1:400 (Baumgartner et al. 1996) gifts from Manzoor Bhat, University of Texas Health Sciences Center, San Antonio, TX, USA], guinea pig anti-Mcr (Hall et al., 2014) 1:400, guinea pig anti-Mtf [(Tiklova et al., 2010) gift from Christos Samakovlis, Stockholm University, Stockholm, Sweden] 1:500, mouse anti-Nrg [clone 1B7 (Bieber et al. 1989) gift from Nipam Patel, University of California, Berkeley, Berkeley, CA, USA] 1:10, mouse anti-Uif (Hall et al., 2014) 1:800, rabbit anti-GFP (Clontech, 632677) 1:800, DAPI 1:800. Secondary antibodies (Jackson ImmunoResearch Laboratories) were used at 1:800. Images were obtained using an Olympus FV1000 confocal microscope equipped with Fluoview software. ImageJ (Schneider, Rasband, and Eliceiri 2012) was used for cropping and rotation of photomicrographs used to compile figures in Adobe Illustrator (version CS6).

Quantitative Cuticle Analysis

Eggs were collected on AJ agar for four hours and subsequently aged for 48 hours. Embryos were collected that failed to crawl away after the 48 hour window. The embryos were placed on slides, dechorionated, mounted in Hoyer's medium, and stored on a slide warmer overnight.

Lethal Phase Analysis

Experiment was conducted to determine the stage at which mutant embryos arrest their development. All *Drosophila melanogaster* lines were crossed to balancers with a YFP marker for unambiguous identification of mutant and non-mutant embryos. Embryos were collected on apple juice agar plates with a smear of yeast paste for 1hr and aged for 17 hours at 25°C. Embryos were fixed and stained as described by Fehon et al., 1991 using a modified rotational speed of 150rpm to prevent shearing of the mutant embryos. Fisher's Exact Test was used for statistical analysis.

Organogenesis morphometric analysis and nuclear quantification

Confocal Z-series were collected of lateral view stage 16 salivary glands and analyzed as previously described (Chung and Andrew 2014).

Acknowledgements

We would like to thank Manzoor Bhat, Arash Bashirullah, the BDSC, and VDRC for fly stocks; Manzoor Bhat, Christos Samakovlis, Nipam Patel, and the DSHB for antibodies; and Brian Ackley for the use of his Olympus FV1000 confocal microscope.

Section 3.6 Figures

Figure 3.1

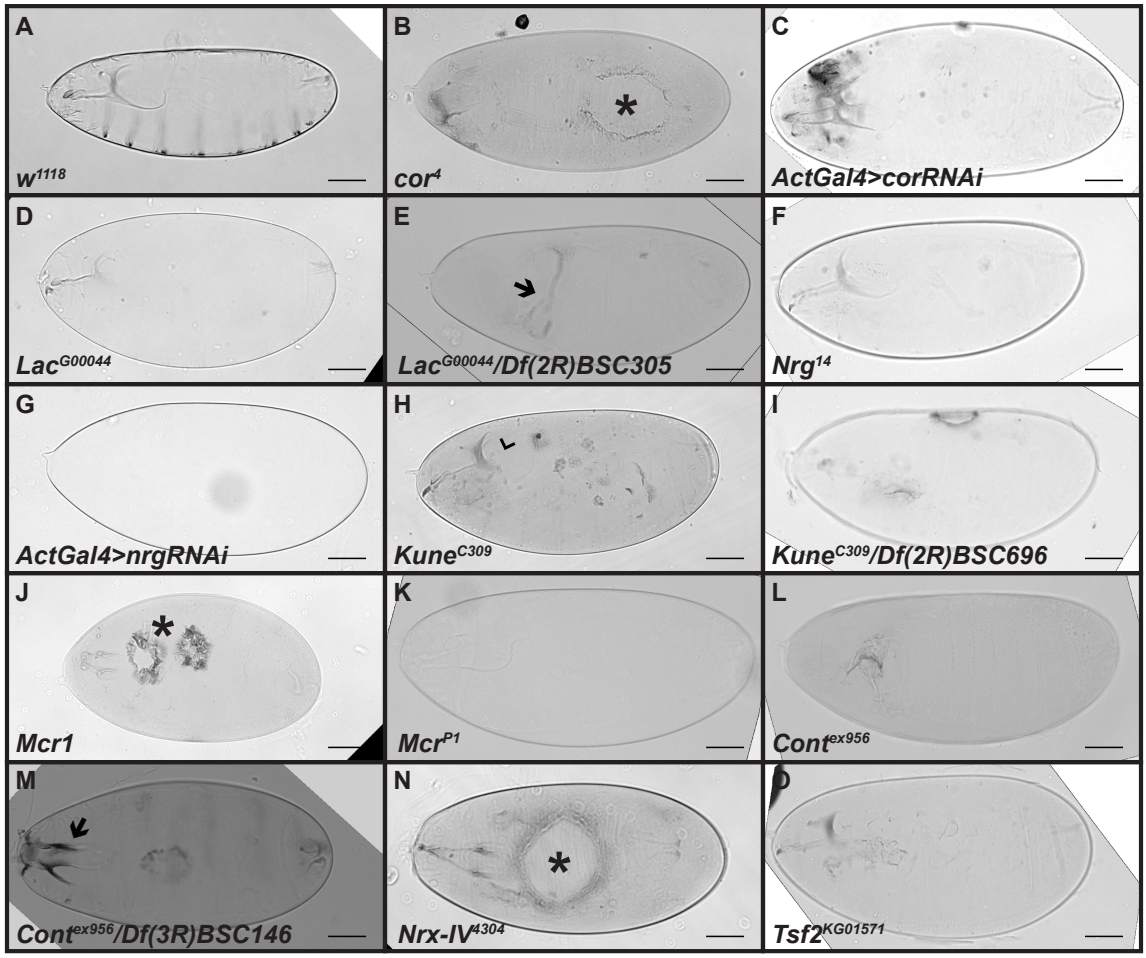

Figure 3.1

Mutations in SJ genes leads to defects in head involution and dorsal closure. Cuticle preparations of a w^{1118} (wild type) embryo (A), SJ mutant embryos (B, D, F, H, J, K, L, N, and O), transheterozygote embryos (E, I, and M), and *ActGal4*>SJ RNAi lines (C,G), all positioned with the anterior to the right and posterior to the left. The dorsal surface is positioned up or facing. Note the severe defects in head involution marked by arrows (E and M), defect in head skeleton morphology designated by arrowhead (H), and dorsal holes marked by asterisks. Scale bars 100um.

Figure 3.2

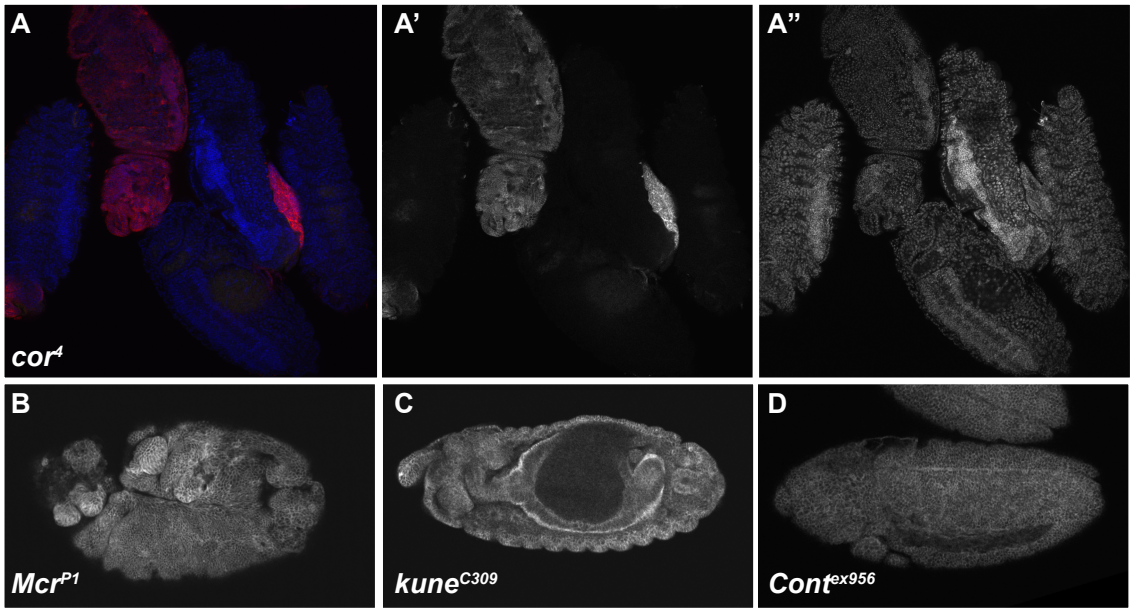

Figure 3.2

SJ mutant animals arrest their development prior to the formation of a functional occluding junction. Confocal optical sections of embryos stained with alpha-spectrin and DAPI (A) were staged using morphological markers. Mutant embryos were observed that failed to secrete a cuticle before stage 17 (A') and that arrested development at various developmental time points (B, C, and D).

Figure 3.3

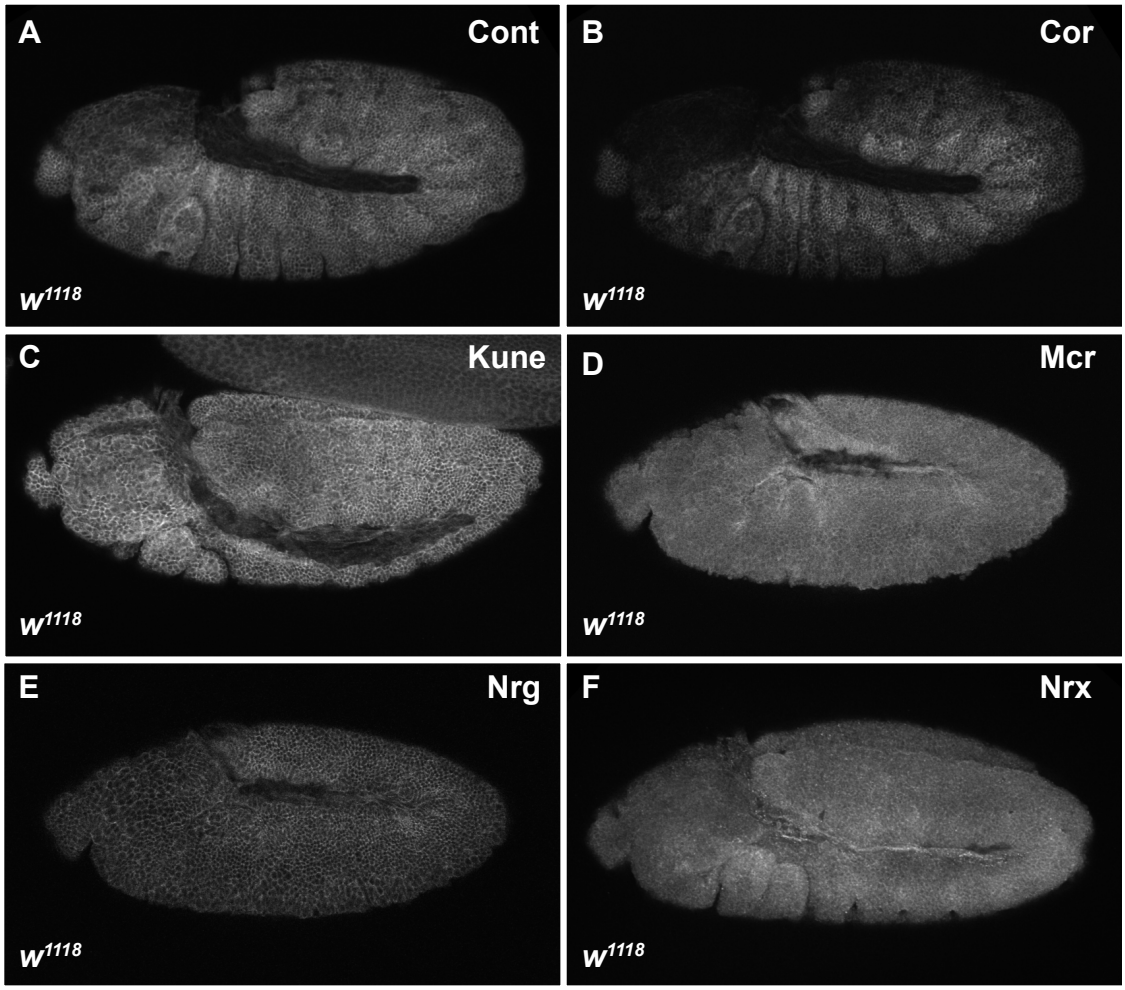
A
Cont
w^{1118}
B
Cor
w^{1118}
C
Kune
w^{1118}
D
Mcr
w^{1118}
E
Nrg
w^{1118}
F
Nrx
w^{1118}

Figure 3.3

SJ proteins are expressed and associated with the membrane at stage 10 of embryogenesis. Confocal sections of stage 10 and 11 w^{1118}embryos demonstrate that Contactin (A), Cor (B), Kune (C), Mcr (D), Nrg (E), and Nrx-IV(C') are expressed in the epithelium, where they appear to be associated with the membrane.

Figure 3.4

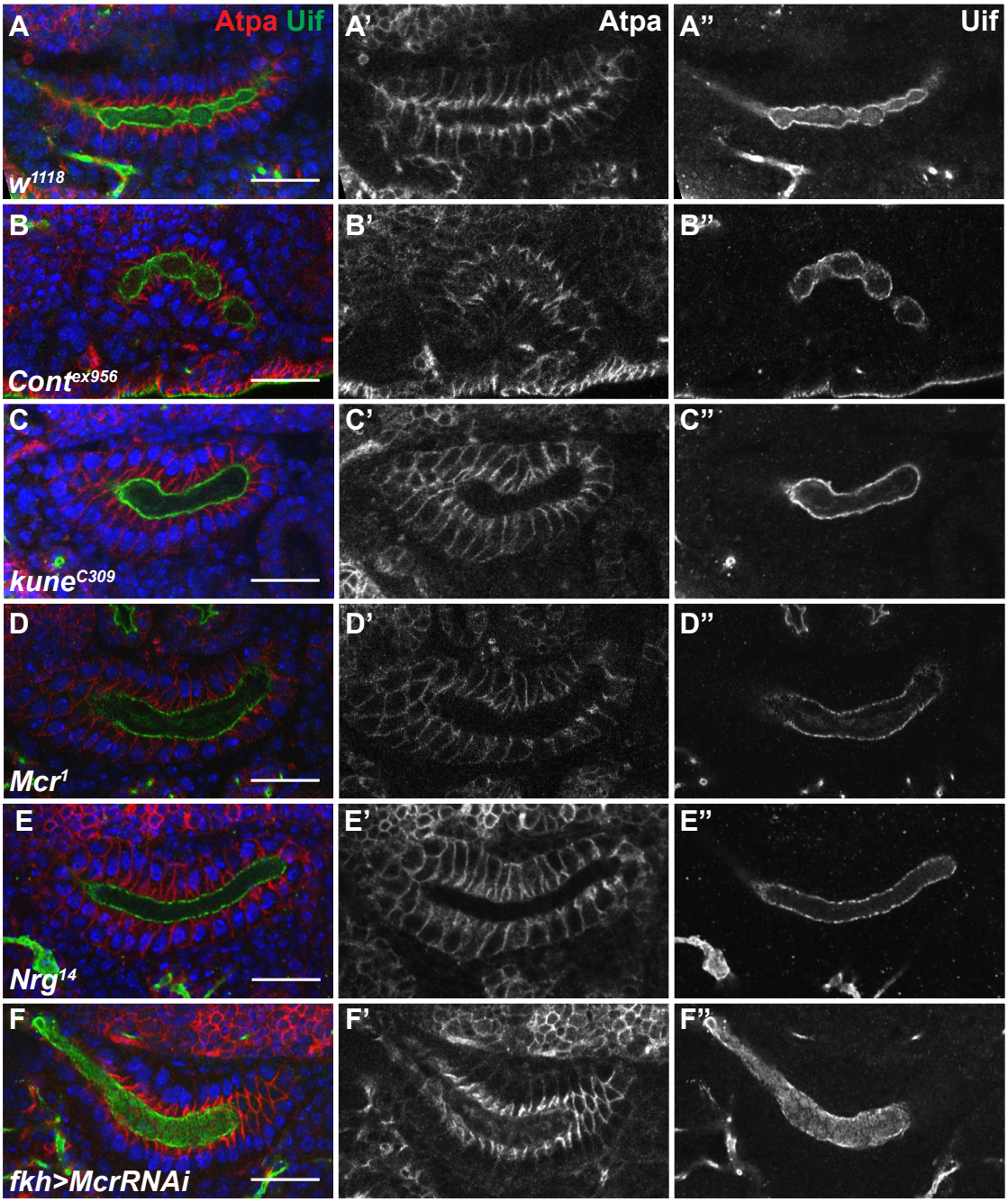
A
Atpa Uif
w1118
A'
Atpa
A''
Uif
B
Cont ex956
B'
B''
C
kune C309
C'
C''
D
Mcr 1
D'
D''
E
Nrg 14
E'
E''
F
fkh>McrRNAi
F'
F''

Figure 3.4

SJ mutant salivary glands exhibit abnormal morphology.

(A-F) Confocal optical sections were selected, from z-stacks used for quantification of SG phenotypes, that revealed the largest number of cells in cross-section with the lumen stained with Atp-alpha (A'-F') to outline cells and Uif (A"-F") to mark the apical membrane in contact with the lumen. w^{1118} (A) SGs have elongated glands with most cells visible at a single cross-section compared to $Cont^{ex956}$ (B), $kune^{C309}$ (C), and Mcr^{1} glands. Nrg^{14} glands have a similar elongation as wild type. Scale bars: 20um

Figure 3.5

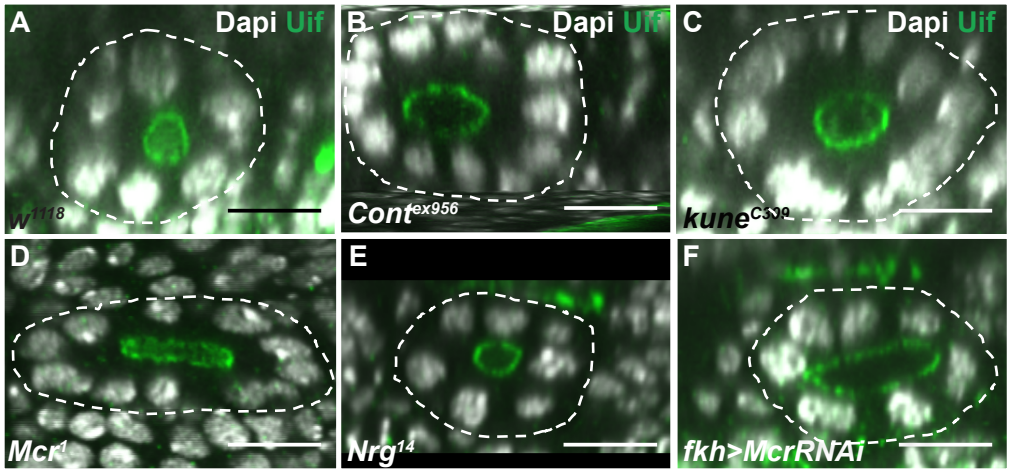
A
Dapi Uif
w1118
B
Dapi Uif
Cont ex956
C
Dapi Uif
kune C539
D
Mcr1
E
Nrg14
F
fkh>McrRNAi

Figure 3.5

Mutations in SJ genes lead to abnormal cellular rearrangements during SG organogenesis. Confocal z-series rendered in xz transverse cross-section stained with Uif to mark the apical membrane in contact with the lumen and DAPI to label the nuclei reveals a higher number of cells in (B) $Cont^{ex956}$,(C) $kune^{c309}$, (D) Mcr^{1}, and (E) *fkh>McrRNAi* but not (E) Nrg^{14} SGs when compared to (A) w^{1118}. Scale bars: 100 pixels.

Figure 3.6

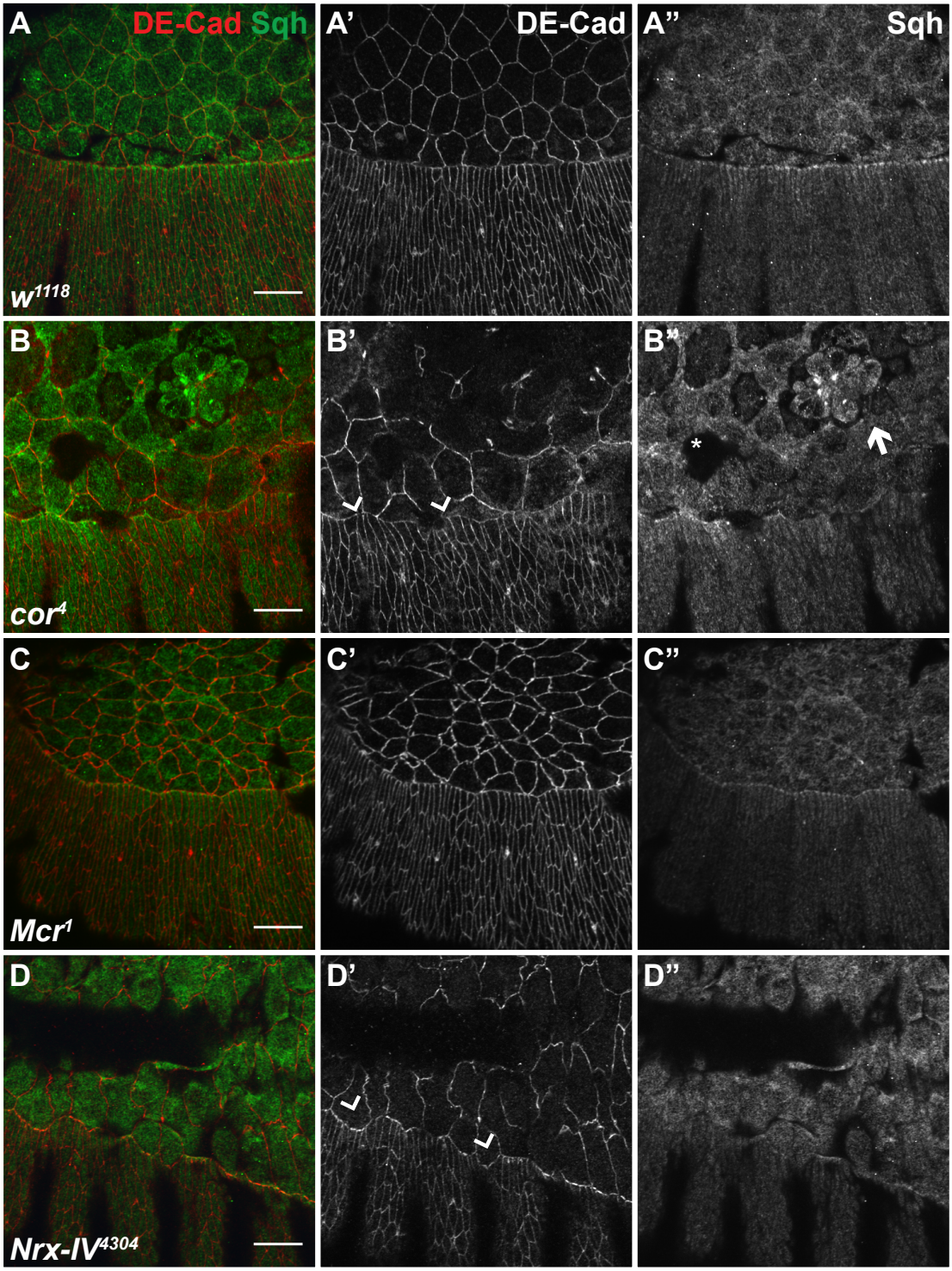
A
DE-Cad Sqh
A'
DE-Cad
A''
Sqh
w1118
B
B'
B''
cor4
C
C'
C''
Mcr1
D
D'
D''
Nrx-IV4304

Figure 3.6

Loss of *coracle* and *Neurexin-IV* leads to abnormal DME organization and a loss of AS integrity. Confocal sections of stage 13 embryos immunostained with DE-Cad and Sqh show (A) w^{1118} embryos have an organized DME with DE-Cad (A') at the leading edge and evenly spaced clusters of Sqh (A") indicating that migration of the lateral epidermis is uniform. In comparison, animals mutant for *cor* (B) and *Nrx-IV* (D) show scalloping of the DME (arrowheads) when stained with DE-Cad (B' and D'). Slight scalloping of the DME is also observed in (C') Mcr^{1}. Sqh staining (A"-D") reveals regions of apoptotic cells (B", arrow) and individual cells in cor^{4} (B) animals that appear to lack medial apical Sqh staining (B", asterisk).

Figure 3.7

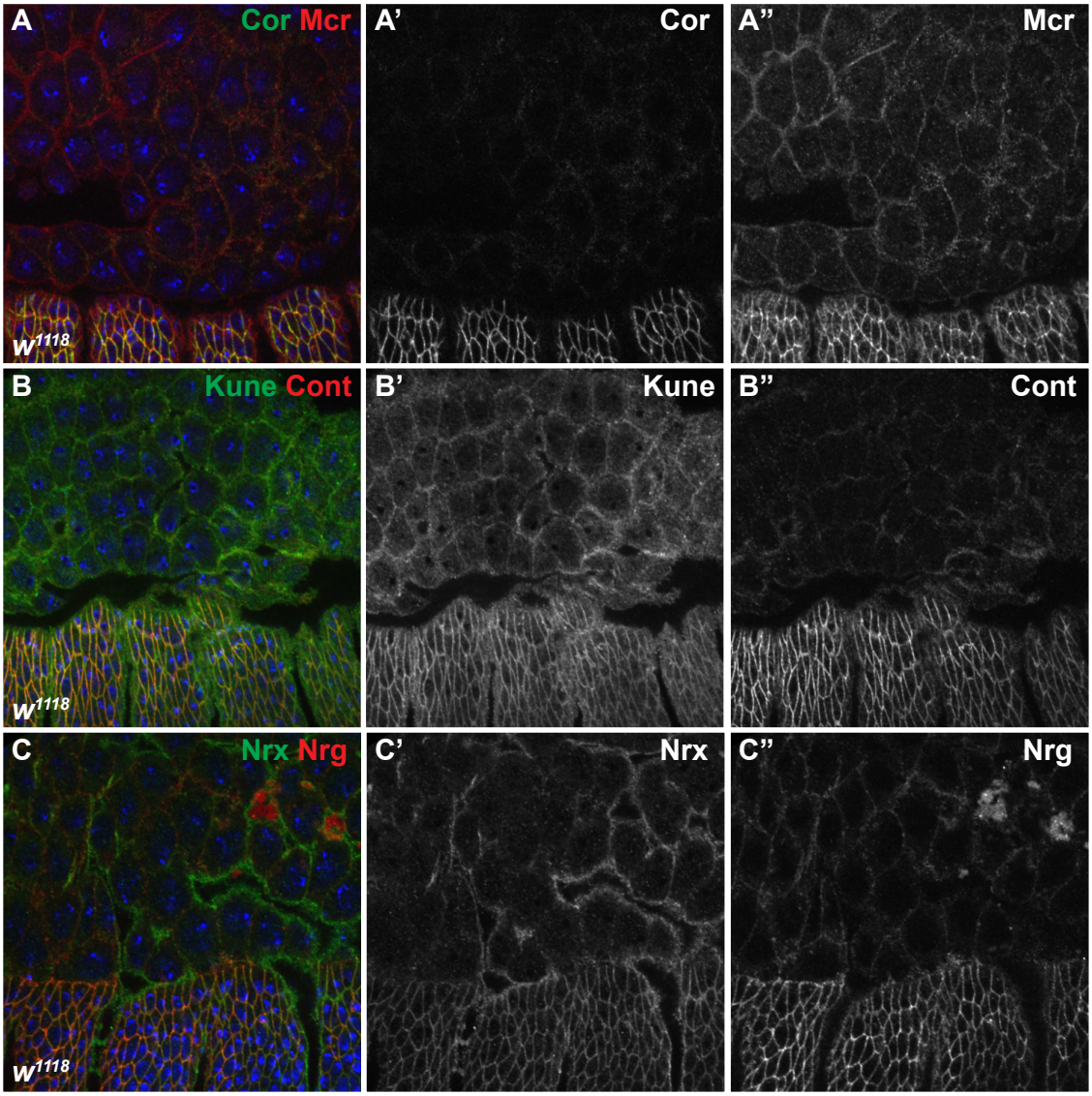
A
Cor Mcr
w1118
A'
Cor
A"
Mcr
B
Kune Cont
w1118
B'
Kune
B"
Cont
C
Nrx Nrg
w1118
C'
Nrx
C"
Nrg

Figure 3.7

SJ proteins are expressed in the AS at the start of DC. Confocal sections of stage 12 w^{1118}embryos demonstrate that Cor (A'), Mcr (A"), Kune (B'), Cont (B"), Nrx-IV(C') and Nrg (C") are expressed in the AS, where they appear to be associated with the membrane.

Figure 3.8

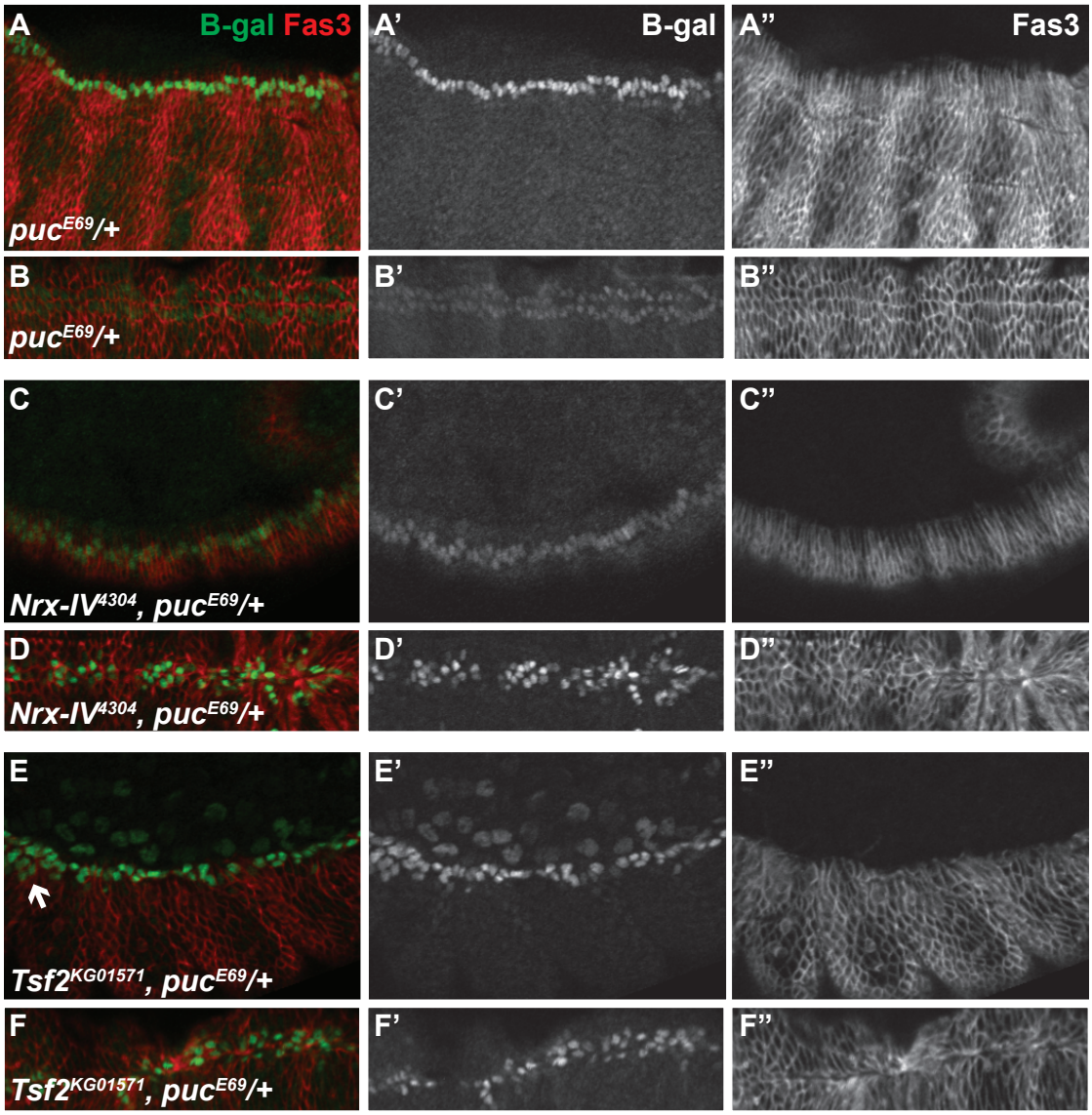
A
B-gal Fas3
puc^E69/+
A'
B-gal
A''
Fas3
B
puc^E69/+
B'
B''
C
Nrx-IV^4304, puc^E69/+
C'
C''
D
Nrx-IV^4304, puc^E69/+
D'
D''
E
Tsf2^KG01571, puc^E69/+
E'
E''
F
Tsf2^KG01571, puc^E69/+
F'
F''

Figure 3.8

JNK signaling is active in SJ mutant animals.

Embryos immunostained with β-gal (A-F, green), to label the expression of LacZ from the enhancer trap at the *puc* locus, and Fas3 (A-F, red) to outline cells indicates that *puc* is expressed in the DME w^{1118} (A'), $Nrx\text{-}IV^{4304}$ (C'), and $Tsf2^{KG01571}$ (E') at stage 13 when JNK activation is required. Organization of puc expressing cells appears abnormal in the SJ mutants (E', arrow). DC defects are present at a moderate level in $Nrx\text{-}IV^{4304}$ and $Tsf2^{KG01571}$ mutants. At stage 16, animals selected due to successful closure, demonstrate puckering and misalignment at the midline (compare D and F with A) indicating that DC has not occurred correctly.

Figure 3.9

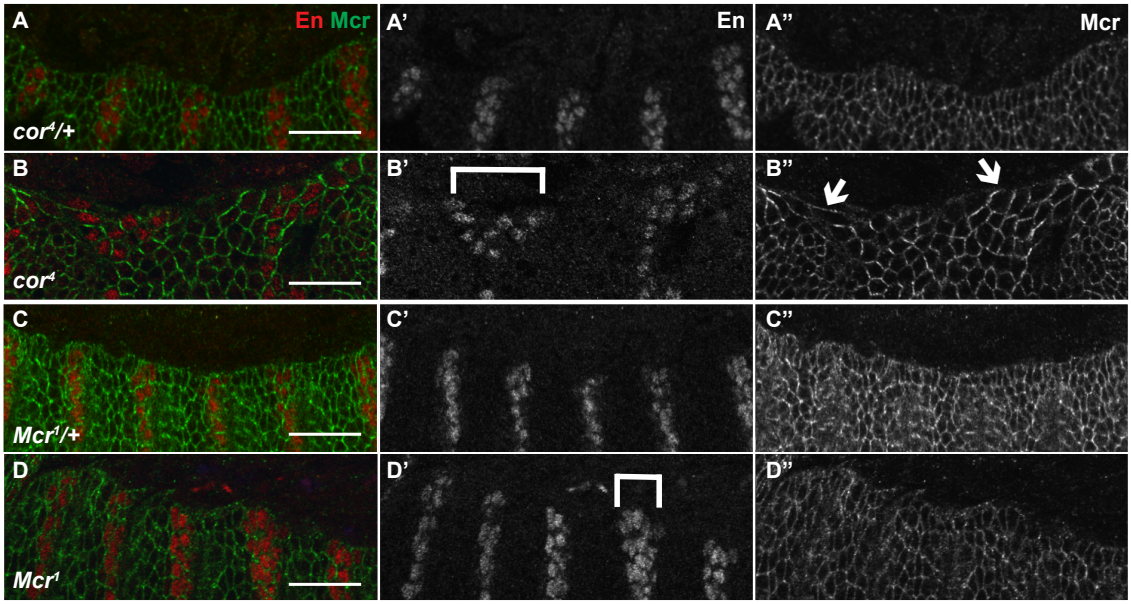

Figure 3.9

SJ mutant animals exhibit abnormal cellular rearrangements and cell shapes in the epithelium during DC. Animals heterozygous for either *cor*^{4} (A) or *Mcr*^{1} (C) were compared to their homozygous siblings (B and D) immunostained for En to label the posterior cells (red and A'-D') and Mcr (green and A"-D"). Animals with mutations in *cor* and *Mcr* exhibit an increased number of En positive cells (brackets B and D) at the DME, indicating that these cells do not maintain their position as the three most posterior cells in each segment, as observed in the heterozygotes (compare A' and C' to B' and D'). Additionally, *cor*^{4} (B") and *Mcr*^{1} (D") mutants exhibit abnormally shaped lateral epithelial cells that do not maintain the elongated and organized structure of their heterozygous siblings (A" and C"), indicating that SJ proteins play a role in acquiring or maintaining proper cell shape during DC.

Tables

Table 3.1

	Empty Phenotype (%)	Dorsal Closure Defective (%)	Head Involution Defective (%)
cont$^{[ex956]}$	22.4 ± 8.6	5.9 ± 1.4	68.7 ± 27.1
Df(3R)BSC146 / cont$^{[ex956]}$	21.3 ± 13.8	6.2 ± 1.9	46.2 ± 14.6
cor$^{[4]}$	53.5 ± 4.5	27.6 ± 2.9	80.5 ± 17.3
kune$^{[C309]}$	50.7 ± 4.5	5.1 ± 5.7	87.2 ± 12.8
Df(2R)BSC696 / kune$^{[C309]}$	31.4 ± 8.0	6.3 ± 2.6	55.8 ± 20.0
Lac$^{[G00044]}$	61.5 ± 12.0	2.6 ± 2.5	81.4 ± 25.4
Df(2R)BSC305 / Lac$^{[G00044]}$	42.9 ± 10.7	5.5 ± 2.7	78.1 ± 5.1
Mcr$^{[1]}$	47.3 ± 19.3	19.5 ± 11.2	97.5 ± 4.2
Mcr$^{[EY07421]}$	28.9 ± 6.5	1.1 ± 1.2	74.7 ± 15.9
Nrg$^{[17]}$	64.6 ± 26.8	1.6 ± 1.4	99.6 ± 0.6
Act5c>nrgRNAi	73.3 ± 33.0	0.9 ± 1.3	72.6 ± 15.1
nrv2$^{[ZCL1649]}$	26.4 ± 16.9	3.0 ± 2.1	96.9 ± 6.3
Nrx-IV$^{[4304]}$	25.4 ± 16.1	41.4 ± 16.9	95.8 ± 3.8
Tsf2[$^{KG01571]}$	26.2 ± 27.3	5.2 ± 3.6	100 ± 0

Table 3.1

All SJ mutant lines show some penetrance of head involution and dorsal closure defects. Mean ± s.e.m. from a minimum of three independent experiments.

Table 3.2

Genotype	Stages 10-15 (%)	Stages 16-17 (%)
Cont^{ex956}	27 ***	73
Cont^{ex956}/TM6b YFP	2	98
cor^{4}	33 ***	67
cor^{4}/CyO YFP	0	100
kune^{C309}	23 *	77
kune^{C309}/CyO YFP	12	88
Lac^{G00044}	5	95
Lac^{G00044}/CyO YFP	1	99
Mcr^{1}	9 ***	91
Mcr^{1}/CyO YFP	0	100
Mcr^{EY07421}	19 ***	81
Mcr^{EY07421}/CyO YFP	1	99
Tsf2^{KG01571}	6 **	94
Tsf2^{KG01571}/TM6b YFP	1	99
Nrg^{14}	31 **	69
Nrg^{14}/FM7c YFP	7	93
nrv2^{ZCL1649}	21 ***	79
nrv2^{ZCL1649}/CyO YFP	4	96
Nrx-IV^{A304}	7 **	93
Nrx-IV^{A304}/TM6b YFP	1	99

Table 3.2

SJ homozygous mutant animals show a statistically different percentage of arrested development than their heterozygous siblings, except *Lac^{G00044}* animals. * $p \leq 0.05$, ** $p \leq 0.001$, *** $p \leq 0.00001$

Table 3.3

Genotype	Number of nuclei around lumenal cross section	Average length of lateral membrane	Average length of apical membrane	Salivary gland P/D length	Salivary gland D/V length
w^{1118}	7.5 ± 0.3 (10)	8.7 ± 0.6	4.6 ± 0.3	85.4 ± 5.5	25.7 ± 2.1
$cont^{ex956}$	9.9 ± 0.9 (10)**	8.6 ± 0.9	4.5 ± 0.4	84.4 ± 6.0	26.3 ± 2.9
$Kune^{C309}$	10.1 ± 1.6 (10)**	9.9 ± 1.3*	4.3 ± 0.5	88.7 ± 11.0	27.7 ± 2.3*
fkh>KuneRNAi	9.4 ± 0.6 (10)**	10.6 ± 1.0**	3.3 ± 0.3**	80.2 ± 8.1	28.7 ± 2.9
Mcr^{1}	9.2 ± 1.1 (10)**	10.1 ± 1.3*	3.9 ± 0.5**	84.3 ± 23.3	28.6 ± 2.8*
fkh>McrRNAi	9.0 ± 1.2 (10)**	10.0 ± 0.7**	3.8 ± 0.5**	83.7 ± 6.2	28.3 ± 3.8*
Nrg^{14}	8.4 ± 1.3 (10)*	8.1 ± 1.3	4.2 ± 0.7	87.6 ± 13.7	22.7 ± 3.2

Table 3.3

***Mcr*^{1} and *Kune*^{C309} SGs have decreased apical and increased lateral membranes.** * $p \leq 0.05$, **$p \leq 0.001$, $p \leq 0.0001$

Chapter IV
Concluding remarks and future directions

Section 4.1 Concluding remarks and future directions

Our findings provide insight into the requirement for SJ proteins during morphogenesis and raise a number of interesting questions for the field to explore. In chapter II, we identified a novel core component of the SJ, *Macroglobulin complement related (Mcr),* in a screen for imaginal disc morphogenesis*.* We revealed an interdependence between two core components of the SJ for occluding function, *Neuroglian (Nrg)* and *Mcr*. In the absence of Mcr, Nrg is no longer localized at the membrane and vice versa, at stage 16 of embryogenesis. Interestingly, if we examine mutant embryos at stage 10, we observe that in these mutant backgrounds, the interdependent protein still localizes to the membrane but is gradually lost during SJ biogenesis. We believe this suggests that the interdependence of these proteins is specific to their role in the SJ and raises the possibility that they function independently of each other at earlier stages of development.

Additionally, we identified that the degree of interdependence between core components of the SJ exhibit variation based upon the tissue being examined. This finding identifies a need for future analyses to be conducted in a tissue-specific manner to identify physical interactions and to further understand the subcellular role of individual SJ genes. Using this approach will also allow for further understanding of the cellular function of genes, such as *Mcr*, that have roles in different biological processes such as SJ organization and function and innate immunity.

The identification of a gene involved in the regulation of paracellular flow between epithelial cells also involved in the regulation of morphogenesis was

surprising. This finding brought into question how *Mcr* contributes to morphogenesis and if this was a pleiotropic effect of *Mcr* or a broader requirement of genes involved in the SJ. A careful analysis of the literature and examination of terminal cuticle phenotypes revealed that SJ genes are involved in morphogenesis throughout development and that this role is independent of their function in the SJ. Using dorsal closure (DC) and salivary gland (SG) organogenesis as models, we concluded in chapter III that SJ proteins contribute to morphogenesis by regulating cell shape changes and rearrangements.

It is important to point out, however, that our data suggests that not all SJ genes function to regulate both cell shape changes and rearrangements. In the context of SG organogenesis, we observe a noticeable difference in the phenotypes of Nrg^{14} and $Cont^{ex956}$ mutants compared with Mcr^{1} and $Kune^{C309}$ mutant animals. This variation in phenotypes could be due to strength of the allele used, maternal contribution, or could indicate that these proteins function in subcomplexes to regulate different cellular mechanisms. Our data suggests that *Mcr, Cont, Kune,* and *Nrg* are required for cellular rearrangements but in the absence of *Nrg* and *Cont,* cell shape is not dramatically altered as it is in the absence of *Mcr* and *Kune*. Using this assay to analyze other SJ mutants, it will be possible to further clarify how SJ genes regulate cell shape changes or rearrangements. Identification of SJ genes in regulating cell shape changes and rearrangements is a novel finding that opens the field to new lines of investigation of the roles of this large group of lateral membrane proteins in regulating morphogenesis. We propose that these proteins function as one complex or as multiple subcomplexes to regulate adhesion along the

lateral membrane, affecting signaling through vesicle trafficking, and/or directly regulating the cytoskeleton.

Recently, a resource was created by Dunst et al. (2015) that allows for the examination of membrane trafficking using endogenously labeled Rab proteins. To examine the role of SJ proteins in regulating signaling through vesicle trafficking, it will be beneficial to cross these labeled Rab lines into SJ mutant backgrounds to examine the dynamics and location of Rab labeled vesicles. Changes in Rab localization or dynamics, using live imaging and fixed tissues, would suggest that SJ proteins either regulate the trafficking of Rabs or possibly function as a scaffolding for vesicle docking. This examination can be extended by inhibiting trafficking using dominant negative Rabs to look for alterations in the trafficking and localization of SJ proteins. Combined with co-localization studies, this will allow for further understanding of how SJ proteins are trafficked in different pathways at different developmental time periods.

Another promising area of study to examine is the role of SJ proteins in regulating cell adhesion. The broad lateral membrane location of SJ proteins, prior to coalescing into the SJ, may allow for this large group of transmembrane adhesion molecules to stabilize cell-cell contacts during developmental events that require dynamic cell shape changes and rearrangements. This may aid in distributing forces during apical membrane constriction or tissue level force propagation to drive morphogenetic events. To examine this possibility, laser ablation may be used to measure the rate of recoil of cell membranes in the absence of SJ components compared with wild type. If the cells are less adhesive in the absence of laterally

localized SJ components, a lower rate of recoil would be expected. Cell adhesion is a major player in regulating cell shape changes and cell rearrangements. We suggest that the dynamic relocalization of SJ proteins during SJ biogenesis serves to regulate cell adhesion by modulating lateral membrane stiffness during cell shape changes and rearrangements.

Finally, individual SJ components may directly interact with cytoskeletal components to regulate cytoskeletal dynamics. We suggest further examining the role of SJ genes in SG morphogenesis to investigate their connection to the cytoskeleton during morphogenesis. *Rho1* was identified by Xu et al. (2008 and 2011) to regulate invagination, migration, and lumen size of the SG by regulating actin polymerization and apical membrane elongation. A loss of *Rho1* results in a failure to expand the apical membrane, which leads to abnormal cellular rearrangements. This phenotype is similar to that of Mcr^{1} and $Kune^{C309}$ mutants, raising the possibility that these genes function in the same or redundant pathway with *Rho1*. Conducting epistasis experiments should allow for further understanding of how these genes interact. Xu et al., (2011) provided a model of two parallel pathways where Rho1 and Rok function together to inhibit Cofilin, allowing for the polymerization of actin and the correct localization of F-actin, contributing to both elongation of apical membrane and cellular rearrangements. In the suggested parallel pathway, Rho1 in conjunction with Rib, limits p-Moe, leading to apical membrane elongation. Based on our findings, Mcr, Kune, Cont, and Nrg would all function in the first proposed pathway downstream of Rho1, because crumbs localizes normally in the absence of SJ proteins, but not in the absence of Rho1 (Fig.

4.1). *Mcr* and *Kune* potentially lie upstream of actin polymerization where they regulate both cell rearrangements and apical membrane elongation. *Cont* and *Nrg* also function to regulate cell rearrangements but not apical membrane length, most likely placing them downstream of *Mcr* and *Kune*. Additionally, if SJ genes are involved in actin polymerization examining cell rearrangements and apical membrane elongation in animals mutant for SJ genes and a loss of function allele for *Cofilin*, which would prevent depolymerization of actin (Xu et al., 2011) could be useful. If the rearrangement and apical membrane elongation phenotypes are suppressed, it would suggest that the SJ component being examined plays a role in regulating actin polymerization. It is possible that these SJ proteins function in a separate redundant pathway or in various combinations within and outside of the Rho1 pathway.

A redeployment of SJ proteins that have the ability to directly interact with cytoskeletal components would allow for these proteins to have a direct regulation of changes in cell shape, orientation of the plane of cell division, or polarize cells undergoing rearrangement. The localization of SJ proteins to the region of the SJ may act to sequester these proteins, limiting their ability to regulate the distribution of forces through adhesion, alter vesicle trafficking to regulate signaling events, and to contribute to cytoskeletal changes. Further investigation into the role of SJ genes in regulating these processes will greatly contribute to extending our understanding of the regulation of foundational biological mechanisms that contribute to development.

Figures

Figure 4.1

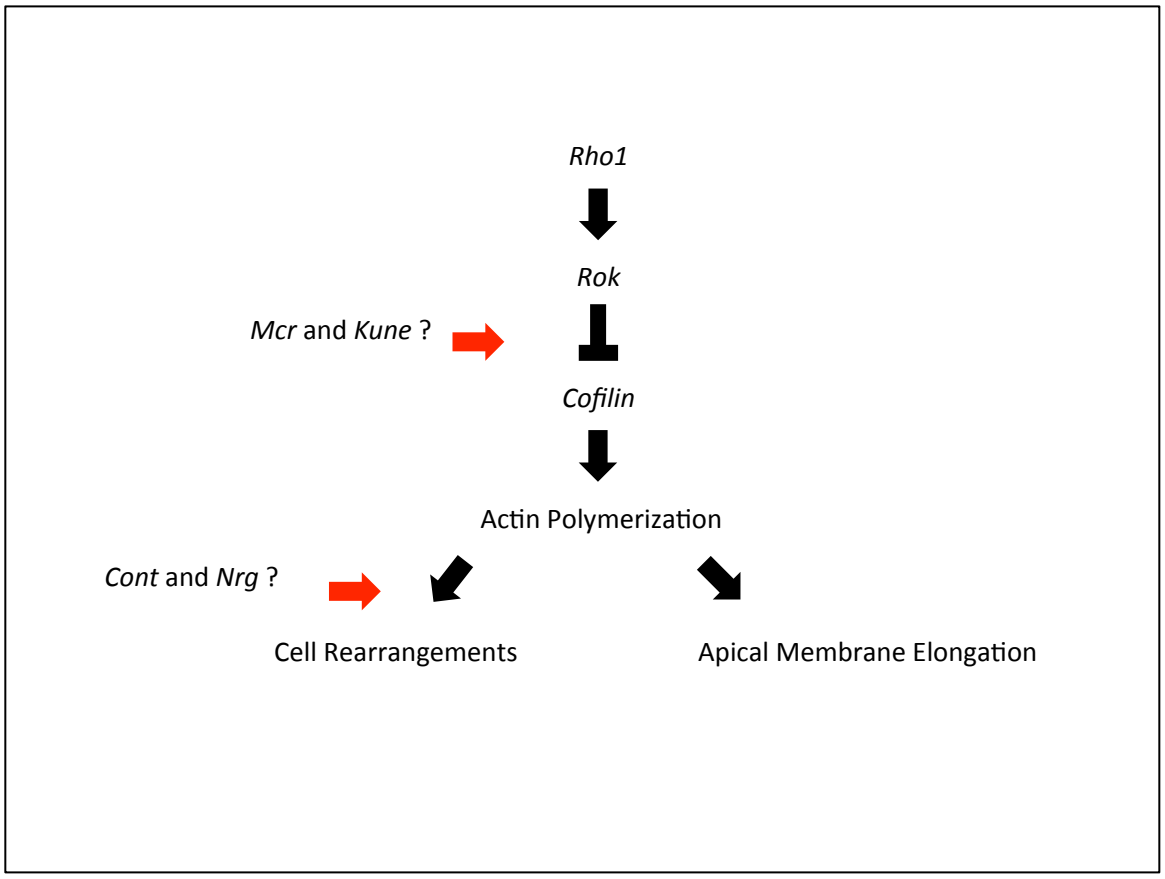

Figure 4.1 Model of SJ genes in regulating SG organogenesis Modified from Xu et al. (2011). *Rho1* and *Rok* function together to inhibit *Cofilin* allowing for the polymerization of actin. We predict that *Mcr* and *Kune* function upstream of actin polymerization, possibly with *Rho1* and *Rok* influencing both cellular rearrangements and apical membrane elongation. Our results support a model where *Cont* and *Nrg* function downstream of actin polymerization where they influence cell rearrangements but not apical membrane elongation.

References

Armstrong, P B, and J P Quigley. 1999. "Alpha2-Macroglobulin: An Evolutionarily Conserved Arm of the Innate Immune System." *Developmental and Comparative Immunology* 23 (4-5): 375–390.

Baumgartner, S, J T Littleton, K Broadie, M a Bhat, R Harbecke, J a Lengyel, R Chiquet-Ehrismann, a Prokop, and H J Bellen. 1996. "A Drosophila Neurexin Is Required for Septate Junction and Blood-Nerve Barrier Formation and Function." *Cell* 87 (6) (December 13): 1059–68. http://www.ncbi.nlm.nih.gov/pubmed/8978610.

Behr, Matthias, Dietmar Riedel, and Reinhard Schuh. 2003. "The Claudin-like Megatrachea Is Essential in Septate Junctions for the Epithelial Barrier Function in Drosophila." *Developmental Cell* 5 (4) (October): 611–20. http://www.ncbi.nlm.nih.gov/pubmed/14536062.

Bender, R C, and C J Bayne. 1996. "Purification and Characterization of a Tetrameric Alpha-Macroglobulin Proteinase Inhibitor from the Gastropod Mollusc Biomphalaria Glabrata." *The Biochemical Journal* 316 (Pt 3: 893–900.

Bieber, a J, P M Snow, M Hortsch, N H Patel, J R Jacobs, Z R Traquina, J Schilling, and C S Goodman. 1989. "Drosophila Neuroglian: A Member of the Immunoglobulin Superfamily with Extensive Homology to the Vertebrate Neural Adhesion Molecule L1." *Cell* 59 (3): 447–460. doi:10.1016/0092-8674(89)90029-9.

Blanchard, Guy B, Sughashini Murugesu, Richard J Adams, Alfonso Martinez-Arias, and Nicole Gorfinkiel. 2010. "Cytoskeletal Dynamics and Supracellular Organisation of Cell Shape Fluctuations during Dorsal Closure." *Development (Cambridge, England)* 137 (16): 2743–2752. doi:10.1242/jcs.078279.

Blasig, I. E., L. Winkler, B. Lassowski, S. L. Mueller, N. Zuleger, E. Krause, G. Krause, K. Gast, M. Kolbe, and J. Piontek. 2006. "On the Self-Association Potential of Transmembrane Tight Junction Proteins." *Cellular and Molecular Life Sciences* 63 (4): 505–514. doi:10.1007/s00018-005-5472-x.

Bou Aoun, Richard, Charles Hetru, Laurent Troxler, Daniel Doucet, Dominique Ferrandon, and Nicolas Matt. 2011. "Analysis of Thioester-Containing Proteins during the Innate Immune Response of Drosophila Melanogaster." *Journal of Innate Immunity* 3 (1) (January): 52–64. doi:10.1159/000321554. http://www.pubmedcentral.nih.gov/articlerender.fcgi?artid=3031515&tool=pmcentrez&rendertype=abstract.

Bradley, Pamela L., Monn Monn Myat, Christy a. Comeaux, and Deborah J. Andrew. 2003. "Posterior Migration of the Salivary Gland Requires an Intact Visceral

Mesoderm and Integrin Function." *Developmental Biology* 257 (2): 249–262. doi:10.1016/S0012-1606(03)00103-9.

Buszczak, Michael, Shelley Paterno, Daniel Lighthouse, Julia Bachman, Jamie Planck, Stephenie Owen, Andrew D. Skora, et al. 2007. "The Carnegie Protein Trap Library: A Versatile Tool for Drosophila Developmental Studies." *Genetics* 175 (3): 1505–1531. doi:10.1534/genetics.106.065961.

Charles, Perrine, Steven Tait, Catherine Faivre-Sarrailh, Gilles Barbin, Frank Gunn-Moore, Natalia Denisenko-Nehrbass, Anne Marie Guennoc, Jean Antoine Girault, Peter J. Brophy, and Catherine Lubetzki. 2002. "Neurofascin Is a Glial Receptor for the paranodin/Caspr-Contactin Axonal Complex at the Axoglial Junction." *Current Biology* 12 (3): 217–220. doi:10.1016/S0960-9822(01)00680-7.

Chow, D a R C, and John G Forte. 1995. "Functional Significance of the Beta Subunit for Heterodimeric P-Type ATPases." *The Journal of Experimental Biology* 198: 1–17.

Chung, Seyeon, and Deborah J Andrew. 2014. "Cadherin 99C Regulates Apical Expansion and Cell Rearrangement during Epithelial Tube Elongation." *Development (Cambridge, England)* 141 (9): 1950–60. doi:10.1242/dev.104166. http://www.ncbi.nlm.nih.gov/pubmed/24718992.

Cibrián-Uhalte, Elena, Adam Langenbacher, Xiaodong Shu, Jau Nian Chen, and Salim Abdelilah-Seyfried. 2007. "Involvement of Zebrafish Na+,K+ ATPase in Myocardial Cell Junction Maintenance." *Journal of Cell Biology* 176 (2): 223–230. doi:10.1083/jcb.200606116.

David, Daryl J V, Alisa Tishkina, and Tony J C Harris. 2010. "The PAR Complex Regulates Pulsed Actomyosin Contractions during Amnioserosa Apical Constriction in Drosophila." *Development (Cambridge, England)* 137 (10): 1645–1655. doi:10.1242/dev.044107.

De Matos Simões, Sérgio, Avantika Mainieri, and Jennifer a. Zallen. 2014. "Rho GTPase and Shroom Direct Planar Polarized Actomyosin Contractility during Convergent Extension." *Journal of Cell Biology* 204 (4): 575–589. doi:10.1083/jcb.201307070.

Dietzl, Georg, Doris Chen, Frank Schnorrer, Kuan-Chung Su, Yulia Barinova, Michaela Fellner, Beate Gasser, et al. 2007. "A Genome-Wide Transgenic RNAi Library for Conditional Gene Inactivation in Drosophila." *Nature* 448 (7150): 151–156. doi:10.1038/nature05954.

Faivre-Sarrailh, Catherine, Swati Banerjee, Jingjun Li, Michael Hortsch, Monique Laval, and Manzoor a Bhat. 2004. "Drosophila Contactin, a Homolog of Vertebrate Contactin, Is Required for Septate Junction Organization and Paracellular Barrier Function." *Development (Cambridge, England)* 131 (20) (October): 4931–42. doi:10.1242/dev.01372. http://www.ncbi.nlm.nih.gov/pubmed/15459097.

Farquhar, Marilyn G., and George E. Palade. 1963. “JUNCTIONAL COMPLEXES IN VARIOUS EPITHELIA Downloaded from Jcb . Rupress . Org on November 16 , 2012 Fixation and Processing of Tissue.” *The Journal of Cell Biology*: 375–412.

Fehon, R G, I a Dawson, and S Artavanis-Tsakonas. 1994. “A Drosophila Homologue of Membrane-Skeleton Protein 4.1 Is Associated with Septate Junctions and Is Encoded by the Coracle Gene.” *Development (Cambridge, England)* 120: 545–557.

Furuse, Mikio. 2010. “Molecular Basis of the Core Structure of Tight Junctions” 2 (1): 14. doi:10.1101/cshperspect.a002907.

Furuse, Mikio, Hiroyuki Sasaki, and Shoichiro Tsukita. 1999. “Manner of Interaction of Heterogeneous Claudin Species within and between Tight Junction Strands.” *Journal of Cell Biology* 147 (4): 891–903. doi:10.1083/jcb.147.4.891.

Géminard, Charles, Nicanor González-Morales, Jean Baptiste Coutelis, and Stéphane Noselli. 2014. “The Myosin ID Pathway and Left-Right Asymmetry in Drosophila.” *Genesis* 52 (6): 471–480. doi:10.1002/dvg.22763.

Genova, Jennifer L, and Richard G Fehon. 2003. “Neuroglian, Gliotactin, and the Na+/K+ ATPase Are Essential for Septate Junction Function in Drosophila.” *The Journal of Cell Biology* 161 (5) (June 9): 979–89. doi:10.1083/jcb.200212054. http://www.pubmedcentral.nih.gov/articlerender.fcgi?artid=2172966&tool=pmcentrez&rendertype=abstract.

Georgiou, Marios, Eliana Marinari, Jemima Burden, and Buzz Baum. 2008. “Cdc42, Par6, and aPKC Regulate Arp2/3-Mediated Endocytosis to Control Local Adherens Junction Stability.” *Current Biology* 18 (21): 1631–1638. doi:10.1016/j.cub.2008.09.029. http://dx.doi.org/10.1016/j.cub.2008.09.029.

Gumbiner, Barry M. 2005. “Regulation of Cadherin-Mediated Adhesion in Morphogenesis.” *Nature Reviews. Molecular Cell Biology* 6 (8): 622–634. doi:10.1038/nrm1699.

Hall, Sonia, Courtney Bone, Kenzi Oshima, Liang Zhang, Molly McGraw, Bethany Lucas, Richard G Fehon, and Robert E Ward. 2014. “Macroglobulin Complement-Related Encodes a Protein Required for Septate Junction Organization and Paracellular Barrier Function in Drosophila.” *Development (Cambridge, England)* 141 (4) (February): 889–98. doi:10.1242/dev.102152. http://www.ncbi.nlm.nih.gov/pubmed/24496625.

Hall, Stephen G., and Allan J. Bieber. 1997. “Mutations in the Drosophila Neuroglian Cell Adhesion Molecule Affect Motor Neuron Pathfinding and Peripheral Nervous System Patterning.” *Journal of Neurobiology* 32 (3): 325–340. doi:10.1002/(SICI)1097-4695(199703)32:3<325::AID-NEU6>3.0.CO;2-9.

Hijazi, Assia, Wilfried Masson, Benoit Augé, Lucas Waltzer, Marc Haenlin, and Fernando Roch. 2009. "Boudin Is Required for Septate Junction Organisation in Drosophila and Codes for a Diffusible Protein of the Ly6 Superfamily." *Development (Cambridge, England)* 136 (13) (July): 2199–209. doi:10.1242/dev.033845. http://www.ncbi.nlm.nih.gov/pubmed/19502482.

Hutson, M Shane, Yoichiro Tokutake, Ming-Shien Chang, James W Bloor, Stephanos Venakides, Daniel P Kiehart, and Glenn S Edwards. 2003. "Forces for Morphogenesis Investigated with Laser Microsurgery and Quantitative Modeling." *Science (New York, N.Y.)* 300 (5616): 145–149. doi:10.1126/science.1079552.

Ile, K. E., R. Tripathy, V. Goldfinger, and a. D. Renault. 2012. "Wunen, a Drosophila Lipid Phosphate Phosphatase, Is Required for Septate Junction-Mediated Barrier Function." *Development* 139 (14): 2535–2546. doi:10.1242/dev.077289.

Jacinto, a, W Wood, T Balayo, M Turmaine, a Martinez-Arias, and P Martin. 2000. "Dynamic Actin-Based Epithelial Adhesion and Cell Matching during Drosophila Dorsal Closure." *Current Biology : CB* 10 (22) (November 16): 1420–6. http://www.ncbi.nlm.nih.gov/pubmed/11102803.

Jankovics, Ferenc, and Damian Brunner. 2006. "Transiently Reorganized Microtubules Are Essential for Zippering during Dorsal Closure in Drosophila Melanogaster." *Developmental Cell* 11 (3): 375–385. doi:10.1016/j.devcel.2006.07.014.

Kaltschmidt, Julia a, Nicola Lawrence, Véronique Morel, Tina Balayo, Beatriz García Fernández, Anne Pelissier, Antonio Jacinto, and Alfonso Martinez Arias. 2002. "Planar Polarity and Actin Dynamics in the Epidermis of Drosophila." *Nature Cell Biology* 4 (12): 937–944. doi:10.1038/ncb882.

Krogh, a, B Larsson, G von Heijne, and E L Sonnhammer. 2001. "Predicting Transmembrane Protein Topology with a Hidden Markov Model: Application to Complete Genomes." *Journal of Molecular Biology* 305 (3): 567–580. doi:10.1006/jmbi.2000.4315.

Krupinski, Thomas, and Greg J Beitel. 2009. "Unexpected Roles of the Na-K-ATPase and Other Ion Transporters in Cell Junctions and Tubulogenesis." *Physiology (Bethesda, Md.)* 24 (June): 192–201. doi:10.1152/physiol.00008.2009. http://www.ncbi.nlm.nih.gov/pubmed/19509129.

Lamb, R S, R E Ward, L Schweizer, and R G Fehon. 1998. "Drosophila Coracle, a Member of the Protein 4.1 Superfamily, Has Essential Structural Functions in the Septate Junctions and Developmental Functions in Embryonic and Adult Epithelial Cells." *Molecular Biology of the Cell* 9 (12) (December): 3505–19. http://www.pubmedcentral.nih.gov/articlerender.fcgi?artid=25665&tool=pmcentrez&rendertype=abstract.

Langevin, Johanna, Matthew J. Morgan, Carine Rossé, Victor Racine, Jean Baptiste Sibarita, Sandra Aresta, Mala Murthy, Thomas Schwarz, Jacques Camonis, and Yohanns Bellaïche. 2005. "Drosophila Exocyst Components sec5, sec6, and Sec15 Regulate DE-Cadherin Trafficking from Recycling Endosomes to the Plasma Membrane." *Developmental Cell* 9 (3): 365–376. doi:10.1016/j.devcel.2005.07.013.

Laprise, Patrick, Kimberly M Lau, Kathryn P Harris, Nancy F Silva-Gagliardi, Sarah M Paul, Slobodan Beronja, Greg J Beitel, C Jane McGlade, and Ulrich Tepass. 2009. "Yurt, Coracle, Neurexin IV and the Na(+),K(+)-ATPase Form a Novel Group of Epithelial Polarity Proteins." *Nature* 459 (7250) (June 25): 1141–5. doi:10.1038/nature08067. http://www.ncbi.nlm.nih.gov/pubmed/19553998.

Laval, Monique, Christophe Bel, and Catherine Faivre-Sarrailh. 2008. "The Lateral Mobility of Cell Adhesion Molecules Is Highly Restricted at Septate Junctions in Drosophila." *BMC Cell Biology* 9: 38. doi:10.1186/1471-2121-9-38.

Li, Bingbing X., Akiko K. Satoh, and Donald F. Ready. 2007. "Myosin V, Rab11, and dRip11 Direct Apical Secretion and Cellular Morphogenesis in Developing Drosophila Photoreceptors." *Journal of Cell Biology* 177 (4): 659–669. doi:10.1083/jcb.200610157.

Llimargas, Marta, Maura Strigini, Markella Katidou, Domna Karagogeos, and Jordi Casanova. 2004. "Lachesin Is a Component of a Septate Junction-Based Mechanism That Controls Tube Size and Epithelial Integrity in the Drosophila Tracheal System." *Development (Cambridge, England)* 131 (1) (January): 181–90. doi:10.1242/dev.00917. http://www.ncbi.nlm.nih.gov/pubmed/14681183.

Madan, Pavneesh, Keeley Rose, and Andrew J. Watson. 2007. "Na/K-ATPase ??1 Subunit Expression Is Required for Blastocyst Formation and Normal Assembly of Trophectoderm Tight Junction-Associated Proteins." *Journal of Biological Chemistry* 282 (16): 12127–12134. doi:10.1074/jbc.M700696200.

Martín-Blanco, E. 1998. "Regulatory Control of Signal Transduction during Morphogenesis in Drosophila." *The International Journal of Developmental Biology* 42 (3): 363–368.

Maruyama, Rika, and Deborah J. Andrew. 2012. "Drosophila as a Model for Epithelial Tube Formation." *Developmental Dynamics* 241 (1): 119–135. doi:10.1002/dvdy.22775.

Medzhitov, Ruslan, and Charles a Janeway. 2002. "Decoding the Patterns of Self and Nonself by the Innate Immune System." *Science (New York, N.Y.)* 296 (5566): 298–300. doi:10.1126/science.1068883.

Millard, Thomas H, and Paul Martin. 2008. “Dynamic Analysis of Filopodial Interactions during the Zippering Phase of Drosophila Dorsal Closure.” *Development (Cambridge, England)* 135 (4): 621–626. doi:10.1242/dev.014001.

Morin, X, R Daneman, M Zavortink, and W Chia. 2001. “A Protein Trap Strategy to Detect GFP-Tagged Proteins Expressed from Their Endogenous Loci in Drosophila.” *Proceedings of the National Academy of Sciences of the United States of America* 98 (26): 15050–15055. doi:10.1073/pnas.261408198.

Mudiganti, Usharani, Raquel Hernandez, and Dennis T. Brown. 2010. “Insect Response to Alphavirus Infection-Establishment of Alphavirus Persistence in Insect Cells Involves Inhibition of Viral Polyprotein Cleavage.” *Virus Research* 150 (1-2): 73–84. doi:10.1016/j.virusres.2010.02.016. http://dx.doi.org/10.1016/j.virusres.2010.02.016.

Myat, Monn Monn. 2005. “Making Tubes in the Drosophila Embryo.” *Developmental Dynamics* 232 (3): 617–632. doi:10.1002/dvdy.20293.

Myat, Monn Monn, and Deborah J. Andrew. 2002. “Epithelial Tube Morphology Is Determined by the Polarized Growth and Delivery of Apical Membrane.” *Cell* 111 (6): 879–891. doi:10.1016/S0092-8674(02)01140-6.

Nelson, Kevin S, Mikio Furuse, and Greg J Beitel. 2010. “The Drosophila Claudin Kune-Kune Is Required for Septate Junction Organization and Tracheal Tube Size Control.” *Genetics* 185 (3) (July): 831–9. doi:10.1534/genetics.110.114959. http://www.pubmedcentral.nih.gov/articlerender.fcgi?artid=2907205&tool=pmcentrez&rendertype=abstract.

Nilton, Anna, Kenzi Oshima, Fariba Zare, Sunitha Byri, Ulf Nannmark, Kevin G Nyberg, Richard G Fehon, and Anne E Uv. 2010. “Crooked, Coiled and Crimpled Are Three Ly6-like Proteins Required for Proper Localization of Septate Junction Components.” *Development (Cambridge, England)* 137 (14) (July): 2427–37. doi:10.1242/dev.052605. http://www.pubmedcentral.nih.gov/articlerender.fcgi?artid=2889608&tool=pmcentrez&rendertype=abstract.

Oshima, Kenzi, and Richard G Fehon. 2011. “Analysis of Protein Dynamics within the Septate Junction Reveals a Highly Stable Core Protein Complex That Does Not Include the Basolateral Polarity Protein Discs Large.” *Journal of Cell Science* 124 (Pt 16) (August 15): 2861–71. doi:10.1242/jcs.087700. http://www.pubmedcentral.nih.gov/articlerender.fcgi?artid=3148133&tool=pmcentrez&rendertype=abstract.

Patch, Kistie, Shannon R. Stewart, Aaron Welch, and Robert E. Ward IV. 2009. “A Second-Site Noncomplementation Screen for Modifiers of Rho1 Signaling during

Imaginal Disc Morphogenesis in Drosophila." *PLoS ONE* 4 (10). doi:10.1371/journal.pone.0007574.

Paul, Sarah M, Michael J Palladino, and Greg J Beitel. 2007. "A Pump-Independent Function of the Na,K-ATPase Is Required for Epithelial Junction Function and Tracheal Tube-Size Control." *Development (Cambridge, England)* 134 (1): 147–155. doi:10.1242/dev.02710.

Paul, Sarah M, Melissa Ternet, Paul M Salvaterra, and Greg J Beitel. 2003. "The Na+/K+ ATPase Is Required for Septate Junction Function and Epithelial Tube-Size Control in the Drosophila Tracheal System." *Development (Cambridge, England)* 130 (20) (October): 4963–74. doi:10.1242/dev.00691. http://www.ncbi.nlm.nih.gov/pubmed/12930776.

Peralta, X G, Y Toyama, M S Hutson, R Montague, S Venakides, D P Kiehart, and G S Edwards. 2007. "Upregulation of Forces and Morphogenic Asymmetries in Dorsal Closure during Drosophila Development." *Biophysical Journal* 92 (7): 2583–2596. doi:10.1529/biophysj.106.094110.

Pirraglia, Carolyn, Jenna Walters, and Monn Monn Myat. 2010. "Pak1 Control of E-Cadherin Endocytosis Regulates Salivary Gland Lumen Size and Shape." *Development (Cambridge, England)* 137 (24): 4177–4189. doi:10.1242/dev.048827.

Polyakov, Oleg, Bing He, Michael Swan, Joshua W Shaevitz, Matthias Kaschube, and Eric Wieschaus. 2014. "Passive Mechanical Forces Control Cell-Shape Change during Drosophila Ventral Furrow Formation." *Biophysical Journal* 107 (4): 998–1010. doi:10.1016/j.bpj.2014.07.013. http://www.ncbi.nlm.nih.gov/pubmed/25140436.

Rajasekaran, S a, L G Palmer, S Y Moon, a Peralta Soler, G L Apodaca, J F Harper, Y Zheng, and a K Rajasekaran. 2001. "Na,K-ATPase Activity Is Required for Formation of Tight Junctions, Desmosomes, and Induction of Polarity in Epithelial Cells." *Molecular Biology of the Cell* 12 (12): 3717–3732.

Schneeberger, Eveline E, and Robert D Lynch. 2004. "The Tight Junction: A Multifunctional Complex." *American Journal of Physiology. Cell Physiology* 286 (6): C1213–C1228. doi:10.1152/ajpcell.00558.2003.

Schneider, Caroline a, Wayne S Rasband, and Kevin W Eliceiri. 2012. "NIH Image to ImageJ: 25 Years of Image Analysis." *Nature Methods* 9 (7): 671–675. doi:10.1038/nmeth.2089. http://dx.doi.org/10.1038/nmeth.2089.

Shaye, Daniel D, Jordi Casanova, and Marta Llimargas. 2008. "Modulation of Intracellular Trafficking Regulates Cell Intercalation in the Drosophila Trachea." *Nature Cell Biology* 10 (8): 964–970. doi:10.1038/ncb1756.

Shindo, Masayo, Housei Wada, Masako Kaido, Minoru Tateno, Toshiro Aigaki, Leo Tsuda, and Shigeo Hayashi. 2008. "Dual Function of Src in the Maintenance of Adherens Junctions during Tracheal Epithelial Morphogenesis." *Development (Cambridge, England)* 135 (7): 1355–1364. doi:10.1242/dev.015982.

Smith, Benjamin E, and Robert E Braun. 2012. "Germ Cell Migration across Sertoli Cell Tight Junctions." *Science (New York, N.Y.)* 338 (6108) (November 9): 798–802. doi:10.1126/science.1219969. http://www.ncbi.nlm.nih.gov/pubmed/22997133.

Solon, Jerome, Aynur Kaya-Çopur, Julien Colombelli, and Damian Brunner. 2009. "Pulsed Forces Timed by a Ratchet-like Mechanism Drive Directed Tissue Movement during Dorsal Closure." *Cell* 137 (7): 1331–1342. doi:10.1016/j.cell.2009.03.050.

Sottrup-Jensen, Lars, Ole Sand, Lene Kristensens, and Georg H Fey. 1989. "The Alpha-Macroglobulin Bait Region." *The Journal of Biological Chemistry* 264: 15781–15789.

Stroschein-Stevenson, Shannon L, Edan Foley, Patrick H O'Farrell, and Alexander D Johnson. 2006. "Identification of Drosophila Gene Products Required for Phagocytosis of Candida Albicans." *PLoS Biology* 4 (1) (January): e4. doi:10.1371/journal.pbio.0040004. http://www.pubmedcentral.nih.gov/articlerender.fcgi?artid=1310651&tool=pmcentrez&rendertype=abstract.

Takeichi, Masatoshi. 2014. "Dynamic Contacts: Rearranging Adherens Junctions to Drive Epithelial Remodelling." *Nature Reviews. Molecular Cell Biology* 15 (6): 397–410. doi:10.1038/nrm3802. http://www.ncbi.nlm.nih.gov/pubmed/24824068.

Tepass, Ulrich, and Volker Hartenstein. 1994. "The Development of Cellular Junctions in the Drosophila Embryo." *Developmental Biology* 161 (2) (February): 563–596. doi:http://dx.doi.org/10.1006/dbio.1994.1054. http://www.sciencedirect.com/science/article/pii/S0012160684710542.

Tiklová, Katarína, Kirsten-André Senti, Shenqiu Wang, Astrid Gräslund, and Christos Samakovlis. 2010. "Epithelial Septate Junction Assembly Relies on Melanotransferrin Iron Binding and Endocytosis in Drosophila." *Nature Cell Biology* 12 (11) (November): 1071–7. doi:10.1038/ncb2111. http://www.ncbi.nlm.nih.gov/pubmed/20935638.

VanHook, Annalisa, and Anthea Letsou. 2008. "Head Involution in Drosophila: Genetic and Morphogenetic Connections to Dorsal Closure." *Developmental Dynamics* 237 (1): 28–38. doi:10.1002/dvdy.21405.

Vining, Melissa S., Pamela L. Bradley, Christy a. Comeaux, and Deborah J. Andrew. 2005. "Organ Positioning in Drosophila Requires Complex Tissue-Tissue

Interactions." *Developmental Biology* 287 (1): 19–34. doi:10.1016/j.ydbio.2005.08.017.

Violette, Michelle I., Pavneesh Madan, and Andrew J. Watson. 2006. "Na+/K+-ATPase Regulates Tight Junction Formation and Function during Mouse Preimplantation Development." *Developmental Biology* 289 (2): 406–419. doi:10.1016/j.ydbio.2005.11.004.

Wang, Lei, Janelle Evans, Hillary K. Andrews, Robert B. Beckstead, Carl S. Thummel, and Arash Bashirullah. 2008. "A Genetic Screen Identifies New Regulators of Steroid-Triggered Programmed Cell Death in Drosophila." *Genetics* 180 (1): 269–281. doi:10.1534/genetics.108.092478.

Wang, Shenqiu, Satish Arcot Jayaram, Johanna Hemphälä, K. a. Senti, Vasilios Tsarouhas, Haining Jin, and Christos Samakovlis. 2006. "Septate-Junction-Dependent Luminal Deposition of Chitin Deacetylases Restricts Tube Elongation in the Drosophila Trachea." *Current Biology* 16 (2): 180–185. doi:10.1016/j.cub.2005.11.074.

Wang, Yu-Chiun, Zia Khan, Matthias Kaschube, and Eric F. Wieschaus. 2012. "Differential Positioning of Adherens Junctions Is Associated with Initiation of Epithelial Folding." *Nature* 484 (7394): 390–393. doi:10.1038/nature10938.

Ward, Robert E, Liang Schweizer, Rebecca S Lamb, and Richard G Fehon. 2001. "A Cytoplasmic Component of the Septate Junction , Provides."

Ward, Robert E, Robert E Ward Iv, Rebecca S Lamb, Rebecca S Lamb, Richard G Fehon, and Richard G Fehon. 1998. "A Conserved Functional Domain of." *Cell* 140 (6): 1463–1473.

Ward, Robert E., Janelle Evans, and Carl S. Thummel. 2003. "Genetic Modifier Screens in Drosophila Demonstrate a Role for Rho1 Signaling in Ecdysone-Triggered Imaginal Disc Morphogenesis." *Genetics* 165 (3): 1397–1415.

Williams, Michael J. 2007. "Drosophila Hemopoiesis and Cellular Immunity." *Journal of Immunology (Baltimore, Md. : 1950)* 178 (8): 4711–4716. doi:178/8/4711 [pii].

Wirtz-Peitz, Frederik, and Jennifer a Zallen. 2009. "Junctional Trafficking and Epithelial Morphogenesis." *Current Opinion in Genetics & Development* 19 (4) (August): 350–6. doi:10.1016/j.gde.2009.04.011. http://www.pubmedcentral.nih.gov/articlerender.fcgi?artid=2752435&tool=pmcentrez&rendertype=abstract.

Woods, Daniel F., J. O Wen Wu, and Peter J. Bryant. 1997. "Localization of Proteins to the Apico-Lateral Junctions of Drosophila Epithelia." *Developmental Genetics* 20

(2): 111–118. doi:10.1002/(SICI)1520-6408(1997)20:2<111::AID-DVG4>3.0.CO;2-A.

Wu, Victoria M, Joost Schulte, Alexander Hirschi, Ulrich Tepass, and Greg J Beitel. 2004. "Sinuous Is a Drosophila Claudin Required for Septate Junction Organization and Epithelial Tube Size Control." *The Journal of Cell Biology* 164 (2) (January 19): 313–23. doi:10.1083/jcb.200309134. http://www.pubmedcentral.nih.gov/articlerender.fcgi?artid=2172325&tool=pmcentrez&rendertype=abstract.

Wu, Victoria M, Marcus H Yu, Raehum Paik, Swati Banerjee, Zhiguo Liang, Sarah M Paul, Manzoor a Bhat, and Greg J Beitel. 2007. "Drosophila Varicose, a Member of a New Subgroup of Basolateral MAGUKs, Is Required for Septate Junctions and Tracheal Morphogenesis." *Development (Cambridge, England)* 134 (5) (March): 999–1009. doi:10.1242/dev.02785. http://www.pubmedcentral.nih.gov/articlerender.fcgi?artid=1955473&tool=pmcentrez&rendertype=abstract.

Xu, N., G. Bagumian, M. Galiano, and M. M. Myat. 2011. "Rho GTPase Controls Drosophila Salivary Gland Lumen Size through Regulation of the Actin Cytoskeleton and Moesin." *Development* 138 (24): 5415–5427. doi:10.1242/dev.069831.

Xu, Na, Benison Keung, and Monn Monn Myat. 2008. "Rho GTPase Controls Invagination and Cohesive Migration of the Drosophila Salivary Gland through Crumbs and Rho-Kinase." *Developmental Biology* 321 (1): 88–100. doi:10.1016/j.ydbio.2008.06.007.

Yamazaki, Yuji, Reitaro Tokumasu, Hiroshi Kimura, and Sachiko Tsukita. 2011. "Role of Claudin Species-Specific Dynamics in Reconstitution and Remodeling of the Zonula Occludens." *Molecular Biology of the Cell* 22 (9): 1495–1504. doi:10.1091/mbc.E10-12-1003.